THE PREDICTION OF CIVIL ENGINEERING PROBLEMS IN THE ARCTIC BY MEANS OF DUAL-CHANNEL I-R SCANNING AND AEROCHROME INFRARED PHOTOGRAPHY
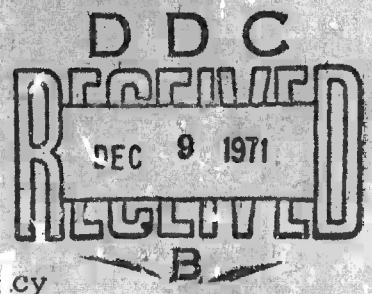
by

Leonard A. LeSchack, Frederick H. Morse, Wm. R. Brinley, Jr.
Nancy G. Ryan and Robert B. Ryan

Semi-Annual Technical Report #1

November 1971

DEVELOPMENT AND RESOURCES TRANSPORTATION CO.

1111 UNIVERSITY BLVD. WEST, SUITE G-7   SILVER SPRING, MARYLAND 20902, U.S.A.
TELEPHONE 301-649-1670

D D C

RECEIVED
DEC 9 1971
B

DISCLAIMER NOTICE

THIS DOCUMENT IS THE BEST
QUALITY AVAILABLE.

COPY FURNISHED CONTAINED
A SIGNIFICANT NUMBER OF
PAGES WHICH DO NOT
REPRODUCE LEGIBLY.

THE PREDICTION OF CIVIL ENGINEERING PROBLEMS IN
THE ARCTIC BY MEANS OF DUAL-CHANNEL I-R SCANNING
AND AEROCHROME INFRARED PHOTOGRAPHY

by

Leonard A. LeSchack, Frederick H. Morse, Wm. R. Brinley, Jr.
Nancy G. Ryan and Robert B. Ryan

Semi-Annual Technical Report #1

November 1971

DEVELOPMENT AND RESOURCES TRANSPORTATION CO.

1111 UNIVERSITY BLVD. WEST, SUITE G-7   **SILVER SPRING, MARYLAND 20902, U.S.A.**
TELEPHONE 301·649·1670

Principal Investigator: Leonard A. LeSchack

Scientific Officer: Director, Arctic Program
                     Earth Sciences Division
                     Office of Naval Research
                     Department of the Navy
                     800 North Quincy Street
                     Arlington, Virginia 22217

Short Title of Work: Subsurface I-R Imagery

Effective Date of Contract: 15 April 1971

Contract Expiration Date: 14 April 1972

Amount of Contract: $110,932.00

DOCUMENT CONTROL DATA - R&D

(Security classification of title, body of abstract and indexing annotation must be entered when the overall report is classified)

1. ORIGINATING ACTIVITY (Corporate author)	2a. REPORT SECURITY CLASSIFICATION
Development & Resources Transportation Co. 1111 University Boulevard W. Silver Spring, Maryland 20902	Unclassified
	2b. GROUP N/A

3. REPORT TITLE

The Prediction of Civil Engineering Problems in the Arctic by Means of
Dual-Channel I-R Scanning and Aerochrome Infrared Photography

4. DESCRIPTIVE NOTES *(Type of report and inclusive dates)*
Semi-Annual Technical Report, 15 April-31 October 1971

5. AUTHOR(S) *(Last name, first name, initial)*
Le Schack, Leonard A., Morse, Frederick H., Brinley, Wm. R., Jr.,
Ryan, Nancy G. and Ryan, Robert B.

6. REPORT DATE	7a. TOTAL NO. OF PAGES	7b. NO. OF REFS
November 1971	38 + 4 Appendices	18
8a. CONTRACT OR GRANT NO. N00014-71-C-0396	9a. ORIGINATOR'S REPORT NUMBER(S) D&RTCo., #7	
b. PROJECT NO. NR 307-339		
c. ARPA Order #1772 (31 Mar 71)	9b. OTHER REPORT NO(S) (Any other numbers that may be assigned this report)	
d. Program Code 1N10	None	

10. AVAILABILITY/LIMITATION NOTICES

Qualified requestors may obtain copies of this report from DDC.

11. SUPPLEMENTARY NOTES Monitored by Office of Naval Research Arctic Program (Code 415) Arlington, Virginia 22217	12. SPONSORING MILITARY ACTIVITY Advanced Research Project Agency 1400 Wilson Boulevard Arlington, Virginia 22209

13. ABSTRACT

The feasibility of detecting massive ice in permafrost by sensing the associated surface thermal anomalies with an airborne synchronous dual-channel infrared (I-R) line scanner is discussed in this first semi-annual report. Three broad areas of research are involved: (a) the determination and quantification by both mathematical modeling and ground truth field studies of significant parameters useful in detecting any thermal anomalies caused by near surface ice in permafrost, (b) the modification of a standard quantitative I-R scanner to synchronously sense and record radiation emitted in the 4.5-5.5 and 8-12 micron bands, and (c) the processing electronically of the recorded information to obtain the ratio and product imagery used to delineate the thermal anomalies sought. As was originally proposed by the Development & Resources Transportation Co., the ratio signal, by producing imagery which approaches an emissivity ratio map, appears to assist significantly in differentiating effects due to temperature from those due to emissivity--inseparable in conventional "thermal" mapping. Comparison of the ratio map of an area with the thermal maps in the 4.5-5.5 and 8-12 micron bands, and especially with the product imagery map, distinguishes anomalous regions due primarily to temperature. Field ground truth studies, including extensive permafrost probing and near-surface temperature measurements taken at hourly intervals over several days, were conducted for correlation with the airborne imagery. Drilling of one
(Continued on supplement)

DD FORM **1473** 1 JAN 64

DD Form 1473

#13, Abstract, Continued

ridge-shaped permafrost structure, located by probing in an area corresponding
to a polygonal structure seen on the imagery, revealed more ice in the cores
than would have been anticipated by random drilling. It is believed that these
structures are the sides of ice polygons seen on the I-R imagery but not
observable in standard aerial photography. Further analyses of these data
are needed before conclusive statements can be made; however, both the dual-
channel scanner and the discussed approach to detection of ice within the
permafrost appear to be useful tools for arctic engineering and warrant further
study.

14. KEY WORDS	LINK A		LINK B		LINK C	
	ROLE	WT	ROLE	WT	ROLE	WT
Arctic Civil Engineering						
Airborne Remote Sensing – Alaska						
Permafrost – Alaska						
Infrared Imagery – Alaska, High Resolution, Large Scale						
Aerochrome Infrared Photography – Alaska						
Ice-Polygonal, wedges, lenses						
Imagery Enhancement -Thermal I-R						
Ratio and Product Imagery -Thermal I-R						
Airborne Line Scanner-Synchronous Dual Channel I-R						

INSTRUCTIONS

1. **ORIGINATING ACTIVITY:** Enter the name and address of the contractor, subcontractor, grantee, Department of Defense activity or other organization (*corporate author*) issuing the report.

2a. **REPORT SECURITY CLASSIFICATION:** Enter the overall security classification of the report. Indicate whether "Restricted Data" is included. Marking is to be in accordance with appropriate security regulations.

2b. **GROUP:** Automatic downgrading is specified in DoD Directive 5200.10 and Armed Forces Industrial Manual. Enter the group number. Also, when applicable, show that optional markings have been used for Group 3 and Group 4 as authorized.

3. **REPORT TITLE:** Enter the complete report title in all capital letters. Titles in all cases should be unclassified. If a meaningful title cannot be selected without classification, show title classification in all capitals in parenthesis immediately following the title.

4. **DESCRIPTIVE NOTES:** If appropriate, enter the type of report, e.g., interim, progress, summary, annual, or final. Give the inclusive dates when a specific reporting period is covered.

5. **AUTHOR(S):** Enter the name(s) of author(s) as shown on or in the report. Enter last name, first name, middle initial. If military, show rank and branch of service. The name of the principal author is an absolute minimum requirement.

6. **REPORT DATE:** Enter the date of the report as day, month, year; or month, year. If more than one date appears on the report, use date of publication.

7a. **TOTAL NUMBER OF PAGES:** The total page count should follow normal pagination procedures, i.e., enter the number of pages containing information.

7b. **NUMBER OF REFERENCES:** Enter the total number of references cited in the report.

8a. **CONTRACT OR GRANT NUMBER:** If appropriate, enter the applicable number of the contract or grant under which the report was written.

8b, 8c, & 8d. **PROJECT NUMBER:** Enter the appropriate military department identification, such as project number, subproject number, system numbers, task number, etc.

9a. **ORIGINATOR'S REPORT NUMBER(S):** Enter the official report number by which the document will be identified and controlled by the originating activity. This number must be unique to this report.

9b. **OTHER REPORT NUMBER(S):** If the report has been assigned any other report numbers (*either by the originator or by the sponsor*), also enter this number(s).

10. **AVAILABILITY/LIMITATION NOTICES:** Enter any limitations on further dissemination of the report, other than those imposed by security classification, using standard statements such as:

  (1) "Qualified requesters may obtain copies of this report from DDC."

  (2) "Foreign announcement and dissemination of this report by DDC is not authorized."

  (3) "U. S. Government agencies may obtain copies of this report directly from DDC. Other qualified DDC users shall request through

    _____."

  (4) "U. S. military agencies may obtain copies of this report directly from DDC. Other qualified users shall request through

    _____."

  (5) "All distribution of this report is controlled. Qualified DDC users shall request through

    _____."

If the report has been furnished to the Office of Technical Services, Department of Commerce, for sale to the public, indicate this fact and enter the price, if known.

11. **SUPPLEMENTARY NOTES:** Use for additional explanatory notes.

12. **SPONSORING MILITARY ACTIVITY:** Enter the name of the departmental project office or laboratory sponsoring (*paying for*) the research and development. Include address.

13. **ABSTRACT:** Enter an abstract giving a brief and factual summary of the document indicative of the report, even though it may also appear elsewhere in the body of the technical report. If additional space is required, a continuation sheet shall be attached.

It is highly desirable that the abstract of classified reports be unclassified. Each paragraph of the abstract shall end with an indication of the military security classification of the information in the paragraph, represented as *(TS), (S), (C),* or *(U)*.

There is no limitation on the length of the abstract. However, the suggested length is from 150 to 225 words.

14. **KEY WORDS:** Key words are technically meaningful terms or short phrases that characterize a report and may be used as index entries for cataloging the report. Key words must be selected so that no security classification is required. Identifiers, such as equipment model designation, trade name, military project code name, geographic location, may be used as key words but will be followed by an indication of technical context. The assignment of links, rules, and weights is optional.

FOREWORD

This first Semi-Annual Technical Report under Office of Naval Research Contract N00014-71-C-0396, ARPA Order #1722 dated 31 March 1971, covers research conducted by the Development and Resources Transportation Co. (D&RTCo)from the signing of the contract (10 June 1971) to date. The program objective has been to investigate the feasibility of using dual-channel infrared (I-R) scanning with Aerochrome Infrared photography to detect massive ice within the permafrost in Alaska. The major efforts during the reporting period were devoted to identifying the significant parameters for measurement in the field; determining what their expected magnitudes would be and how best to measure them. In the field phase, using projected data values, these measurements were made at several locations in Alaska. Accordingly, this report will be devoted primarily to a discussion of the methodologies used in the conduct of the field program and of the types of data collected. Additionally, some preliminary analysis of the data is is presented.

ACKNOWLEDGEMENT

THE PREDICTION OF CIVIL ENGINEERING PROBLEMS IN THE ARCTIC BY MEANS OF DUAL-CHANNEL I-R SCANNING AND AEROCHROME INFRARED PHOTOGRAPHY

by

Leonard A. LeSchack, Frederick H. Morse, Wm. R. Brinley, Jr.
Nancy G. Ryan and Robert B. Ryan

November 1971

SUMMARY

PURPOSE OF THE RESEARCH PROGRAM

Background – The Problem

Engineering construction in areas underlain by permanently frozen ground (permafrost) has long been a problem in the Arctic. The USSR has found this to be one of their most severe constraints in Arctic engineering construction; the United States and Canada encountered similar problems, particularly in the building of the DEWLINE stations. Currently, civil engineers are faced with route selection problems, over extensive zones of continuous and discontinuous permafrost, prior to construction of a large diameter pipeline from Prudhoe Bay to Valdez, Alaska.

In connection with initial surveys for the proposed pipeline, an extensive core-drilling program was essential to determine the engineering characteristics of the subsurface and the ability of the ground to support the pipeline and its associated facilities. The fact that the line was to traverse extensive regions of permafrost was known--the nature of the underlying permafrost was not. R&M Engineering and Geological Consultants of Fairbanks (R&M), under contract to the pipeline consortium is currently conducting the core-drilling program. The services of R&M were also retained by the Development and Resources Transportation Company (D&RTCo.) for the program described herein. As core-drilling progressed, engineers were disturbed to note that many of the cores contained substantial thicknesses of ice. The ice appeared at apparently random borehole locations as lenses, wedges, and other forms of varying thickness. Construction in areas where permafrost has a substantial ice content is almost predestined to fail as the ice responds to disruption of the thermal regime. A method is needed, therefore, to locate and delineate such areas of massive

ice without an extensive and expensive program of core drilling required literally every few meters. Remote sensing techniques appear to offer a potential solution, and warrant further investigation.

Standard and Conventional Photo-Interpretation

The extensive literature, published in the US, the USSR, and Canada shows a consensus that the phenomenon of the ice-wedge polygon is an important key to determine the presence (or absence) of massive ice in permafrost. In areas with shallow depths to permafrost (such as the North Slope of the Brooks Range) conventional aerial photography clearly identifies polygonal structures and Aerochrome Infrared photography has also proven to be a boon in such applications. In areas other than on the North Slope or where patterned ground is not clearly visible, conventional photographic interpretation techniques are insufficient to determine the presence of such ice with the degree of certainty and resolution required. A more positive method of determining such phenomena in near-real-time is needed.

I-R Scanning in the Arctic

Based upon records of previous experiments with standard I-R scanning in the Arctic, the D&RTCo. proposed a potential solution to the problem described above. Although the majority of previous I-R work in this area employed single channel scanners, D&RTCo. proposed to use a <u>synchronous dual-channel scanner</u> in which two wavebands of I-R radiation could be examined simultaneously. D&RTCo. studies, conducted in late 1970, concluded that a dual-channel scanner had excellent promise as a tool by which massive ice inclusions in permafrost might be detected. A proposal was made to the Director, Advanced Engineering, ARPA in which field experiments were to be conducted employing these techniques. An ARPA Order was issued in March 1971, and the Contract was signed in June.

GENERAL METHODLOGY, CHRONOLOGY AND DESCRIPTION OF ACTIVITIES

The D&RTCo. Program is divided into three major phases. These are:

- Literature search, instrumentation preparation, field site selection, establishment of a field operational plan, thermal modelling - PHASE I

- Field program - PHASE II

- Data reduction, data analyses, and documentation - PHASE III

This summary and the first Semi-Annual Technical Report accompanying it discuss the first two phases of the program.

PHASE I - Methodology

Phase I consisted of the following activities:

- Review of studies in the areas of permafrost and Arctic engineering problems including visits to CRREL, the Willow Run Laboratories and the CRREL permafrost tunnel at Fairbanks.

- Development of appropriate techniques for implementation of dual-channel I-R scanning and giving appropriate guidance to the instrument contractor for the construction of the specialized I-R scanning equipment.

- Development of a thermal model to describe the anomalies being sought.

- Detailed examination of the borehole logs, prepared by R&M, to determine areas for more concentrated study in the field.

- Design and fabrication of special equipment required for the ground truth data collection portion of the field program.

- Development of a field program to obtain the required data prior to the onset of snow.

PHASE I - Chronology

Phase I was completed in late July 1971 and included field reconaissance by the Principal Investigator of candidate sites in Alaska, and the detailed examination of borehole data prepared by R&M from boreholes at the sites. On the basis of the field reconaissance, examination of Aerochrome Infrared aerial photography made available by the United States Geological Survey, and detailed plotting of core-logs, four major sites were selected for the field program. These were at Sourdough, Shaw Creek Flats, Hess Creek, and Barrow.

Daedalus Enterprises, Inc. (DEI) modified and tested the dual-channel I-R Scanner. Special field instrumentation was designed, fabricated and tested at D&RTCo. and high-accuracy radiation measurement instruments were acquired.

Close coordination was maintained during this phase with the Willow Run Laboratories of the University of Michigan. This organization had done extensive work in the areas of I-R scanning and thermal modeling, and therefore was chosen to perform the thermal modeling for this program.

PHASE II - The Field Program

The field program was divided into two major operations.

iii

- Airborne operation
- Ground operation

Both of these operations were closely coordinated, and were, of necessity, carried on simultaneously. They are separately described in the paragraphs that follow.

Airborne Operations: A Piper "Aztec" was fitted with the airborne scanner on 19 August and immediately dispatched to the Sourdough area. Two sites, referred to as "Sourdough North" and "Sourdough South" were overflown under varying conditions of weather and time of day. The aircraft was based nearby, permitting immediate processing and examination of the imagery for information that would be of value to the ground party. At the conclusion of the operations in the Sourdough area, the aircraft proceeded to the site of special DOD research activities in the Pt. Barrow Area. Overflights were made of a series of arctic research activities in the region including several CRREL sites, the sites of the ARPA Surface Effect Vehicle Test Program and the IBP Tundra Biome Program. At the conclusion of these activities, the aircraft returned to the ground party, which, having completed its work in the Sourdough area, had proceeded to the Shaw Creek Flats Site.

The data gathered at the Shaw Creek Flats Site indicated that this should be the area for investigation in depth by both ground and air means. The Hess Creek Site was excluded from investigations during this phase of the program due to logistic and time limitations. In addition to the employment of the I-R scanner, selected aerial photography was taken of all the sites of interest to the program. Low-level Kodacolor photography taken of the Shaw Creek Flats Site by helicoper proved a valuable bridge between the activities of the ground party and Phase III data analyses.

Ground Operations: At both the Sourdough and Shaw Creek Flats Sites the ground party carried out similar activities. At the latter site, additional data were gathered. Basic ground truth collection procedures were as follows:

- Locating previously identified boreholes which had significant ice content and marking the holes with high-visibility signal panels for ease of identification on airborne imagery.

- Establishing navigational "check points" to guide the overflights.

- Establishing appropriate ground control. Area is poorly mapped, and "benchmarks" are few. Control had to be established independent of existing geodetic data.

- Describing significant elements of the vegetation by species and size.

iv

After the decision was made to concentrate the field investigations at the Shaw Creek Flats Site, the following additional activities were carried out.

- Detailed ground control was established, based upon compass bearings. NW/SE and NE/SW "transects" were made

- A probe of depth to top of frozen ground layer was made along each transect at 1/2 meter intervals and logged with appropriate environmental data.

- 21-element thermistor arrays were established at two sites, their location guided by rapid interpretation of both airborne imagery and ground probe data, and continuous environmental readings were made at critical times of day and night.

- Detailed (1/2m spacing) probe activities were carried out in areas at which imagery indicated likelihood of polygonal formations.

- An experimental core-drilling operation was conducted at one point of interest, at which a polygon ridge anomaly had been identified; this resulted in finding segregated ice at depths of 50 and 100 cm.

The ground party concluded its field activity on 11 September 1971.

PRELIMINARY CONCLUSIONS

The field program was concentrated at the Shaw Creek area and conclusions presented below represent a preliminary analysis of both the airborne imagery and associated ground data from that area.

- The dual-channel I-R scanner has near-real-time capability of providing assistance to engineers in the field. In the test area, polygonal structures were identified, based upon rapid processing, using a field processing unit. Pre-dawn imagery appeared to have the greatest significant information. Polygons undetected by conventional reconaissance means, are, on the basis of these limited experiments, apparently detected by use of this technique. The authors believe that the existence of polygons, with their associated ice-wedges, may be determined with greater confidence in areas of discontinuous permafrost or in areas where there is no visible surface expression, with the techniques described in the report.

- On the basis of initial imagery examination it is evident that the dual-channel system offers considerable promise for identifying ice wedge polygons. Applying contemporary image-enhancing techniques to the D&RTCo. data appear to offer only limited

capabilities in the identification of polygons. D&RTCo. has offered an alternative technique, which, even in these early stages of study appears to present marked advantages over the techniques commonly employed in I-R image enhancement for other purposes. The D&RTCo. procedure involves a comparison of the ratio and product of the two-channel imagery. The procedure has, to date, shown a remarkable capability for identifying ice-wedge polygons that appear undetectable by other means. The potential of this imagery processing tool appears to be very significant and has just begun to be realized.

IMPLICATIONS TO THE DEPARTMENT OF DEFENSE

The Department of Defense has, of recent years, shown increasing interest in the Arctic, as evidenced by their sponsorship of the Arctic Surface Effect Vehicle Program, their recent overview study of DOD-sponsored arctic research programs, and their sponsorship of CRREL and ONR research in the North. The program reported upon herein is in a position to support ongoing and planned DOD activities in the Land Arctic, particularly in areas underlain by permafrost. The program has demonstrated that:

- The use of I-R scanning has a significant, but undeveloped potential to locate and identify massive ice in permafrost. The availability of this capability to engineers who must engage in arctic construction in such areas is considered to be of value.

- Dual-channel I-R scanning offers even greater capabilities of identifying such ice masses. At present, image enhancement techniques that will make the greatest use of this capability are confined to the laboratory. It is, however, preeminently feasible to adapt such capability to the field; thus giving the user vital data concerning the engineering characteristics of permafrost in near-real-time.

- It appears that contemporary, conventional image-enhancement techniques, although suited to other interpretations, are less suited to the identification of ice-wedge polygons in permafrost than the "ratio-product" methodology now under study by the D&RT Co.

FURTHER RESEARCH IMPLICATIONS

The role of civil engineering in the Arctic is expected to grow with greater DOD and civil interests in the area. In addition, the Corps of Engineers maintains both a civil and military role in Alaska--an area in which civil and military functions have typically been closely inter-related. With increased interest in both the Land and Ocean Arctic Regions, the requirements for facilities construction is also expected to grow. It is vital that the civil engineer operating in the Arctic be fitted with the best tools of the trade.

To date, permafrost engineering has been a costly, "learn by experience" activity. The techniques initiated in this program offer the potential to take some of the guesswork out of engineering operations there. The techniques discussed have not been subjected to detailed, analytical examination, however, and therefore represent only a limited sampling of employment of instrumentation, correlation with ground truth, and analyses. Such limitations are inherent to the extremely limited time afforded by the short Alaskan field season. Before the promise of the techniques initiated in this feasibility study may be implemented with fullest confidence, a more comprehensive research program should be undertaken.

ABSTRACT

The feasibility of detecting massive ice in permafrost by sensing the associated surface thermal anomalies with an airborne synchronous dual-channel infrared (I-R) line scanner is discussed in this first semi-annual report. Three broad areas of research are involved: (a) the determination and quantification by both mathematical modeling and ground truth field studies of significant parameters useful in detecting any thermal anomalies caused by near surface ice in permafrost, (b) the modification of a standard quantitative I-R scanner to synchronously sense and record radiation emitted in the 4.5-5.5 and 8-12 micron bands, and (c) the processing electronically of the recorded information to obtain the ratio and product imagery used to delineate the thermal anomalies sought. As was originally proposed by the Development & Resources Transportation Co., the ratio signal, by producing imagery which approaches an emissivity ratio map, appears to assist significantly in differentiating effects due to temperature from those due to emissivity--inseparable in conventional "thermal" mapping. Comparison of the ratio map of an area with the thermal maps in the 4.5-5.5 and 8-12 micron bands, and especially with the product imagery map, distinguishes anomalous regions due primarily to temperature. Field ground truth studies, including extensive permafrost probing and near-surface temperature measurements taken at hourly intervals over several days, were conducted for correlation with the airborne imagery. Drilling of one ridge-shaped permafrost structure, located by probing in an area corresponding to a polygonal structure seen on the imagery, revealed more ice in the cores than would have been anticipated by random drilling. It is believed that these structures are the sides of ice polygons seen on the I-R imagery but not observable in standard aerial photography. Further analyses of these data are needed before conclusive statements can be made; however, both the dual-channel scanner and the discussed approach to detection of ice within the permafrost appear to be useful tools for arctic engineering and warrant further study.

TABLE OF CONTENTS

Table of Contents (Continued

THE PREDICTION OF CIVIL ENGINEERING PROBLEMS IN
THE ARCTIC BY MEANS OF DUAL-CHANNEL I-R SCANNING
AND AEROCHROME INFRARED PHOTOGRAPHY

by

Leonard A. LeSchack, Frederick H. Morse, Wm. R. Brinley, Jr.
Nancy G. Ryan and Robert B. Ryan

1. INTRODUCTION AND RATIONALE FOR RESEARCH

One of the most extensive civil engineering projects planned in Alaska
is the construction of a pipeline from Prudhoe Bay on the North Coast to
Valdez on the South Coast. A massive preliminary survey effort was con-
ducted within the past few years by the Trans-Alaska Pipeline System (now
Alyeska Pipeline Service Co.) and one of their contractors, R & M Engineer-
ing & Geological Consultants (R&M) of Fairbanks, to determine the near-
surface geology of the proposed route and to locate the extent of permafrost
in the discontinuous region. This survey involved preparing an aerial photo
mosaic of the route using the available black and white photography taken
at a scale of 1:47,350 and obtaining geological ground truth by drilling
along this route. The drilling program was, and continues to be, an
extensive and costly effort; hundred of boreholes are being sunk to bedrock
or gravel beds to determine the nature of the "active" layer and the potentially
unstable permafrost layer. Boreholes were spaced an average of two miles
apart along the trail, with some occasional clustering in areas of special
interest.

A drilling program of this nature is the usual precursor to the final survey
for a road or pipeline project, and this Alaskan survey was considerably more
costly than a similar program in the temperate zone, owing to higher logistic
costs. A prime purpose of any such survey is to determine the capability of the
subsurface structure to bear, without shifting, contracting or expanding, the
weight of a roadway or structure emplaced along the survey route. It was,
therefore, very disturbing to the contracting engineers to discover, at appar-
ently random drill sites, substantial thicknesses of ice in the drill core
sections. The ice is formed in lenses, strata, wedges and other shapes. It
is commonly found in the Arctic and has been described in the literature[1,2,3,4].
These masses are significant to engineers because, being nearly pure
ice, they respond to temperature changes by relatively rapid, large scale
volumetric changes. Temperature changes may be caused by seasonal changes
in incident solar energy; extensive changes in the vegetation cover such as
due to land clearing; or by the construction of a roadbed or structure above
the ice body. Such large scale volumetric changes in the near-surface
geologic column could easily precipitate an engineering catastrophe.

- 1 -

The Alyeska experience is perhaps the most recent and largest scale example of the extensive engineering problems encountered in construction projects in the Arctic. The problem of near-surface ice structures is important to all arctic military construction whether it be large projects such as airstrips, roadways or pipelines, or small projects such as radar sites or buildings. It seems obvious that a point by point drilling survey, while providing positive information on the presence or absence of massive ice at each drill site, is too costly for use in a continuous survey. As a possible alternative, the Development and Resources Transportation Co. (D&RTCo.) proposed that by airborne remote sensing techniques, large areas could be efficiently surveyed and the presence of ice in engineeringly significant amounts could be determined. This report presents the progress to date on this research.

1.1 Standard Photo-Interpretation

The engineers conducting the Alyeska survey[5] observed that:

> "Due to photo age, photo quality and scale,
> as well as a near total lack of ground truth
> data in many areas, variation between actual
> ground conditions and those conditions thought
> to exist based on photo interpretation will oc-
> cur. One example is massive ground ice, par-
> ticularly lenses. In several cases this ice
> form, where known to exist based on drill hole
> data, showed no surface expression whatever.
> Thus, it is not possible to pin-point all mass-
> ive ice forms based on photo interpretation
> alone. In other instances, where polygonal
> ground patterns are visible, the presence of
> massive ground ice (wedges) can generally
> be predicted with a high degree of accuracy.
> It is also pointed out that in some instances
> the presence of permafrost can effectively
> mask the normal relationships between soil
> types and surface expression."

It should be observed that these engineers were hampered by the age and small scale of the photography available to them. Large scale Aerochrome Infrared* photography would have helped their interpretation effort considerably, although the authors believed at the time that appropriate infrared scanning (I-R) techniques would provide much more useful engineering information.

---

*Formerly known as Ektachrome Infrared Aero film (type 8443).

1.2 Standard I-R Scanning in the Arctic

Several experiments have been conducted in Alaska to determine the value of standard I-R imagery for examining the tundra. Horvath and Lowe[6] showed, for example, that I-R scanning in the 8-14 micron range was very useful for detecting frozen and dry bed lakes on the tundra, both of which were barely visible on standard aerial photography owing to snow cover, and certainly not distinguishable one from another. Unfortunately, the emitted radiation, (Q), is a function of not only the absolute temperature (T) of a given point on the ground, which is the parameter of greatest interest, but also of the emissivity (ϵ) of the material at that point. This emissivity too, could be a useful engineering parameter as recently demonstrated by Vincent[7]. However, I-R scanners detect a signal which is a complex combination of these two variables, thus complicating the interpretation. Currently used procedures of assuming values for ϵ can produce significant interpretation errors as pointed out by several workers in this field[8,9,10].

1.3 The Dual-Channel I-R Scanner

In late 1970, the D&RTCo. conducted preliminary studies that suggested that considerable value would accrue to interpretation of I-R scanning imagery obtained in the Arctic if two wavelength channels were scanned simultaneously. In this technique, a given point in space is sensed simultaneously in two different wavelength bands. Present I-R scanning equipment generally is sensitive to radiation either in the 2-5 micron or 8-14 micron range, depending on the sensor utilized. The radiation received at the sensor is the sum of the energy emitted from the surface, the sky radiance reflected by the surface, both modified by atmospheric absorption, and the energy emitted by the atmosphere between the sensor and the surface. Under certain conditions assumed by the authors, the dominant energy received at the sensor is that emitted from the surface, which may be represented as

$$\dot{Q} = \epsilon F_{\lambda_1 - \lambda_2}(T)$$

where $F_{\lambda_1 - \lambda_2}(T)$ is the fraction of the total emissive power that is emitted in the wavelength interval $\lambda_1 - \lambda_2$. If two channels are recorded simultaneously, one such equation is produced for each band:

$$\dot{Q}_{4-5} = \epsilon_{4-5} F_{4-5}(T)$$

$$\dot{Q}_{8-12} = \epsilon_{8-12} F_{8-12}(T)$$

- 3 -
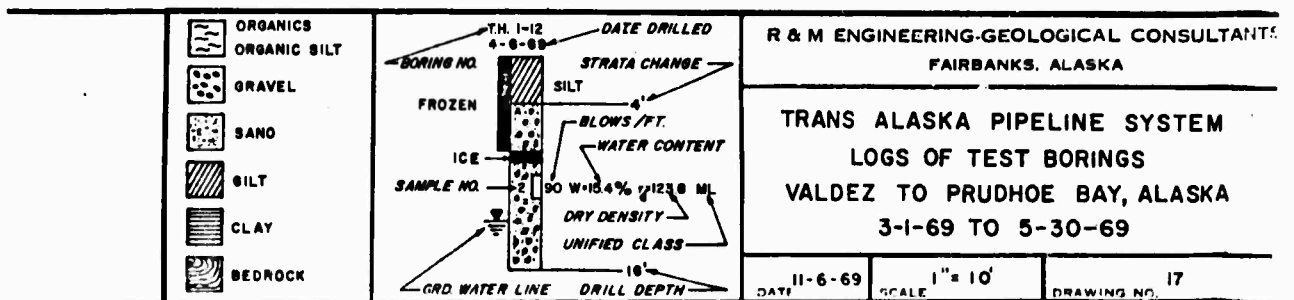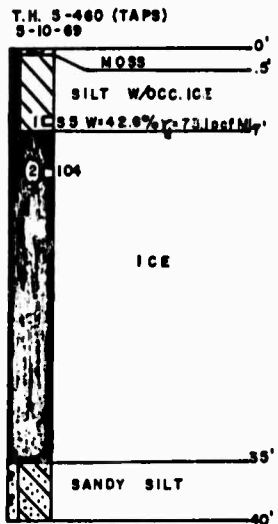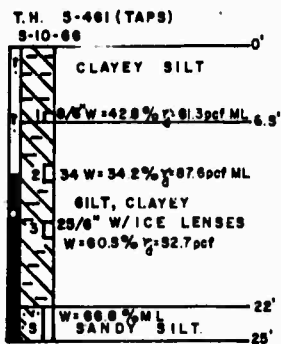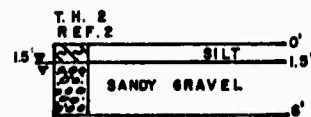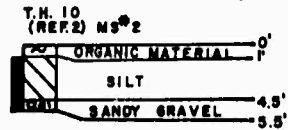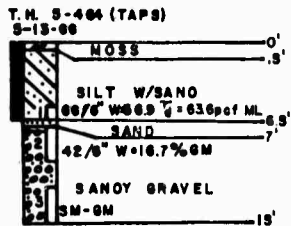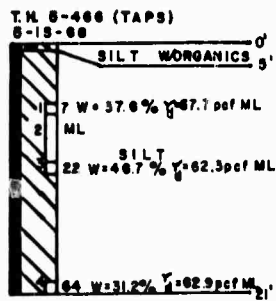
FIGURE 1: An Example of Several Drill Cores in the General Area of Fairbanks, Alaska, Taken Along the Pipeline Route. Note the Significant Thickness of Ice in Hole T.H. 5-460. Locations of the Boreholes are Shown in Figure 2.

The subscripts indicate the nominal wavelength range of each channel. The emissivity varies as a function of wavelength for each material scanned (for example see Buettner and Kern[11]); the function F is also wavelength dependent. The absolute temperature (T) in both equations would be the same for any given point simultaneously scanned. A ratio of the two signals $\dot{Q}_{4-5}$ and $\dot{Q}_{8-12}$ would, for this simplified model, equal the ratio $\epsilon_{4-5}/\epsilon_{8-12}$ and, over the temperature range of interest, this emissivity ratio is a function essentially of the material scanned and not the local temperature. If the ratio signal, rather than either single channel signal is now plotted, a map of surface emissivity ratios is produced. These data can be color-enhanced for contour emphasis. This, in itself could have engineering significance if adequate ground truth studies were made and emissivity ratios known. Of major significance, however, is the separation of the effect of the emissivity of the surface material from the overall radiation response. If the emissivity ratio map is now compared with a color-contoured map obtained by processing the 8-12 micron signal alone, regions of different surface temperature can be identified and theoretically be related to the presence of ice lenses.

A dual-channel scanner that can simultaneously produce the above two functions was constructed for D&RTCo, by Daedalus Enterprises, Inc., a leading manufacturer of I-R scanning equipment, for the discussed research. A description of the equipment is given in Section 2.2 and in greater detail in Appendix A.

1.4 Preliminary Thermal Modelling

Figure 1 shows several drill cores obtained by Alyeska, in the Fairbanks area, during their survey. The locations of these drill holes are shown in Figure 2. Examination of the cores shows the diversity of materials encountered in a relatively small area and particularly, a typical hole at which a substantial ice lens was found. When this ground surface is subjected to a significant increase in net solar energy input over a relatively short time interval, the response of the surface temperatures will reflect the local variations in subsurface composition. There are two types of solar energy increases; these correspond to sunrise (on a daily scale) and springtime (on an annual scale). The response of surface temperatures in the Arctic to daily changes is influenced by a thin sub-surface layer ranging in thickness from a few centimeters to approximately a meter, depending on the nature of the material. This temperature response has been studied by Weedfall at Ogoturuk Valley, Alaska[12]: Figure 3 from his study, shows that maximum and minimum diurnal temperature changes do not propagate downward sufficiently far to produce measurable effects at the surface of anomalies of interest in this study. It can be seen, however, from Figure 4, taken from the same study, that where temperature maxima and minima are recorded monthly from April to August, the warming effect resulting from the onset of springtime can be felt to a considerably greater depth (e.g. from this
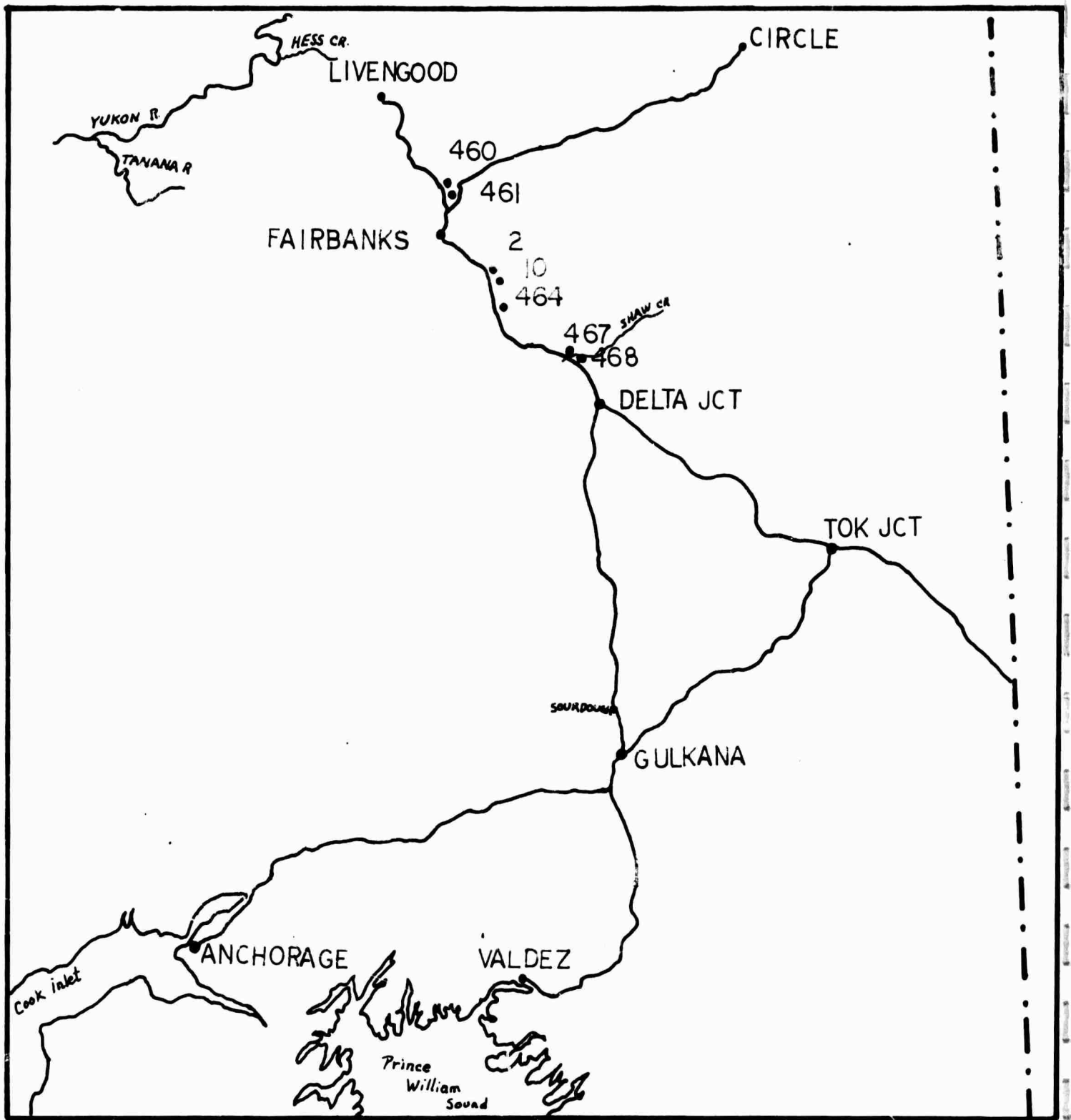
FIGURE 2: Map of Anchorage-Fairbanks Area Showing Locations of Borehole Data Shown in Figure 1.
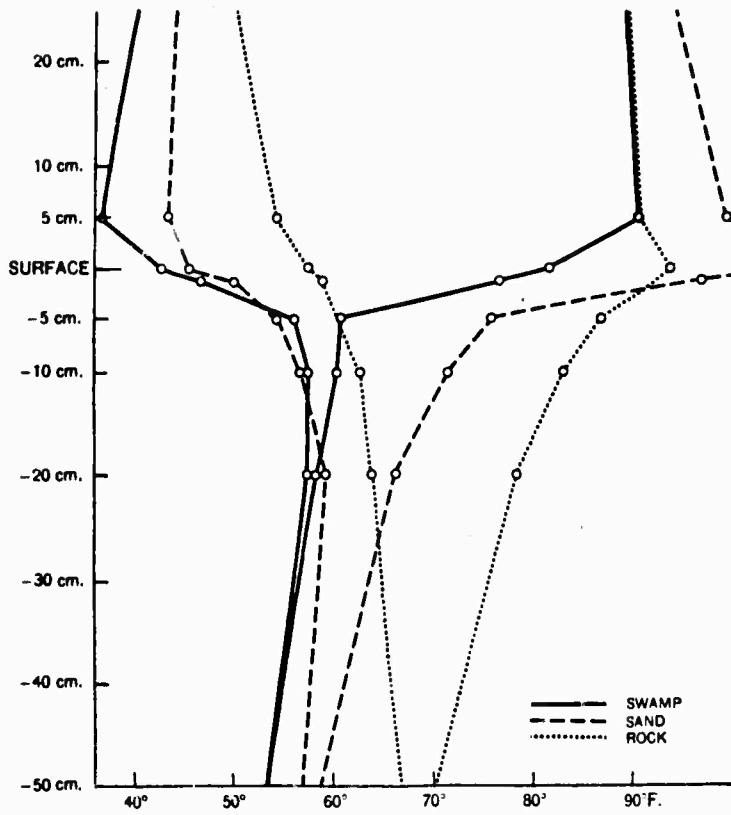
FIGURE 3: (Above) Tempera-
ture Profiles Showing Average
Maxima and Minima for Swampy,
Sandy and Rocky Soil in the
Arctic. (After Weedfall,
Ref. 12).
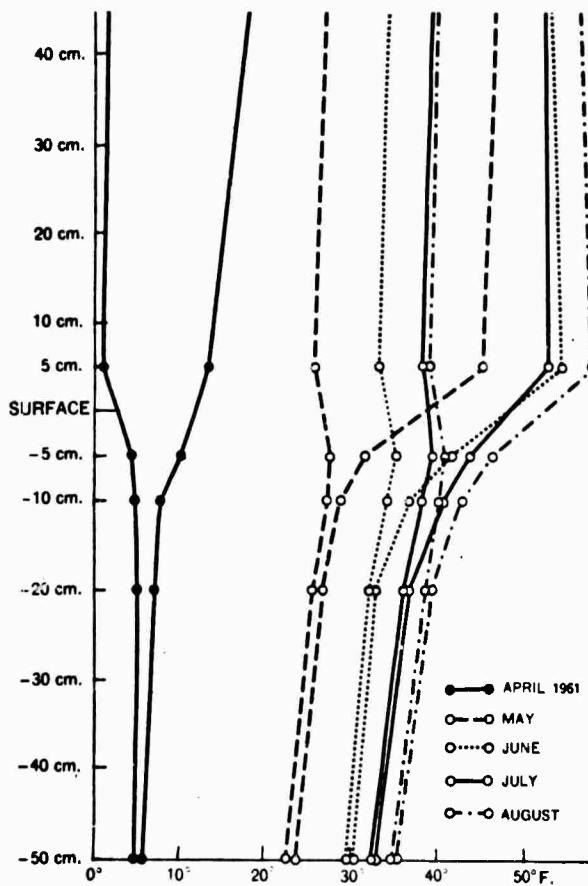
FIGURE 4: (At Left) Maximum
and Minimum Averages of 13
Stations in Ogotoruk Valley,
Alaska. (After Weedfall,
Ref. 12).
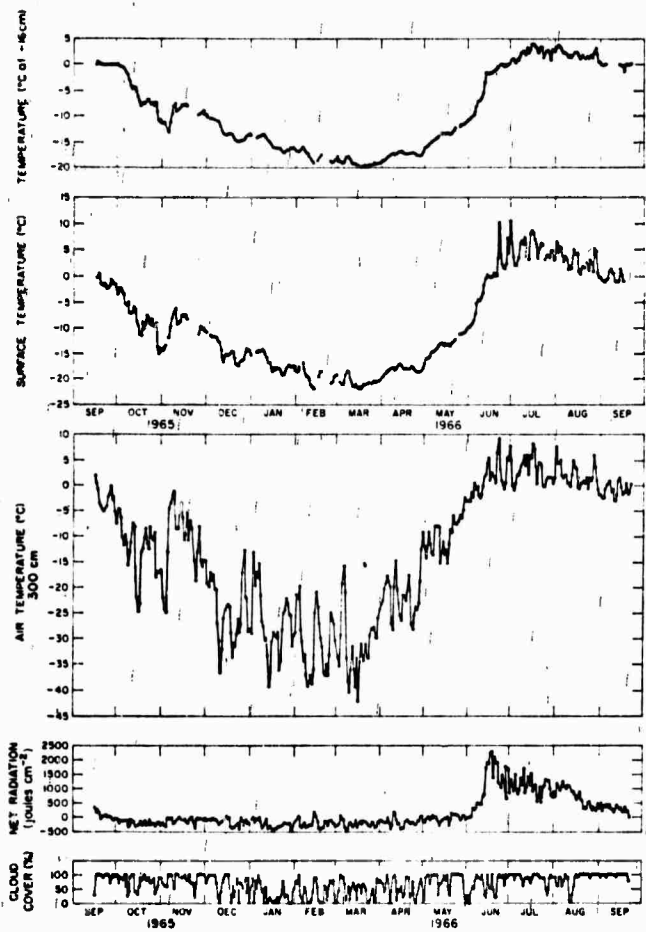
FIGURE 5: The Annual Course of Tundra Temperatures at the Surface and at 16 cm. Levels. (After Kelley and Weaver, Ref. 13).

Figure, a maximum thermal penetration depth of 2.5 m was extrapolated).
This suggests that ice anomalies, which from the Alyeska drill hole data
appear to be found at depths of 0.5-2.5 m, could be expected to influence
the temperature profile. It therefore appears that any anomaly of interest
in this work must be examined with respect to its response to the seasonal
increase in net insolation rather than a diurnal increase. A typical insola-
tion increase and its effect on the surface, air and sub-surface temperatures
is shown in Figure 5, based on studies conducted at Barrow, Alaska by Kelley
and Weaver [13].

Figure 6 shows the temperature-time response of a uniform media (frozen
ground in winter) and that of the same material that includes an ice lens.
Initially, after the relatively large solar energy input flux, the increase in
the ground temperature in both cases propagates downward at the same rate
as the ground thaws. At a time t* the temperature disturbance reaches the
depth corresponding to the top of the ice lens. For all subsequent times
the temperature profiles in the two cases will differ. The surface tempera-
ture of the uniform media would then rise above the temperature of the sur-
face over the ice lens. The time-dependent surface temperature difference
is represented in Figure 7. The time at which the temperature disturbance
first reaches the ice lens, t*, depends on the depth of the lens, as well as
the composition of the material above it. Preliminary calculations indicated
that t* would typically range from 38 days to 85 days, and the maximum sur-
face temperature difference would occur shortly after the onset of Fall. The
maximum surface temperature difference depends primarily on the convective
heat transfer rate at the surface as well as the depth of the ice lens and the
composition of the overlying material. The preliminary calculations indicated
that anomalies ranging from $4C^o$ to $0.4C^o$ could be expected. Temperature
differences of this magnitude would be readily sensed by the I-R scanning
system intended for this project.

1.5 Research Plan

Using the above theory as a guide, the below outlined program
was implemented:

1.5.1 Close examination was made of infrared imagery and Aero-
chrome Infrared photography taken by the U.S.G.S. along certain sections
of the pipeline route.

1.5.2 A Daedalus Enterprises, Inc Model DEI 110 airborne I-R
scanner was modified so that dual-channel, synchronous imagery within the
4.5-5.5 and 8-12 micron band was obtained. Appropriate mixing and processing
of these signals was expected to separate the emissivity function from the
surface temperature patterns being sought.

SOLAR RADIATION

SOLAR RADIATION

TEMPERATURE

MAX. SURFACE TEMP.
WITH ICE LENS BELOW

INCREASING TIME
AFTER ONSET OF
SOLAR RADIATION
INCREASE

SURFACE
MATERIAL

DEPTH

ICE
LENS

(0°C)
(32°F)

TEMPERATURE

MAX. SURFACE TEMP.
WITHOUT ICE LENS BELOW

INCREASING TIME
AFTER ONSET OF
SOLAR RADIATION
INCREASE

SURFACE
MATERIAL

DEPTH
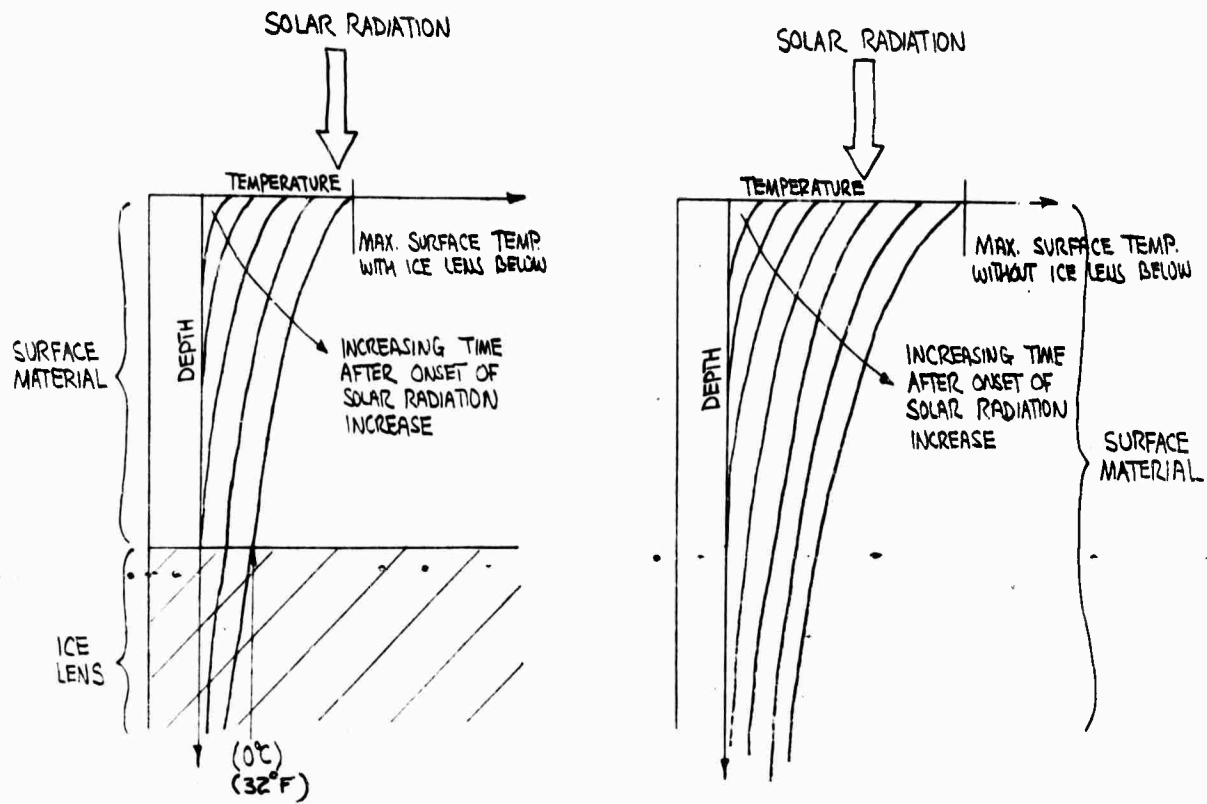
FIGURE 6: Temperature Profiles in Surface Material With and Without Ice Lens Present
at Various Times After the Onset of Springtime Solar Radiation Increase.

WITHOUT ICE LENS
BELOW SURFACE

WITH ICE LENS
BELOW SURFACE

t*, Time at Which Temperature
Disturbance Reaches Top
Surface of Ice Lens.

SURFACE TEMPERATURE

TIME AFTER ONSET OF SOLAR RADIATION INCREASE
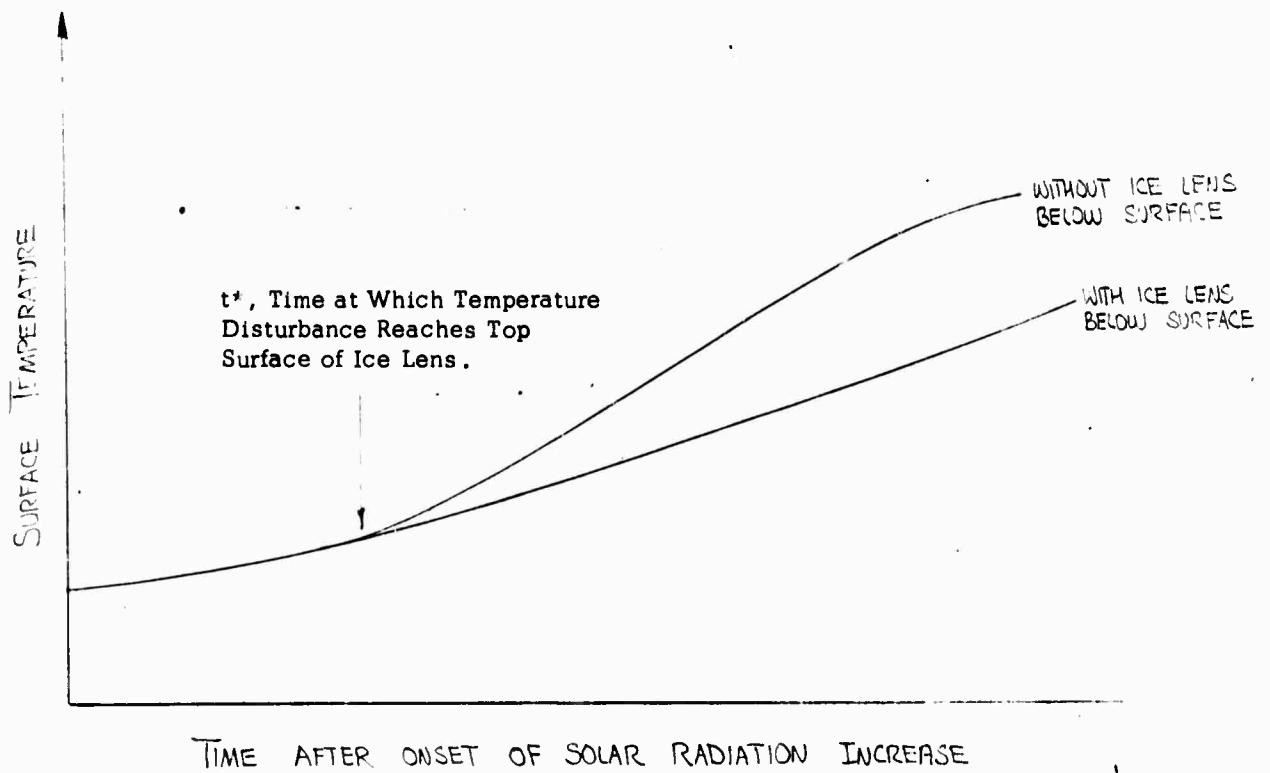
FIGURE 7: Surface Temperature as a Function of Time After onset of Springtime
Solar Radiation Increase.

- 10 -

1.5.3 <u>Site Location and surveying was conducted of chosen</u>
<u>Alaskan test sites for subsequent overflights with the modified scanner</u>.
The test sites were selected with the assistance of R & M Engineering &
Geological Consultants of Fairbanks, the company that conducted the orig-
inal boring survey. The sites ideally included both "textbook" examples
of ice lenses beneath a single, homogeneous surface layer with no plant
cover as well as the more common situations with more complicated geology
and plant cover.

1.5.4 <u>Mathematical thermal modelling studies were made of several</u>
<u>typical geologic sections under a variety of solar, surface temperature and</u>
<u>surface wind inputs</u>. Such a computer model has been developed at the
University of Michigan and was used in an attempt to determine the
magnitudes of the expected thermal anomalies under various ambient
conditions and for various typical surface compositions.

1.5.5 <u>Field Survey</u>. The chosen areas in Alaska, both along the
proposed pipeline route and at the Tundra Biome project near Barrow, were
surveyed so that both surface geology and vegetation maps could be correlated
with the airborne imagery of these sites. Surface weather observations and
surface temperature measurements were made at the time of overflight.

2. INSTRUMENTATION

Two major instrumentation systems were developed for the field phase of
this research: (a) an airborne I-R line scanner modified by the manufac-
turer (Daedalus Enterprises, Inc.) for the airborne phase of the operation.
Modification was carried out according to D&RTCo.'s specifications for
obtaining high resolution dual-channel thermal imagery. (b) A portable,
compact, signal conditioner/readout device was designed and fabricated
by D&RTCo. for use in the acquisition of thermal ground truth data.

2.1 The Dual-Channel Scanner

The major requirements for the line scanner were that it provide
<u>synchronous</u>, dual channel I-R imagery and be able to resolve temperature
differences of less than $0.3C^{O}$ with a spatial resolution of 3 milliradians
or less. Daedalus Enterprises, Inc., under subcontract to D&RTCo.,
modified their Quantitative Scanning Radiometer, Model DEI110, by inserting
a dichroic mirror in the path between the scanning mirror and the original
detector and adding a second detector. The incoming energy was thus
separated in such a manner that, by transmission through the mirror,
the 8-12 micron detector received more than 90% of the incident energy in
its wavelength interval, while by reflection, the 4-5 micron detector

received essentially all of the incident energy in its wavelength interval.

The scanner output is recorded on magnetic tape thus permitting the collection of the complete dynamic range of signals (including the two internal reference "black body" signals) for later playback and subsequent enhancement. The operating characteristics are listed in Table 1.

TABLE 1: Operating Characteristics of the Daedalus Enterprises, Inc. Dual-Channel Quantitative Scanning Radiometer System.

Operating Wavelengths	4.5-5.5 and 8-12 Microns
Aperture	5-inch
Focal Length	6-inch
Optical Aperture (effective)	f/2
Scan Rate	80 scans/second
Total Field of View	77° 20'
Instantaneous Field of View	2.5 Milliradians
Temperature Resolution	0.10°
V/H	0.2
Roll Correction	$\pm 5^{\circ}$
Reference Source	2 controllable thermal blackbodies
Reference Range	$-10^{\circ}C$ to $+40^{\circ}C$ with respect to scan-head heat sink
Sensor Indicator Range	$-10^{\circ}C$ to $+50^{\circ}C$

2.2 The Signal Conditioner/Readout Device

The signal conditioner/readout was designed specifically to display temperature variations as sensed by thermistor arrays. It not only had to meet the requirement for portability and small size, but have a low power consumption, and a non-ambiguous readout with resolution to four significant figures. With the above constraints, a Hewlett-Packard Digital Panel Meter, Model 3431A, factory assembled to operate within a range of 8.8 to 15.2 DCV, was chosen as the readout device. The meter has overload and under range indicators, variable sample rate, BCD output, annunciators, and hold and trigger capabilities along with a reliable LED display.

For obtaining surface and subsurface temperatures for correlation with the airborne data, a system with resolution and accuracy comparable to or better than that of the airborne system was required. Yellow Springs Instrument Co. (YSI) 700 Series Thermistor Probes and "Thermivolt" signal conditioner met these requirements. YSI fabricated, on special order, a quantity

of probes with leads 27 meters in length. These were to be used, along with standard lead length YSI probes, in various array configurations during field operations. The "Thermivolt" signal conditioner was modified to operate from a common power supply, a rechargable nickle-cadmium battery on loan to D&RTCo. from NASA-Goddard Space Flight Center.

The system (Figure 8) accepts up to twelve inputs, any one selectable for signal conditioning and subsequent readout by low contact resistance, push button, leaf switches. The type of signal conditioning, amplifier, gain, etc., is selected by a series of rocker switches. The system also contains a chopper stabilized operational amplifier for conditioning the output of an Eppley precision spectral pyranometer.

3. THERMAL MODELLING

It has become increasingly apparent that a qualitative interpretation of the processes leading to a particular thermal image is, at best, able to provide just a general understanding of the surface under investigation. Simplistic, qualitative.concepts, such as hot-spot detection, have only limited utility in describing natural processes, since much of the significant information of causative thermal relationships is too complex for an unsophisticated study to disclose. Full utilization of the potential of thermal-infrared remote sensing requires both qualitative and quantitative understanding of the interaction of the surface under study and the associated environment. The qualitative understanding is based on geological, botanical and topographical features, while the quantitative understanding can be obtained through the application of realistic theoretical modeling techniques in which each significant form of thermal interaction is described and the parametric effects of each factor can be investigated. Such a thermal model has been developed by the Willow Run Laboratories of the University of Michigan (U.of M). This model was modified in an attempt to verify the surface thermal anomalies previously estimated by a less-detailed analysis and discussed in the introduction.

Preliminary examination of the output of this model, which displays temperature of each layer as a function of time, indicated that, at the surface, the temperature anomalies being sought were significant. However, careful examination of the vertical temperature profiles generated by this model showed that they were sufficiently different from typical measured profiles to indicate that a realistic model has not yet been developed. It appears that the U.of M.model as presently written can not appropriately account for the energy requirements associated with the phase change of water during freezing and thawing. A discussion of the model used is contained in Appendix B.

- 13 -
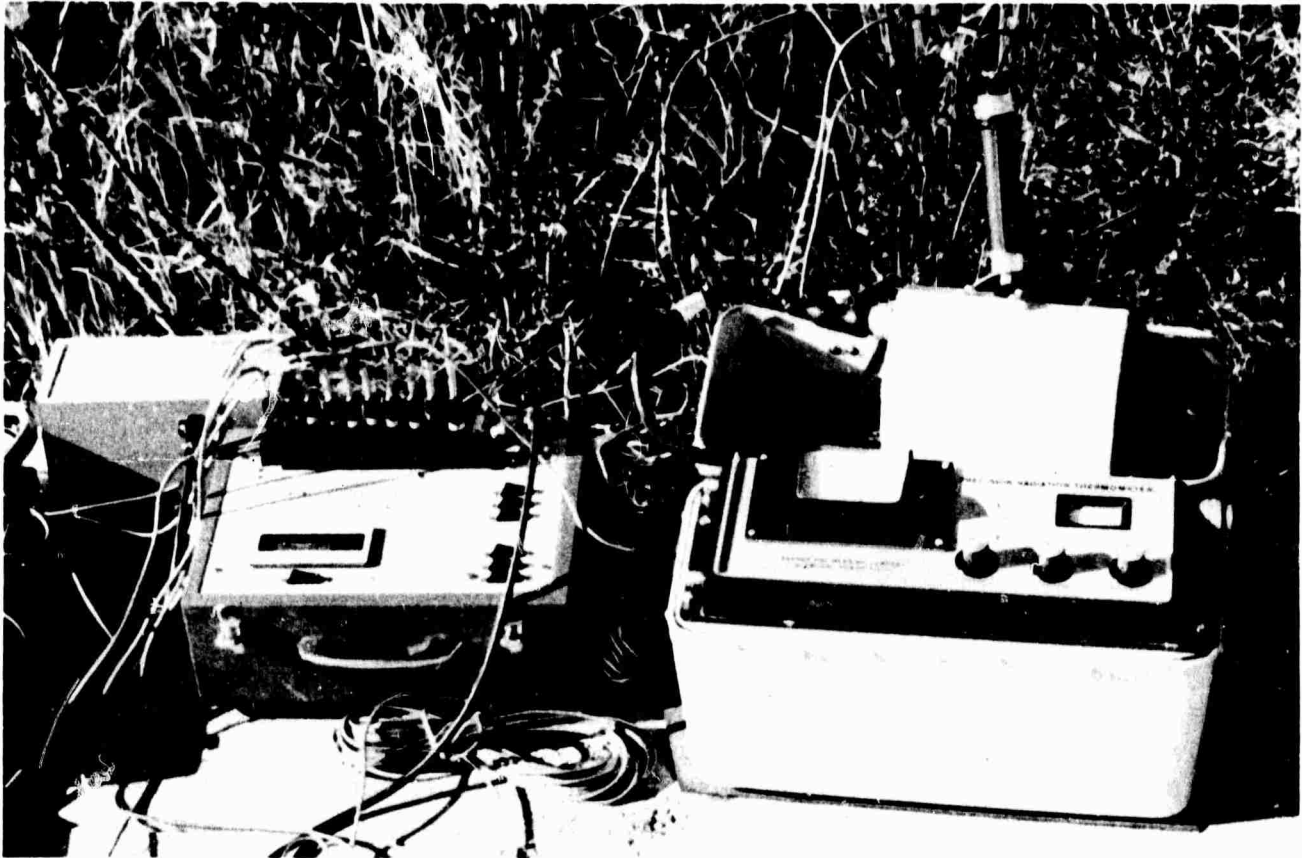
FIGURE 8: Pictured Above is the Signal Conditioner/Readout Device
(at left) Connected to the Thermistor Array, at the Shaw Creek Flats
Site. At Right is the Barnes PRT-5 Precision Radiation Thermometer,
Provided Courtesy of Daedalus Enterprises Inc.

4. FIELD PROGRAM

4.1 Preliminary Site Investigation

Four potential sites for the field program, in addition to the well-studied sites at Barrow, were chosen by the Principal Investigator with the assistance of R & M Engineering & Geological Consultants. R & M is the firm that conducted the borehole survey for Alyeska and thus has considerable knowledge of the near-surface geology along the pipeline route. The sites picked were selected since they have a large number of boreholes already in place, are "textbook" examples of uncomplicated near-surface geology with substantial quantities of ice in the permafrost, and for logistical convenience. The sites were as follows:

4.1.1 Sourdough North: there were 21 boreholes in a 1 by 3 km area at the point where the pipeline is presently planned to cross the Gulkana River. The site is 1.6 km northwest of Sourdough along the Richardson Highway. The site included a well-drained gravel outwash area, some lower flatlands with notable thermokarst features and some forested areas. Of the 21 boreholes in the area, four had significant ice at depths less than 3m.

4.1.2 Sourdough South: there were 48 boreholes in a 2 by 3 km area where the pipeline was originally expected to cross the Gulkana River, before the route was changed to Sourdough North. The site is 4.3 km south-southwest of Sourdough on the Richardson Highway. The area has gently rolling hills, is forested and is well drained. Of the 48 boreholes in the area, 10 had significant ice within 3 m of the surface. Both Sourdough Sites are approximately 30 km north of Gulkana (See Figure 9).

4.1.3 Shaw Creek Flats: this site, located at mile 281 on the Richardson Highway, has very little tree cover. The vegetation is primarily muskeg. At one point along the planned pipeline route, four boreholes were sunk within a radius of 10 m. This was done, according to the boring log, to investigate a freeze polygon. Of the four holes drilled, two had significant ice at less than 3 m from the surface and two had none. The Shaw Creek Flats Site is approximately 30 km northwest of Big Delta (See Figure 9).

4.1.4 Hess Creek: Along the proposed pipeline, extending 4 km south of the point at which it crosses Hess Creek, are 12 boreholes where massive ice varying from 10 m to 15 m thick has been found. The area is heavily wooded and very hilly. The site was included in the preliminary site selection study because such large thickness of essentially pure ice were encountered with no observable surface expression. The site is approximately 125 km northwest of Fairbanks.

- 15 -
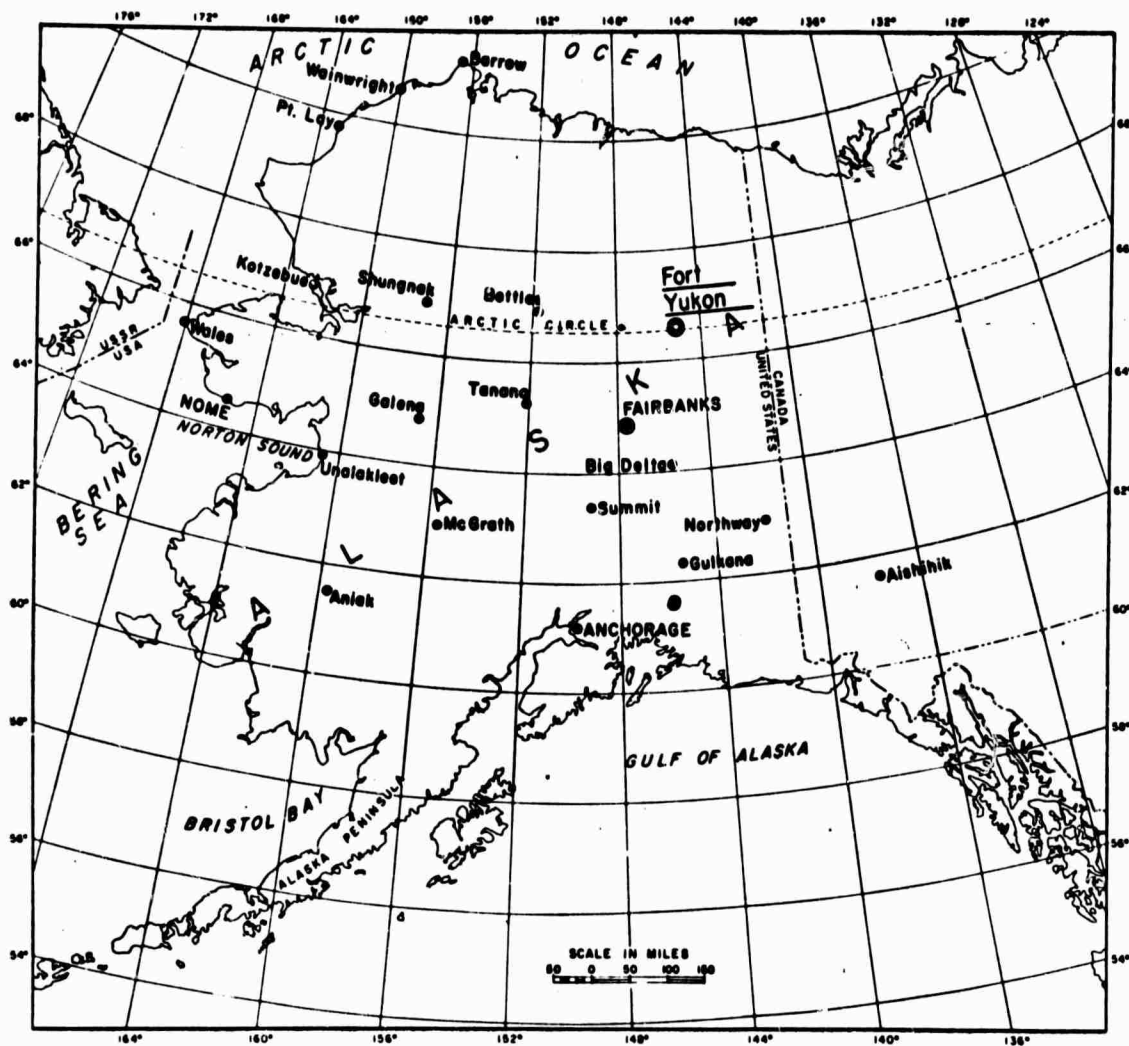
Figure 9: Map of Alaska
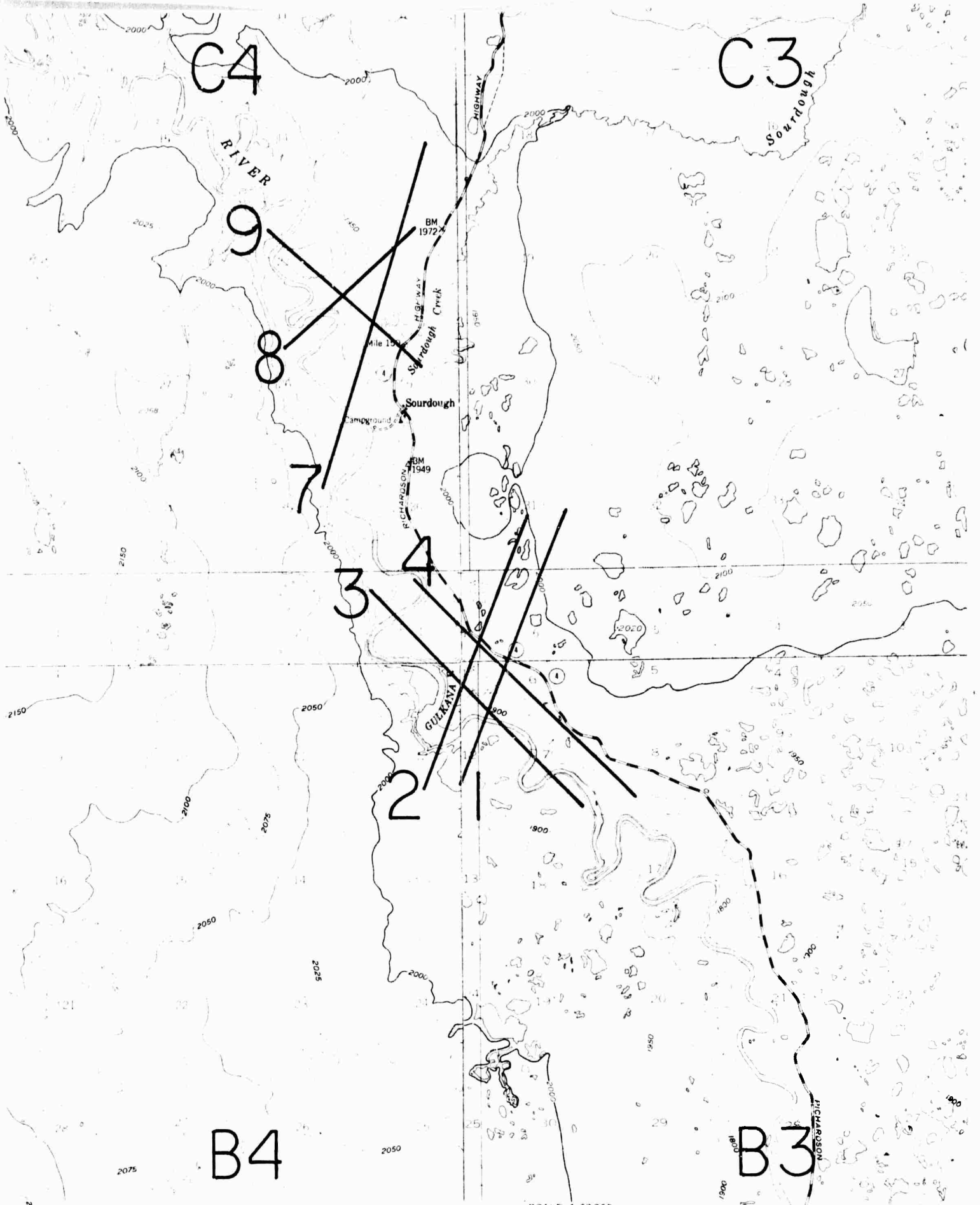
C4

C3

B4

B3

RIVER

Sourdough

Sourdough Creek

HIGHWAY

RICHARDSON Highway

BM 1972

Mile 15

Sourdough

Campground

BM 1949

GULKANA RIVER

RICHARDSON

9

8

7

4

3

2

SCALE 1 63360

CONTOUR INTERVAL 100 FEET
DOTTED LINES REPRESENT 50 FOOT CONTOURS
DATUM IS MEAN SEA LEVEL
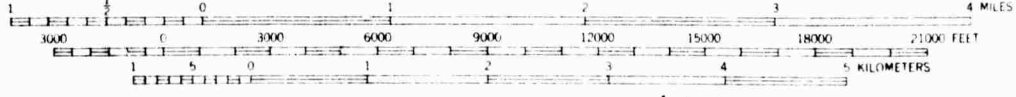
TRUE NORTH

MAGNETIC NORTH

APPROXIMATE MEAN
DECLINATION, 1950

16b

1   0   1   2   3   4 MILES
3000   0   3000   6000   9000   12000   15000   18000   21000 FEET
1   .5   0   1   2   3   4   5 KILOMETERS

FIGURE 10: The Flight Lines at the Sourdough Sites are Shown. (Gulkana Quadrangle). See Appendix C for Details.

16a

FIGURE 11: The Flight Lines at the Barrow Site are Shown (Barrow, Alaska). The Flight Lines Cover Several CRREL Sites (Lines 1,2,8), the IBP Tundra Biome Site (Lines 1,2) and the SEV Sites (Lines 5,6).

16c

ALASKA

BARROW

3

3 KM

7

8

16d
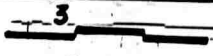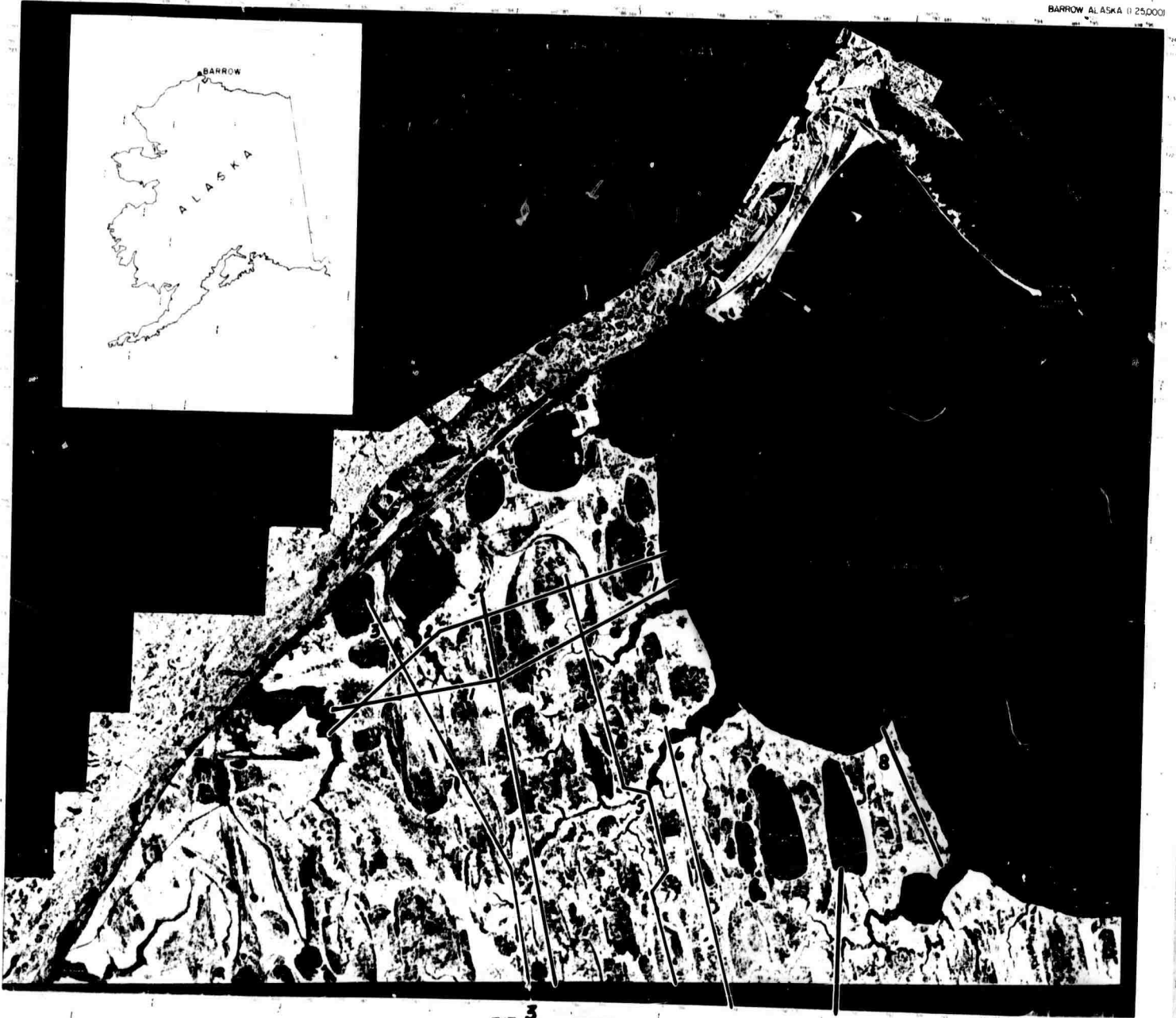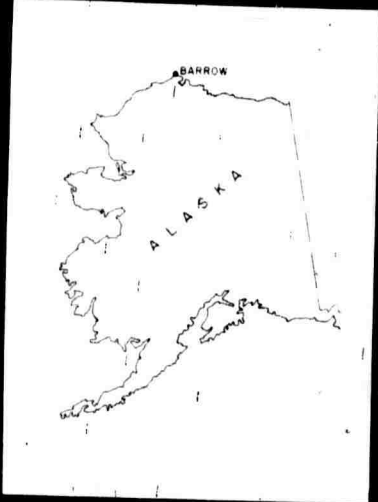
FIGURE 12: The Flight Lines at the Shaw Creek Flats Site are Shown
(Big Delta Quadrangle). The "X" Marks the Area Where the Major Portion
of the Field Work at this Site was Conducted. See Appendix C for Details

16e

B5

B4

Cabin

Keyston

CREEK FLATS

Shaw

Creek

CREEK

Caribou

3

35

T 7 S

Shaw

Shaw Creek

VABM
1123

1

T 8 S

RICHARDSON

2

1

RIVER

HIGHWAY

2

SHAW   CREEK   FLA

11

12

7

8

16

SHAW

14

13

18

17

17

925

23

24

19

20

22

23

TANANA

RICHARDSON

950

26

HIGHWAY

26

25

Timber

1000

35

36

RIVER

36

BM
999

5

1000

VABM

A5

A4

1125

16f
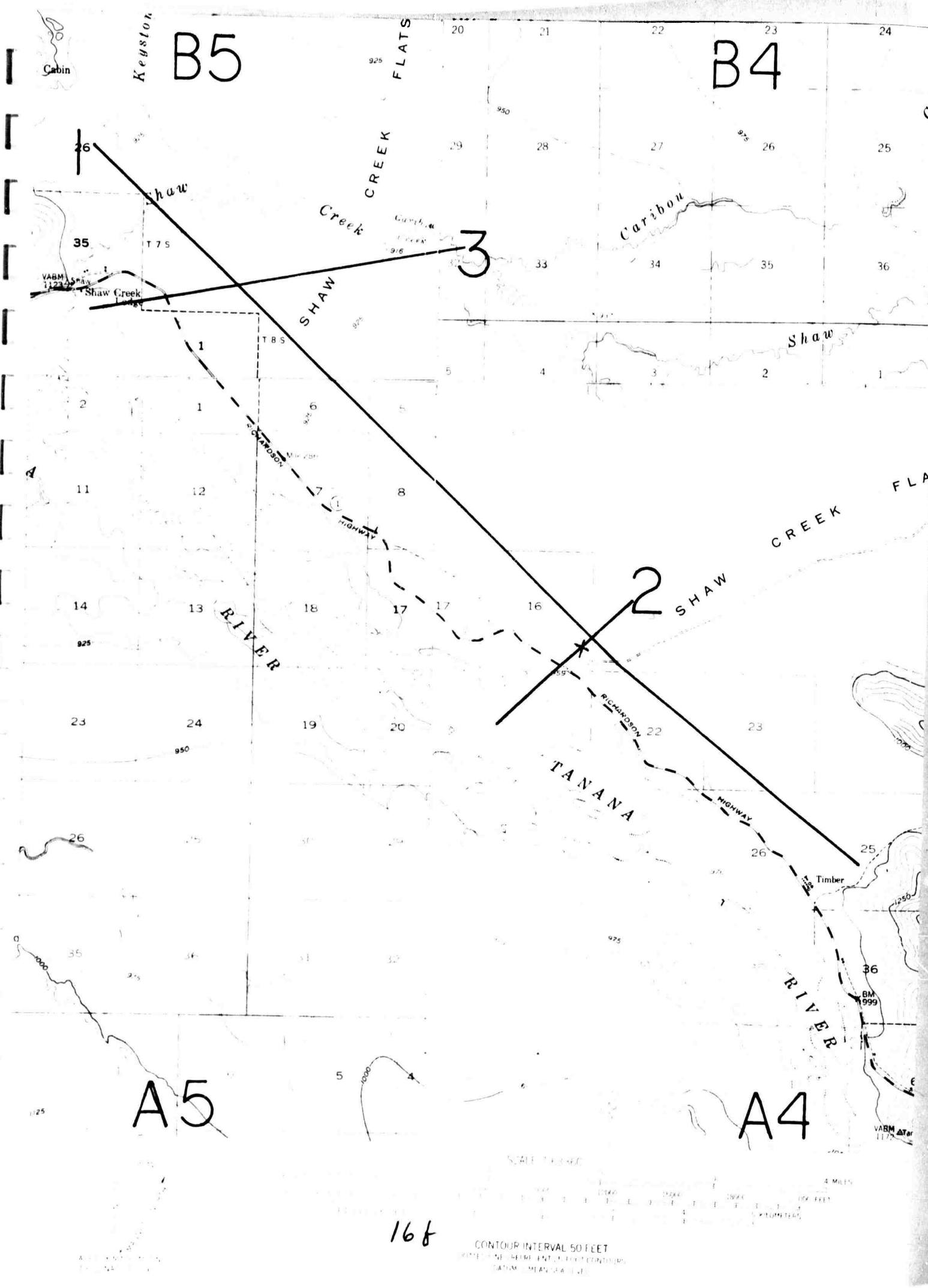
SCALE

4 MILES

CONTOUR INTERVAL 50 FEET

DATUM MEAN SEA LEVEL

4.2 Airborne Program

Figures 10, 11 and 12 show maps of the areas where airborne dual-channel I-R imagery was flown. The flight lines are drawn on the maps and are keyed for easy reference to the Flight Log (Appendix C).

4.3 Ground Program

The ground truth data gathering effort was almost entirely spent at the Shaw Creek Flats Site and consisted of the following measurements:

• Two distinct thermistor arrays were emplaced. The first array was established to measure temperature as a function of time of the surface vegetation and organic mat within a radius of 10 m. A few of the thermistors at one location of this array consistently indicated lower temperatures than would have been expected when compared with other thermistor measurements from another portion of the array, suggesting that the array which was randomly placed, may have been established across a thermal anomaly. Measurements at this array were taken every hour for a period of 3 days.

• The second array was "L" shaped and located so as to straddle the supposed anomaly. All thermistor elements were buried to a depth of 10 cm.

• A Barnes PRT-5 portable radiometer was used to determine both sky radiation at the times of overflight, and to collect ground surface radiation over the permafrost profile transects and thermistor arrays for correlation with these data, respectively.

• Surface weather observations were taken at each site at the times of overflight. The observations made were wet and dry bulb air temperatures and wind speed. Standard weather observations reported by the airfield closest to the site under study, and taken during the period of overflights, were also obtained.

• Selected transects were surveyed and permafrost probes were made at half-meter intervals. The probe, a calibrated aluminum rod with a point at one end, was pushed through the relatively soft, unfrozen ground or "active layer" until it stopped at the permanently frozen ground, which, at this location, varies between 0.2m and 1.5 m, beneath the surface. This depth of active layer, is, in late August when the measurements were made, close or equal to the depth to permafrost. The profiles so produced do vary considerably and certain peaks were believed to be associated with massive ice in the permafrost.

NOT REPRODUCIBLE

FIGURE 13: Oblique Aerial Photograph (Approximate
Altitude = 100m) of the Strangmoor Area of Shaw Creek
Flats Where Preliminary Studies were Conducted.
(Note the Hummocky Surface of the Terrain).
Tracked Vehicle Trails Made by the Drillers are
Clearly Seen. A Cluster of Three Boreholes was
Made at the Area Seen in the Center of the
Photograph.

18

4.4   Description of Shaw Creek Flats Environment--Taiga Biome-Type

In Delta (Illinoian) time, broad gravel plains extended northward
into the Shaw Creek Flats over which the braided Tanana River and assoc-
iated outwash streams meandered. In late Quaternary (Wisconsin) time,
the Donnelly Glaciation occurred in the area and some sand dune formation
developed at the southeast edge of the flats. Wind-blown silt (loess)
was abundant and deposited over the sand dunes and moraine. In post-
Wisconsin time additional loess was deposited over the dunes of Wisconsin
age resulting in the loess covering of 0.3 to 1.5 m presently found.

Old channels and meander scars similar to those described by
Johnson and Vogel,[15] are imprinted in the vegetation of Shaw Creek Flats.

Bog species dominate extensive areas of muskeg and tend to
segregate along a moisture gradient. On older flood plains no longer sub-
ject to flooding, changes in micro-topography occur (which either reflect
the original flood plain surface or differential peat deposition) that cause
a moisture gradient. In the strangmoor area of Shaw Creek Flats (Fig-
ure 13), abrupt hummocks or sinuous peaty ridges rise above the surrounding
bog and, as determined by R & M borehole data, are ice-cored or contain
ice-rich silt.

Much of the research was conducted in an area approximately 300
meters north of mile 281. At that location in May 1970, R & M drilled holes
TH 8-2, 8-3, 8-4 and 8-5 on the borders and within a "freeze polygon". The
positioning of these boreholes is shown in Figure 14a; Figure 14b shows the
subsurface section with ice inclusions as suggested by these data (Figure 14c).
It is believed that this type of near-surface geology exists throughout the area.

No polygonal structures were visible in existing (1:12000) aerial
photography of the areas east of Shaw Creek though some visible structures
occur in areas west of Shaw Creek. The U.S.G.S. has classified the
surficial geology of the Flats as perennially frozen silt, undifferentiated
and of Quaternary age (Figure 15). Although massive ice wedges are known
to be present in this type of silty soil overlying gravel, generally little to
no visible ice was found in the silt deposits and no visible ice was en-
countered in gravels by R & M boring crews[16].

The area of Shaw Creek Flats north of mile 285 on the Richardson
Highway is poorly drained and underlain by permafrost at shallow depths as
described by Péwé (1965)[17]. Along the southern boundary of the area are
extensive stands of larch (Larix laricina). The center of the Flats, which
Pewe describes as appearing to be a stabilized strangmoor, or string bog
(See Figure 13), is clearly evident in existing small scale photography.
The area does contain more vegetation than indicated by Péwé i.e., sedge
tussock, (Eriophorum sp) and sedges (Carex sp), as well as some "quaking

- 19 -
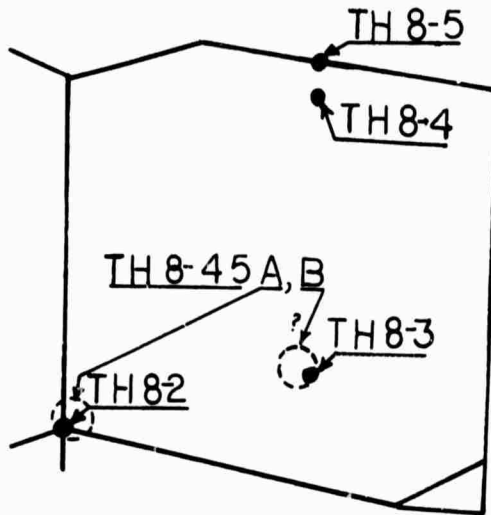
(a)   POLYGON As Reconstructed From R&M Logs of Test Borings.
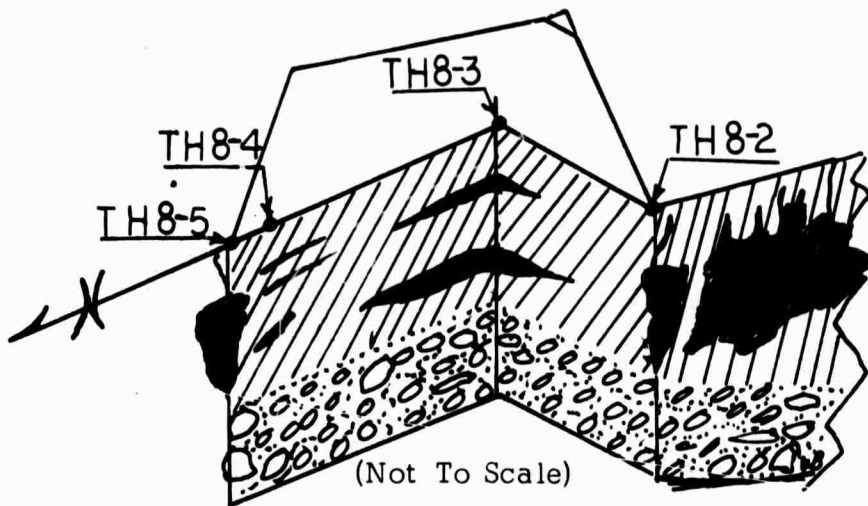
(b)   Section Of Subsurface Structure As Suggested By R&M Logs.

FIGURE 14: A Cluster of Boreholes was Sunk in 1970 by R & M Within
a Visible "Freeze Polygon". The Polygon was Reconstructed in (a) from
Field Notes of R & M Geologists. Examination of the Borehole Logs
Suggested the Near-Surface Geologic Section Sketched in (b). The Cores
are Shown in (c) Opposite. It is Seen that Significant Quantities of Ice
are Found at the Border of the Polygon. This Area is the Center of
the Shaw Creek Flats Site Surveyed by D&RT Co.

T.H. 8-2   8-42-8
S-19-70   All Samples SI

89 Occ. to Consid. Visible Ice 0'-3' $V_x + V_f$
1
   ORGANIC SILT
2 100 +
                                      3'
3 84
   Consid. Visible Ice 3'-8.75' ICE + ML
4 100 +
   ICE - TR. SILT
5 73
   Estimate 95% Visible Ice
6 100 +
                                      8.75'
7 100 +
   Occ. Visible Ice 8.75'-11' $V_x + V_f$
   SAND w/ TR GRAVEL
                                      11'

T.H. 8-3   8-42-8
S-18-70

SI 1 S6, 48.4%, 49.4 pcf, OL   0'
       ORGANIC SILT
SI 2 100 +, 255.6%, 17.6pcf   1'(APPROX.)
       Little Visible Ice 0'-6' $V_s + V_c$
SI 3 100 +, 63.7%, 45.7pcf
       SILT w/TRACE TO SOME SAND
SI 4 100 +, 118.0%, 33.1pcf, ML
       Some Vis Ice 6'-10' $V_x + V_f$
SI 5 100 +, 165.7%, 25.3 pcf
SI 6 100 +, 71.1%, 50.0 pcf
       Little Vis Ice 10'-12' $V_x + V_f$
SI 7 100 +, 42.5%, 63.3 pcf   10'
       SAND w/ TR. SILT
Se 8 100 +, 37.7%
       SANDY GRAVEL   11'
                                    12'

T.H. 8-4   8-42-8
S-19-70   All Samples SI

1 ORGANIC MATERIAL   0'
   100 +, 145.3%, 24.7pcf
   Some Visible Ice 0.5'-1' V_s 1'(APPROX.)
2 100 +, 164.1%, 23.5pcf, OL
   ICE - ORGANIC SILT w/ TR. SAND
3 Consid. Vis Ice 1'-4' ICE + OL
   Est 50% Vis. Ice
   100 +, 111.3%, 48.7pcf   4'
4 100 +, 177.5%, 25.1pcf, ML
   Some Visible Ice 4'-8' $V_x + V_f$
5 100 +, 72.4%, 53.9pcf
   SILT w/ TR. SAND   8'

T.H. 8-45A   8-42-8
6-28-70
                                    0'
   Little Visible Ice 0.5'-3.5' V_f
   ORGANIC SILT
                                    3.5'
   Consid. Visible Ice 3.5'-10' ICE+ML

   ICE - SILT
                                    10'
   Little Visible Ice 10'-27' V_f

   Scattered Boulders 20'-35'

   SANDY GRAVEL,
   NUMEROUS COBBLES
                                    35'

T.H. 8-45B   8-42-8
7-5-70
                                    0'

   SILT

                                    11'
   SANDY GRAVEL
                                    13'

T.H. 8-S   8-42-8
5-19-70
   Little Vis Ice 0'-3' V_f 0'
   ORGANIC SILT w/ TR. SAND
SI 1 100 +, 113.7%, 30.0 pcf, OL
                                    3'
SI 2 100 +, 1000% +
       ICE - TR ORGANIC SILT
SI 3 100 +, 1000% +
       Cons Vis Ice 3'-7.5' ICE + OL
SI 4 100 +, 1000%
       Estimate 90% Visible Ice
SI 5 100 +, 87.0%, 43.3 pcf, ML   7.5'
       SILT w/ TR. SAND
       Some Vis Ice 7.5'-10.5' V_f
Ss 6 100 +, 53.3%, 68.2 pcf   10'
       SANDY GRAVEL   10.5'

LEGEND:
ORGANIC MAT'L
SILT
CLAY
SAND
GRAVEL
VISIBLE ICE
BEDROCK

Boring No. ——— T.H.7-1   B-04-D ◄—— Location
Date Drilled ——— 12-25-70 ◄—— All Samples SI
Sampler Method   0'
Water Table ——— ▽   90, 15.4%, 123.6pcf, ML ◄— Blows/Ft
                              ◄— Water Content
Sample No. ———   ◄— Dry Density
                              ◄— Unified Class
Frozen Ground ———   5
                            ◄— Strata Change
                            ◄— Ice Description V_f
                            ◄— Drill Depth   7'

(c)

- 21 -

FIGURE 15: U. S. Geological Survey Open File Map of the Surface Geology Along the Proposed Pipeline Route at the Shaw Creek Flats Site (Big Delta Quadrangle.

- 22 -

bogs". Not only were dwarf birch (Betula glandulosa) present on ridges
in the center of the Flats, but also white spruce (Picea glauca), black
spruce (Picea mariana) and incidents of white birch (Betula papyrifera)
and willow (Salix sp.).

Of the two areas, the former appears to be somewhat higher in
elevation than much of the latter and therefore presents a better drained,
more solid substrate which is reflected by the vegetation found there.
See Appendix D.

Subsurface temperatures encountered were generally on the order of
$-7^{o}C$ to $0^{o}C$ with the majority of the readings being close to $0^{o}C$. Because
of this proximity to the phase boundary of water, the permafrost should be con-
sidered sensitive to changes in the thermal environment. According to
Alyeska reports[18]"...in the Shaw Creek Flats area ice wedges were found in
the silts that overlie the frozen gravels. Polygonal ground is present
throughout the flats. Localized massive ice was encountered in the low
rolling hills between Shaw Creek and the Salcha River. Some of this ice was
found in the lower and generally shaded parts of the valleys; however, there
were no good surface indicators for the presence of massive ice. The
majority of the ice in the fine grained soils falls in the category of well
bonded with no excessive ice. However, visible ice, in the form of
pore ice (visible crystals), veins and veinlets was common. Both vertical
and horizontal orientation of the veins occurs and generally the thickness
is on the order of 1/4 inch or less....

...the entire section between the Tanana and Salcha Rivers is generally
frozen with only a few exceptions. ...Approximately nine miles of the
proposed route crosses Shaw Creek Flats where ice wedges are present.
North of Shaw Creek and to the Salcha River, the low rolling hills have numer-
ous areas where massive ice is found...."

4.5 Discussion of Field Data Acquisition

The sites actually studied during the field phase of the research were
chosen from among the preliminary four sites primarily according to favor-
able logistic and weather conditions existing at the outset of the field program.
With the installation of the I-R scanner and camera in the aircraft completed
on 19 August 1971, the nearest sites with favorable weather were Sourdough
North and South. Seven missions were flown over both these sites, which
are only a few kilometers apart. Surface weather and sky radiation tempera-
ture measurements were made during several of the overflights. Between
20-22 August, two predawn missions were flown a day apart and four con-
secutive missions at approximately six-hour intervals were flown, all over
the same flight lines, at altitudes varying from 230 m to 1200m. Both
panchromatic and Aerochrome Infrared coverage were taken during daylight
hours.

On 22 August, the weather at Barrow, which had been bad for airborne operations for the previous week, had moderated. Since, typically, breaks in Barrow weather do not last long during this season, it was decided to fly there then and begin operations immediately. A day was lost returning to Anchorage for aircraft repairs, and then, on 23 August, the aircraft was flown to Barrow. Two missions were flown there before the weather once again began to deteriorate; these were flown over the same flight lines, between 0206 and 0309 hrs and 1724 and 1843 hrs on 24 August at altitudes of 300 m and 150 m respectively. Panchromatic photography was taken during the daylight mission. Since the imagery was flown over sites where significant ground truth studies were or are being conducted, i.e., several CRREL sites, the IBP Tundra Biome Site, the pipeline site and the SEV Test Track Site (See Figure 12), the D&RTCo. ground party did not conduct ground truth studies of its own at Barrow but continued working at the Sourdough and Shaw Creek Flats Sites.

During the period that the aircraft was at Barrow, the ground party began field investigations at the Shaw Creek Flats Site. The aircraft was then flown back to this site from Barrow and, based at the Big Delta Airfield, began missions on 26 August. Five missions were flown over the same flight lines at 2148-2250 hrs on 26 August and at 0432-0505 hrs, 1054-1224 hrs, 2131-2209 hrs on 27 August. Flights were made at altitudes of 230 m, 600 m and 1200 m. Aerochrome Infrared coverage was obtained during a daylight flight. (See Figure 11). The Flight Log for the above missions is included as Appendix C.

The typical ground program at each field site included the following activities designed to guarantee close ground control with the subsequent airborne survey:

• Locating several closely spaced boreholes showing both large as well as small quantities of ice in the permafrost.

• Marking these boreholes or nearby control points with large panels easily visible from the air.

• Conducting a general geological and botanical survey of the area and flagging significant areas and points.

• Probing at close intervals along surveyed lines for depth to permafrost.

• Emplacing thermistor arrays (21 elements) at and below the surface to obtain direct measurement of temperature patterns and their time variations (completed only at Shaw Creek Flats Site).

The ground party, in addition to making surface weather observations and sky radiance measurements concurrently with the overflights, also conducted the program described above. As work at this site progressed and field-processed imagery was made available it became clear that this site, of the four, was least complicated geologically and botanically, and the study of the feasibility of the concept being tested should be concentrated here. Accordingly, it was decided that the Hess Creek Site, although having the most massive subsurface ice, was too logistically difficult to reach to spend any further effort on during this present field season. Thus, the remainder of the field program was spent conducting ground truth studies at the Shaw Creek Flats Site. At the close of the field program, a helicopter was used for taking very low level (50m, 100m and 200m) color photography of the site. This provides a high resolution record of this site useful in pinpointing locations of thermistor arrays, marker panels, boreholes and permafrost transects

5. DISCUSSION OF DATA

5.1. Preliminary Analysis

Because of the decision to concentrate the major field effort at the Shaw Creek Flats area, the preliminary analysis of the airborne imagery and associated ground truth has also been focused on this area. The field party had the advantage of having essentially immediate access to the 8-12 micron imagery of the site owing to the utilization of a portable field imagery processing unit. This imagery was taken to the site and used to guide the investigators to features of interest for ground-image correlation. There were adequate geographic and man-made landmarks visible on the imagery to allow this. The most significant patterns observed on the pre-dawn imagery of this site were polygonal structures on the ground which were otherwise not visible from available aerial photography or from the ground. Since in normal engineering practice, when polygonal structure is clearly seen, and not hidden by vegetation as it was at the Shaw Creek Flats Site, it is usually assumed that ice wedges with their associated engineering problems, exist in the permafrost.

At this site, two distinct polygon types were observed on the pre-dawn imagery: (a) warm anomalies associated with narrow channels (approximately 15 cm) of standing water and (b) cool anomalies associates with similar sized water channels lying just below the surface in the organic mat. The difference in the polygonal anomalies is attributed to the different amounts of solar energy absorption by the water associated with each type of anomaly; the exposed water absorbs more energy during the daylight hours and due to its thermal inertia, continues to re-radiate this energy

- 25 -

into the pre-dawn hours while the subsurface water is both effectively
insulated from the solar radiation and, being associated with polygonal
ice,is, and remains, basically cooler than the surrounding terrain.

Guided by the imagery, an easily accessible "cool" polygon was
located and a series of permafrost probes were conducted along transects
spanning the indicated area. By definition, the top of the permafrost
layer is the equilibrium surface between frozen and unfrozen ground at its
deepest average penetration. At the time that these probes were made, the
depth of the active layer actually measured, was very close, if not equal to
the depth to permafrost. Since this depth measured is an isothermal surface,
significant variations of it, not attributable to visible surface causes, could
be attributed to ice within the permafrost. Thus when a significant change
in depth to permafrost was observed on transect profiles, and the depth
anomaly had a ridge-like form located at the area indicated by the imagery,
it was believed that massive ice could be found immediately adjacent to this
ridge. Although a drilling program was not planned during the recent field
phase of the research, a small portable power auger was briefly made avail-
able to the field party and the ridge anomaly was drilled to a depth of 1 m.
In spite of considerable melting of the cores during the course of this drill-
ing, significant veins of ice were found at the 50 cm. and 100 cm. levels.
From their orientation, it appeared that this ice was either horizontal segrega-
tions or part of a feeder network leading to deeper massive ice, similar to
that found within 100 m of this site at Alyeska Test Hole 8-45A. (Figure 16).
Since within a radius of 10 m of 8-45A, three other holes were sunk and of
these, one more had significant ice while two others did not, (Figure 14),
it is believed that had other borings been made during the course of the
present research, away from the flanks of the above-mentioned permafrost
anomaly, no ice would have been found there either.

5.2 Continuing Data Analysis

The above discussion has been based on cursory examination of the
I-R imagery taken at the Shaw Creek Flats Site. In the interval between the
return from the field and the preparation of this report, little time has been
available for the detailed study of all the ground truth data collected at that
site for correlation with the imagery, and essentially no examination has been
made of data obtained at the other sites. It is intended to continue this
correlation with the greatest emphasis being placed on the Shaw Creek Flats site.

With the completion by Daedalus Enterprises, Inc. of the special-
ized playback equipment needed to electronically produce ratio, product and
difference signals between the two channels synchronously scanned, it has
been possible to begin intensive study of the value of dual-channel imagery.
It appears clear at this point, however, that significant value accrues to an
imagery display which presents a mapping of two simultaneously related
parameters over that produced by one. As seen in Figures 17a-d, the ratio

imagery does appear to map areas of equal emissivity essentially independent of temperature effects and, when compared to the single channel imagery, and especially when compared with the product imagery of the same area, effects due to temperature anomalies are outlined. The imagery has been color-enhanced to outline differences in the mapped values when either of the single channel imagery types is compared with the ratio or product signals. Figure 17e shows Aerochrome Infrared photography of most of the area covered by this imagery and Figure 18 is a Stereo-pair of the area.

Since it is possible to get two different surfaces whose emissivity ratios are similar, as in the case of Figure 19, the comparison of ratio imagery with difference imagery of the same area points out the emissivity differences.

In the course of analyzing these data at the Daedalus facilities, their personnel employed contemporary image enhancing techniques. However, for distinguishing polygons, these various edge enhancement techniques (which produce imagery analogous to the first derivative maps familiar to exploration geophysicists) were less successful than the comparison of the ratio and product imagery under investigation by D&RTCo. and described above.

It appears clear from the above discussion that the potential of this imagery processing tool has just begun to be realized, especially in relation to the arctic engineering problem to which it is being applied, and considerable further analysis is required. A significant portion of the continuing work will be devoted toward this end.

6. POTENTIAL ENGINEERING SIGNIFICANCE OF PROGRAM

During the course of the field work in Alaska, contractor engineers as well as engineers at the University of Alaska who were aware of this project, pointed out continually the advantages of knowing locations and depths to permafrost in areas of discontinuous permafrost, and locations of ice wedges, lenses etc. in permafrost wherever found, prior to embarking on construction projects in these areas. If further research shows that, particularly in areas of discontinuous permafrost, polygonal patterns not otherwise seen by means of conventional airborne techniques can now be delineated, then engineers planning projects in these areas can be forewarned of the likelihood of encountering significant amounts of near-surface ice.

N

active layer

permafrost

0'

N   E   S   W   N

10'

20'
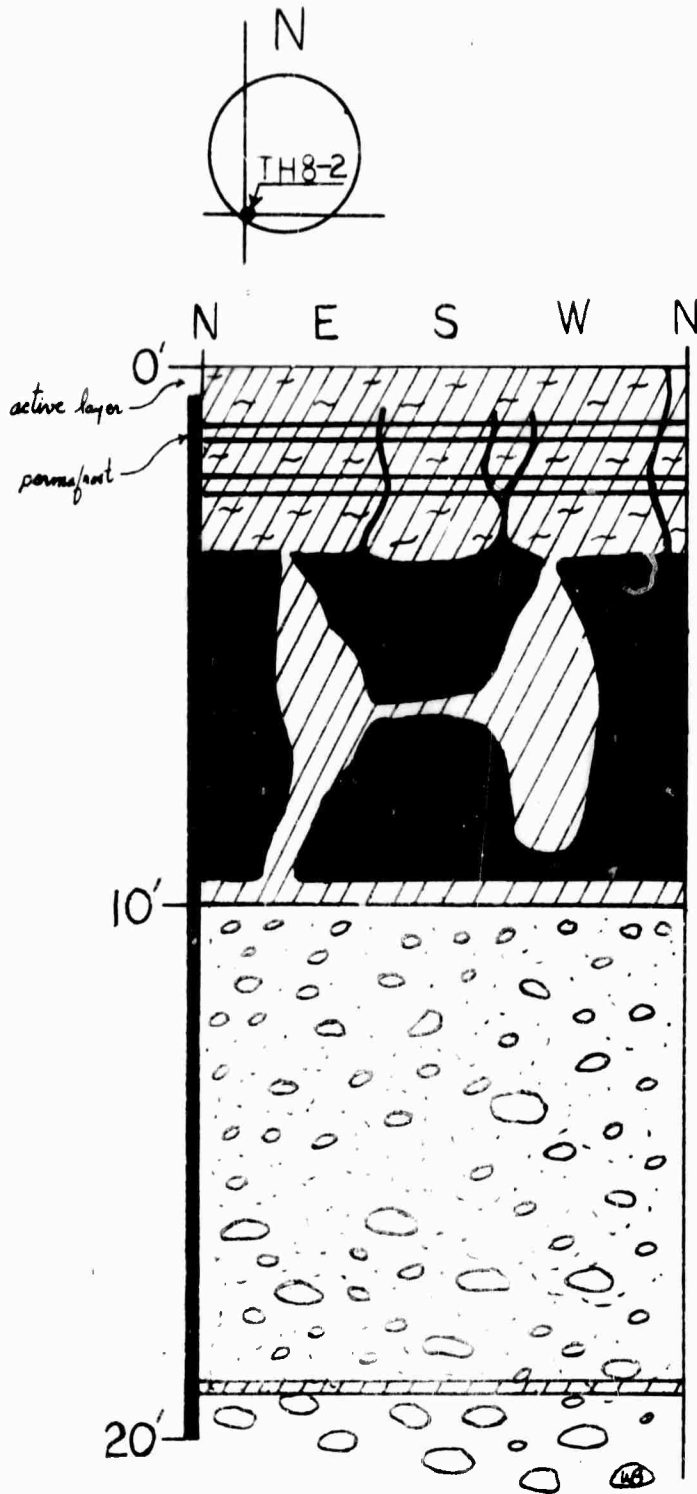
" Dark brown coarse organic silt
w/ice feeders (2"-3") and
horizontal segregation (1/2"-2 1/2")
of clear ice. Feeders are cloudy
w/distinctive structure parallel
to walls of feeders.

ICE-WEDGE ICE
Vert oriented x+1 structure w/air
bubbles. Negligible silt in massive
ice. Trace of feeders (2-3 inch)
can be seen, in massive ice of
wedges, to extend almost to bottom
of ice--do not penetrate into gravel
below.
Silt inclusions are dark to light brown,
w/some blue-gray, coarse silt. Some
organics. No ice segregations noted
w/in silt.

Fine to coarse sand, gravel w/
numerous cobbles. Avg. size 2-3
in. Sand matrix appears to be fine
to medium & well sorted. Ice occurs
as "cement" only--no seggregations
noted

Gray 2-3" silt.

Cobbles w/boulders as well as sand
and medium to coarse gravel."

/// Silt   ~~ Organics   Sand & Gravel   ■ Ice

FIGURE 16: A Large Diameter Auger Hole (Bucket Auger) was Made at
One Corner of the Polygon Illustrated in Figure 14(A). A Geologist
Lowered into the Borehole Made a Drawing and Notes, Part of Which
are Reproduced in the Figure. This Figure Illustrates the Large Quantity
of Ice Found Associated with Polygonal Structures at Shaw Creek Flats.

FIGURE 17 (a-d at Right; e, Below): Compared in This Figure Are Color-Enhanced Sections of The Shaw Creek Flats Imagery Taken at 0450 Hrs. on 28 August 1971 From an Altitude of 230 m. (Flight Line 2). (a) and (b) are Standard Color-Enhanced 4.5-5.5 and 8-12 Micron Imagery, Respectively, Obtained With a Quantitative Scanner. (c) and (d) are the Color-Enhanced Ratio and Product Imagery, Respectively, Produced by D&RTCo. for this Study. For the Purpose of This Comparison, Open Water, Because its Emissivity is Essentially Constant Across the Two Bands, Was Used as a Datum, i.e., The Signal Levels Over the Water for Both the (a) and (b) Outputs Were Made Equal. It is Clear From Examination of (c) That the Ratio Signal Does Reduce Substantially the Effect of Purely Thermal Anomalies as Can be Seen in the Large Expanse of Magenta Associated With Areas of Essentially Similar Emissivities. When This is Compared with Either (a) or (b) Imagery, or Especially with the Product Imagery (d), Anomalies Due Primarily to Thermal Differences are Revealed. Partial Polygonal Structures, for example, Are Obvious in the Product Imagery Whereas on the Aerochrome Infrared Photography (e) They Are Not. The Strip of Three Photographs Was Taken of the Same Area from the Same Altitude on 27 August 1971 at 1200 Hrs. (Flight Line 2). (Scale 1:5000)

- 30 -

(a)

(b)

(c)

(d)

- 31 -

Preceding page blank
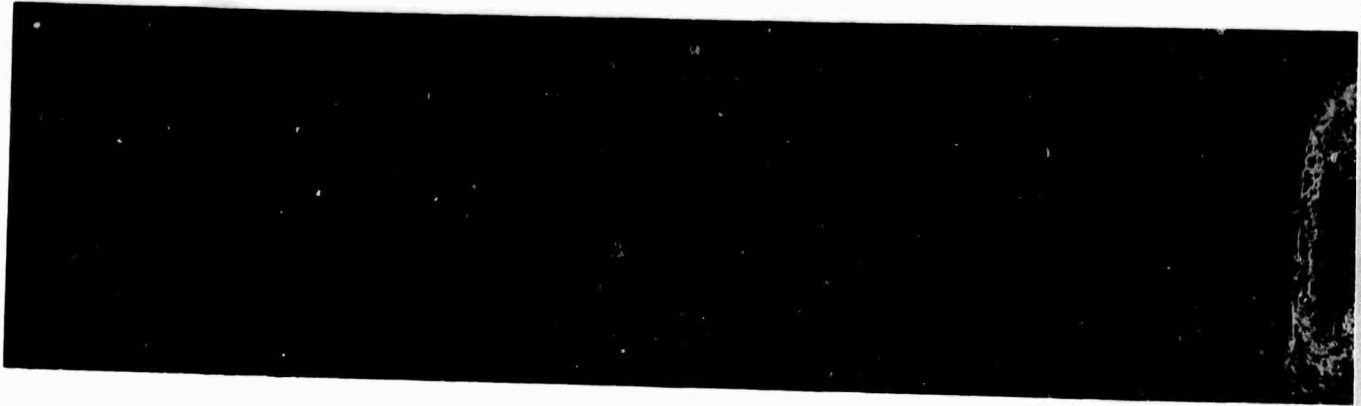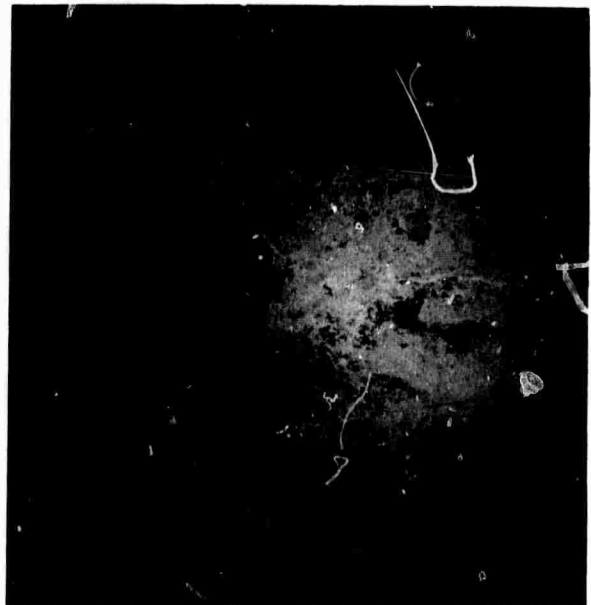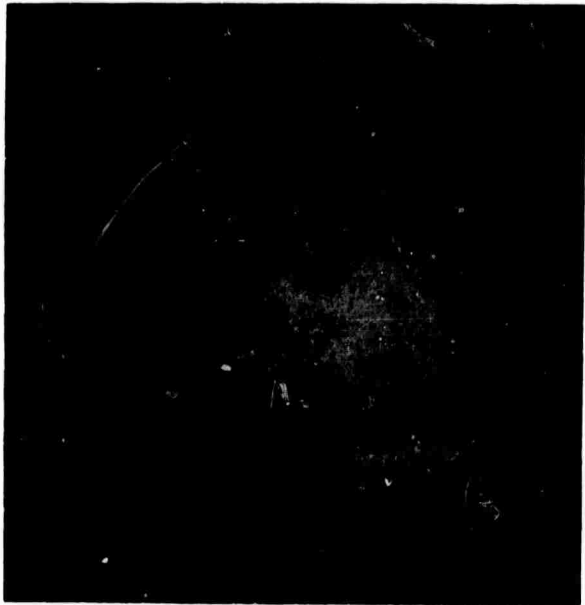
FIGURE 18: An Aerochrome Infrared Stereo-Pair of the Shaw Creek Flats
Area Taken From an Altitude of 1200m on 27 August 1971 at 1200 hrs.
(Scale 1:10,500)

Preceding page blank
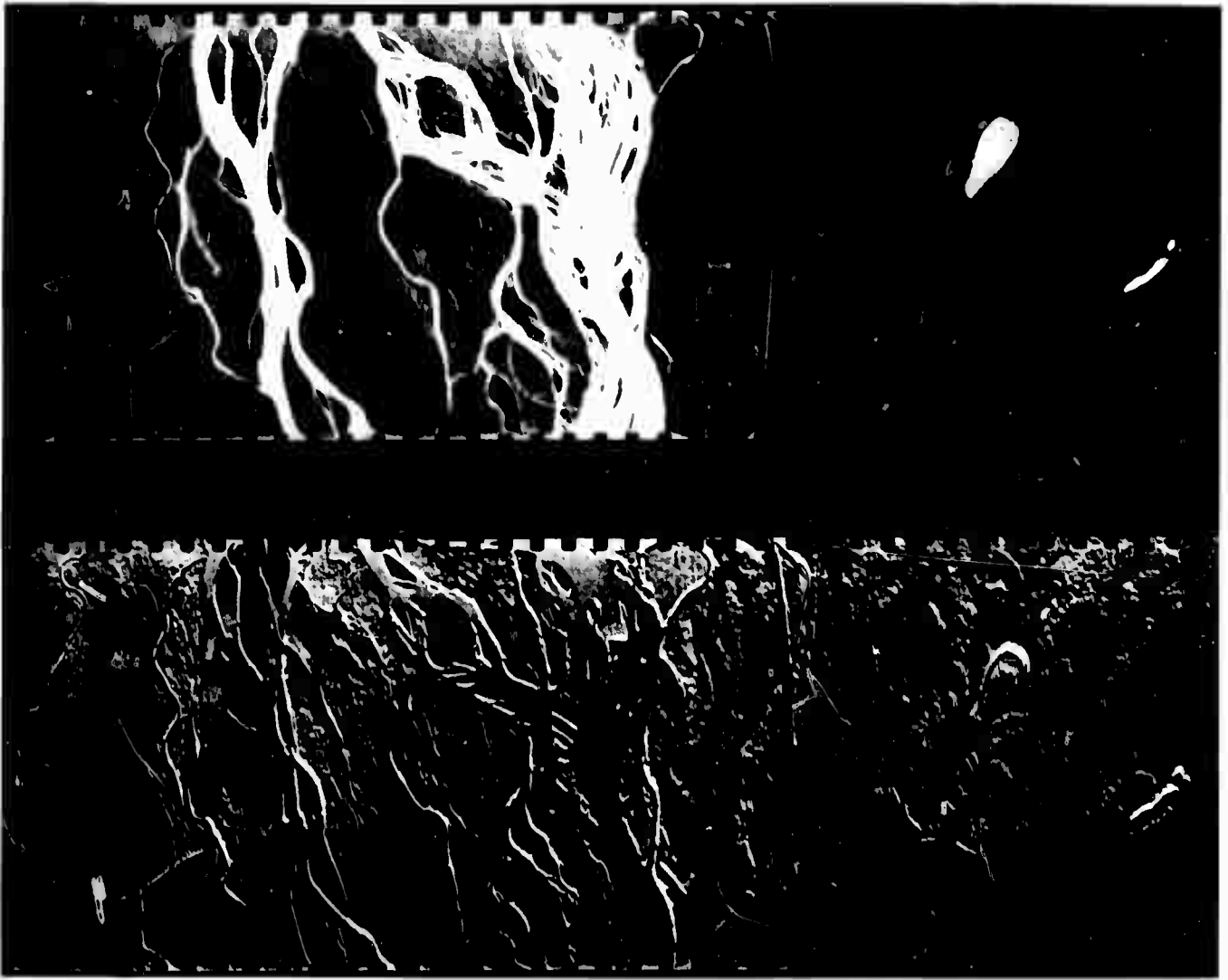
Figure 19: Ratio Imagery (Top) Shows a Relatively Constant Signal Value
For The Islands Seen in The Tanana River (River is Light Area). In Reality
These Islands Have Both Bare Gravel And Vegetation Visible. The
Difference Imagery (Bottom) Delineates These Areas And Eliminates The
Ambiguity. The Imagery Was Taken at 0424 Hrs on 28 August 1971 From
an Altitude of 1200 m.

7. REFERENCES

(1) Drew, J. V. and Tedrow, J.C.F., Arctic Soil Classification and Patterned Ground, _Arctic_, June 1962.

(2) Lewis, C.R., Icing Mound on Sadlerochit River, Alaska, _Arctic_, June 1962.

(3) Burns, J.J., Pingos in the Yukon-Kuskokwim Delta, Alaska: Their Plant Succession and Use by Mink, _Arctic_, Sept. 1964.

(4) Hussey, K. M. and Michelson, R. W., Tundra Relief Features Near Point Barrow, Alaska, _Arctic_, June 1966.

(5) Soil Maps and Soil Borings Data, from Valdez to Prudhoe Bay, R & M Engineering & Geological Consultants, Fairbanks, Alaska, for Alyeska Pipeline Service Co., Nov. 1969.

(6) Horvath, R. and Lowe, D. S., Multispectral Survey in the Alaskan Arctic, _Proc. 5th Symposium on Remote Sensing of Environment_, Univ. of Michigan, April 1968.

(7) Vincent, R. K., Horvath, R., Thomson, F. and Work, E. A., Remote Sensing Data-Analysis Projects Associated with the NASA Earth Resources Spectral Information System, I-R & Optics Lab., Willow Run Labs, Univ. of Michigan, Rpt. 3165-26-T NASA Contract NAS-9-9784, April, 1971.

(8) Myers, V. I., Thermal Infrared Imagery Interpretation as Influenced by the Environment _IEEE 2nd Int'l Geoscience Electronics Symp._ April 1970.

(9) Van Lopik, J., Infrared Mapping: Basic Technology and Geoscience Applications, _GeoScience News_, Jan-Feb 1968.

(10) Kondratyev, K. Ya., Problems of Infrared Atmospheric Spectroscopy Related to the Satellite Determination of Temperature of Underlying Surface, _Fiz Atmosfery i Okeana_, V. 5, No. 6, 1969, p. 616-630.

(11) Buettner, K.J.K. and Kern, C.D., The Determination of Infrared Emissivities of Terrestrial Surfaces, _J. Geophys Res._, March 15, 1965.

(12) Weedfall, R.O., Variation of Soil Temperatures in Ogotoruk Valley, Alaska, Arctic, Sept. 1963.

(13) Kelley, J. J. Jr. and Weaver, D.F., Physical Processes at the Surface of the Arctic Tundra, Arctic, Dec. 1969.

(14) Kersten, Miles S. Thermal Properties of Soils, Bull. No. 28, Univ. of Minn., Inst. of Technology, Eng. Exp. Sta., Vol. L11, #21, June 1, 1949.

(15) Johnson, Philip L. and Vogel, Theodore C., Vegetation of the Yukon Flats Region, Alaska, Res. Rpt. 209, U.S.A. Cold Regions Research & Engineering Laboratory, Hanover, N. H., Nov. 1966.

(16) Alyeska Pipeline Service Co., Soil Investigations, Hogan Hill to Little Salcha River, Alaska, by R & M Engineering & Geological Consultants, pp. B41-B44, Dec. 1970.

(17) Péwé , Troy L., Int'l Assoc. for Quaternary Research, VIIth Congress Guidebook for Field Conf. F, Central & S. Central Alaska, Nebr. Acad. Scis., 1965.

(18) Alyeska Pipeline Service Co., Foreword, Soil Investigations, Hogan Hill to Little Salcha River, Alaska, by R & M Engineering & Geological Consultants, Dec. 1970.

8. GLOSSARY

BCD	Binary coded decimal, a format used in data collection and processing.
DCV	Direct current, volts.
Delta (Illinoian) Time	Mid-Pleistocene epoch.
Dichroic Mirror	A mirror which transmits one wavelength band and reflects a second band.
Edge Enhancement	Process of signal filtering and phase modification which sharply delineates boundaries.
Freeze Polygon	A polygonal structure outlined by frozen melt water during winter periods when there is little vegetation cover.
Insolation	Solar radiation received over a given area.
LED	Light emitting diode--a rugged, high visibility, solid state light source used as indicators and in alphanumeric displays.
Organic Mat	A layer of undecayed organic matter such as moss, leaves, etc., prevalent in cold regions.
Polygonal ground	In this case, due to active, inactive, or fossil ice wedges, a patterning of the surface in the form of various, usually irregular, polygons.
Product Imagery	Imagery produced by electronic analog multiplication of the analog signal of one I-R band by the analog signal of the other I-R band.
Quaking Bogs	A phenomenon in plant succession where a vegetation mat covers a body of water and which quakes when walked upon.

<u>Glossary</u> (Continued)

Quaternary (Wisconsin) Time   Late Pleistocene epoch.

Ratio Imagery   Imagery produced by electronic analog division of the analog signal of one I-R band by the analog signal of the other I-R band.

Thermokarst features   Term used to describe "Karst" or sinkhole and mound phenomena occurring in permafrost areas--due to melting of subsurface ice structures and caused by disturbance of thermal regime.

APPENDIX A

Excerpts from the Daedalus Enterprises, Inc. Model DEI 110
Operating Handbook.
Pages 18 and 19 of this excerpt
have been excluded by the authors.

A 1

This section discusses the basic concepts of airborne line scan systems. The quantitative scanner described in the subsequent sections is a special version of a line scanner from which quantitative thermal information can be derived.

2.1. SCANNING GEOMETRY

Figure 1 is a diagram of a simple scanning optical system. Radiation from the terrain, either emitted or reflected solar energy, is reflected by the scanning mirror to the primary mirror which focuses this radiation into the image plane. A detector element is positioned on the image plane and is usually centered on the optical axis. The detector transduces the radiation into an electrical signal. Several types and configurations of detectors are available for use in line scanners; usually either a photovoltaic or photoconductive quantum detector is selected because of their inherent high sensitivity and fast response. For this discussion, we will assume a single element circular detector of diameter (d) inches.

The instantaneous field of view (IFV) is the basic information element in the line scanning system. It is defined as:

$$IFV = \frac{d}{FL} \tag{1}$$

where   d = linear dimension of detector element

FL = focal length of primary mirror.

A 2

DETECTOR

"N" SIDED SCANNING MIRROR

ROTATION RATE
ω

DETECTOR FIELD OF VIEW
∝

PARABOLIC MIRROR

FOV

H

θ

LINE OF FLIGHT

C

Wg

β
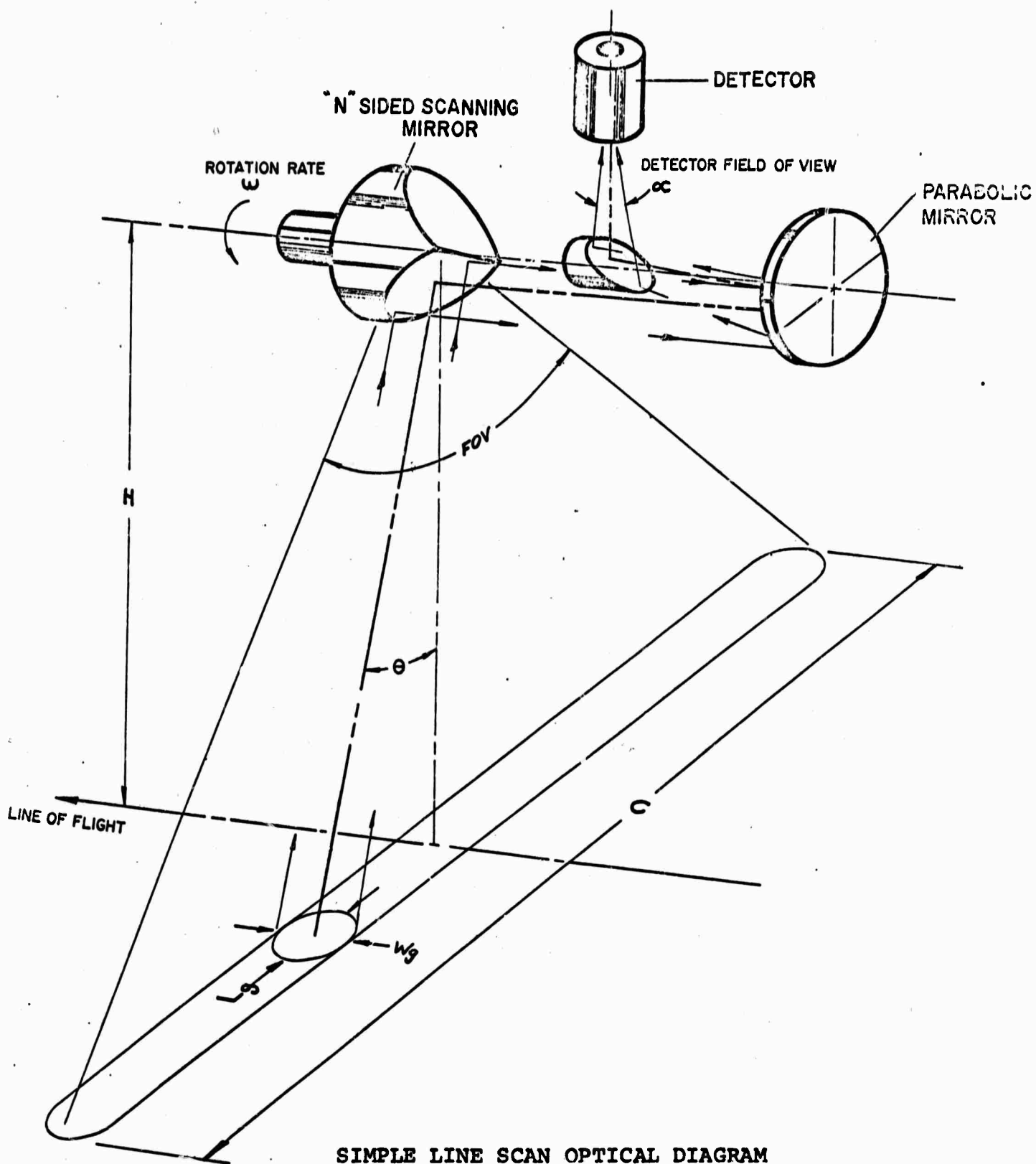
SIMPLE LINE SCAN OPTICAL DIAGRAM
FIGURE 1

A 3

The dimensions are radians. IFV is commonly labeled α.

Considering the static optical condition of figure 1, IFV relates to ground spot size as follows:

$$W_g = \alpha S \tag{2}$$

$$L_g = \alpha S \sec \theta \tag{3}$$

where θ = look angle with respect to true vertical

$S = H \sec \theta$

H = altitude above terrain.

In the dynamic optical condition, the total ground coverage swath width is calculated from the operating altitude, total scan angle (FOV), and IFV.

Referring again to figure 1,

$$C = 2 \left[H \tan \left(\frac{FOV}{2} \right) + \frac{\alpha}{2} H \sec^2 \left(\frac{FOV}{2} \right) \right] \tag{4}$$

For all practical considerations, this is reduced to:

$$C = 2 \left[H \tan \left(\frac{FOV}{2} \right) \right] \tag{5}$$

To aid in visualizing the foregoing discussion, it may be helpful to consider the scanner as a projection lens with finite conjugates which is projecting an image of the detector element onto a flat earth.

Two additional parameters critical to airborne line scanning systems are V/H and $(V/H)_{max}$. V/H (velocity to height ratio) is

a quantity relating specific aircraft operating parameters to final film format. The units are radians/sec. V is aircraft velocity in ft/sec and H is aircraft terrain clearance altitude in feet. $(V/H)_{max}$ is a boundary specification related to the scanning system which specifies the combination of maximum speed and minimum altitude at which continuous ground coverage can be maintained by a given scanning system

$$(V/H)_{max} = \alpha \text{ scan rate} \qquad (6)$$

with the dimensions in radians/sec.

It will be noted that the concept of α in this formula is slightly different than α = IFV = Radians. If this value is put in (6) along with a scan rate in scans/sec., the resultant units are radian scans/sec. There is no contradiction if a concept of a dynamic α is understood. In this concept, α is considered to be the angular width of the scan line and α now has units of radians/scan. Using this in (6) now gives the proper units.

The scan rate of the simple optical system is defined as:

$$\text{Scan Rate} = \frac{\omega}{2\pi} \cdot N \qquad (7)$$

where ω = angular velocity in radians/sec.

N = number of faces on scanning mirror.

The selection of ω and N is a design problem involving mechanics, optics, and electronics and is beyond the scope of this discussion.

It can be seen by restating the formula that

$$V_{max}(\text{ft/sec}) = H(\text{ft}) \; \alpha(\text{rads/scan}) \times S(\text{scans/sec}) \qquad (8)$$

A 5

and that with a fixed value of α and S, H must increase as V increases or for each V there is a minimum H.

2.2. ANALOG SIGNAL GENERATION

The thermal image which is the final output of the airborne line scanning system is built up from a series of data lines generated by the rotation of the scanning mirror and the forward movement of the aircraft. This action causes the detector to receive a continuously changing level of radiation as its field of view is directed toward different areas on the ground. The detector element then transduces this energy level into a voltage analog whose amplitude is proportional to the energy level. Looking again at the static optical system, the detector element is receiving radiation from an area of the terrain within the IFV. The detector element integrates the various energy levels within this area and outputs a voltage proportional to the integrated value of energy. If the scanning mirror is moved, a different area of terrain is within α and a different voltage level is output from the detector. Looking at the dynamic scanner the energy level on the detector element is constantly changing as α is swept through the FOV. The resulting electrical signal from the detector is amplitude variant with time.

The quantities of spatial resolution, thermal resolution, electronic bandwidth, and detector response time are all related to the generation of the analog voltage signal, and are all inter-related in a complex manner. It is beyond the scope of this discussion to treat this in detail. The contribution of each will be

A 6

superficially treated and only some very general expressions will
be developed.

Spatial resolution of a scanning system is generally specified
as α. This is true for bar targets of angular width 2α/line pair
and whose energy difference is equal to the thermal resolution
capability. Actually, a modulation transfer function (MTF) curve
would show signal modulation between 1 line pair = 2α to 1 line
pair = α, at which point there is no modulation. The amount of
usable signal in this region is a function of the target contrast
and the system temperature sensitivity, providing the detector time
constant or the system electronic bandwidth are not limiting factors.

The required system frequency response is a function of α and
ω as they are defined in section 2.1. Assuming the bar chart target
with 1 line pair (1 cycle) = 2α, then

$$FREQ = \frac{\omega}{2\alpha} .$$

This gives sine wave response and assumes detector response time is
infinitely small. To extend the sine wave response to 0 modulation
on the MTF curve

$$FREQ = \frac{\omega}{\alpha} .$$

To approach square wave response, a factor of 1 to 3 is used as a
multiplier. In special cases, this factor may be a function of the
detector time constant; but for fast detectors, 3 is usually used.
Therefore,

$$FREQ = \frac{3\omega}{\alpha} .$$

A 7

2.3. DATA RECORDING

Several techniques of data processing and recording are utilized with airborne line scanner data, but film printout is the most common and is the subject of the following discussion.

The two techniques of film recording most commonly associated with line scanning systems are the glow modulator tube with coupled optics, and the intensity modulated CRT. The end results of both systems are essentially identical, but there are some advantages in both techniques.

The glow modulator printer is the simpler of the two systems to implement. In this system a glow modulator tube is driven by the scanner video signal such that its brightness is proportional to the amplitude of the video signal. An image of the glow tube is focused on the film as a very small spot (typically a few thousandths of an inch in diameter) by a microscope objective lens. This lens is spun by a shaft in synchronism with the scanning mirror such that the glow tube image is swept across the film which is moving proportional to the aircraft V/H. Although the synchronization between the glow tube optics and the scanning mirror can be accomplished with a synchro loop, it is usually accomplished by using a common shaft. This reduces the scanner and recording system to a single unit, and achieves perfect synchronization between data collection and data recording.

In the CRT recording systems, synchronization pulses must be generated by the scanning system to synchronize the CRT sweep with the scanning mirror. These signals along with the scanner video signal are fed to the CRT recording system. The synchronization

A 8

signals trigger a sweep waveform generated by the CRT system which moves the CRT beam on a single line across the CRT face at an angular rate equal to the angular rate of the scanning mirror. This line is swept repetitively for each scan. As the beam is moving across the CRT, its brightness is modulated by the video signal to be proportional to the video signal amplitude. A camera is placed in front of the CRT which images the line transverse to a strip of film being moved proportional to the aircraft V/H.

Several important options are available with this type of recording. By recording the scanner output signals on magnetic tape, a time delay can be introduced between collection and recording. This also gives multiple access to the original data for applying a variety of special processing techniques. A second option is the capability for removing the distortions in the data printout which result from scanning a flat earth at a constant angular rate and then recording the data with a linear sweep waveform. If the CRT beam is swept with a tangent function waveform which is generated from values of the tangent from - FOV/2 to + FOV/2, and the beam brightness is modulated by the derivative of this function, the scan distortions are removed and the density across the film is held constant.

2.4. THE CALIBRATED SCANNER

The typical airborne infrared line scanning system generates data which indicates relative power differences between objects scanned. It is true that the experienced observer can look at the thermal map produced by the average system and say that point A has greater apparent temperature than point B. However, the temperature

A 9

of a given area or the relationship of two temperatures in the same area can only be estimated. To be able to actually make apparent temperature measurements, a system for relating the input energy to output voltage must be devised.

To achieve this situation several initial conditions must be met. First, the video electronics must have DC response. Secondly, all radiation received by the detector must come from the scanning mirror and hence from the area of interest. Finally, the complete electronic chain from detector through final recording must be drift stabilized such that the system responsivity, V/W, (volts output/watts input) is constant. If these conditions are met, the system output can be related to the input.

The output video signal of a quantized scanner bears not only a constant relationship, but also a known relationship to input energy such that the data can be readily converted to energy units and then to apparent blackbody temperature. One approach to achieving this is to calibrate the responsivity of a scanner that meets the above conditions in the laboratory against blackbody standards. Although this approach is feasible, it is not very practical. The vagaries of electronic circuits and infrared detectors make it extremely difficult if not impossible to achieve the stated conditions.

The only practical approach to the quantitative scanner provides two energy reference sources within the scanner optical system so that the unknown radiation collected by the scanner is continuously compared against these reference sources.

The operating sequence and signal flow within the quantitative scanner is as follows. Initially, the operator selects a temperature

A 10

range of interest and adjusts the temperatures of the two refer-
ence sources so that one is near the lower end and one near the
upper end of the temperature range being investigated. These
sources are positioned in the optical system so that they are within
the scanner field of view, one being imaged before and one after
the scan across the terrain. The gain of the video electronics
is adjusted so that the signal difference between the signals of
the two sources is some pre-established ΔV, typically 3-4 volts.
Since the electronics have been designed to be extremely stable in
gain, this ΔV is maintained constant.

To compensate for electronic and detector drift in the quanti-
tative scanner, a reference level feedback is used as follows.
During the scan across each reference source, the signal levels are
sampled and held in separate circuits. After one complete scan,
both source signal levels are stored. These levels are averaged
and this average is inverted and fedback to the first video ampli-
fier stage. Within this stage a zero DC level is established for
the video at the signal level equal to the average of the reference
source signal. This now establishes the reference source signals
at $- \Delta V/2$ and $+ \Delta V/2$, and further establishes that any signal in
the video equal to these levels is the result of the same energy
level on the detector. This continuous feedback also nulls any
signal voltage level drift; and since the sample is updated each
scan, a very rapid drift compensation response is achieved.
Setting the gain of the system with respect to the two reference
sources establishes $\Delta V/\Delta W$. From this dV/dW can be readily esta-
blished with the system responsivity curve.

The accuracy of measurements made by the quantitative scanner of radiation at the scanner aperture is a function of the accuracy with which the temperatures of the reference sources can be determined, as well as their emissivity and uniformity.

A rough estimate of effects of temperature uniformity and emissivity of the reference source can be obtained from the equation for total radiated energy:

$$W = \varepsilon \delta T^4 \qquad (9)$$

where W = total energy

   ε = emissivity

   δ = Stefan-Boltzman constant

   T = absolute temperature.

Assuming small incremental changes in energy and temperature, from W_o to $W_o + \Delta W$ and from T_o to $T_o + \Delta T$, respectively, the ratio of the two equations is:

$$\frac{W_o + \Delta W}{W_o} = \frac{\varepsilon \delta}{\varepsilon \delta} \cdot \frac{(T_o + \Delta T)^4}{T_o^4}$$

If $\Delta T/T_o$ is small, then $(1 + \Delta T/T_o)^4 \simeq 1 + 4(\Delta T/T_o)$ and

$$1 + \left(\frac{\Delta W}{W_o}\right) \simeq 1 + 4\left(\frac{\Delta T}{T_o}\right)$$

or

$$\Delta T \simeq \left(\frac{T_o}{4}\right)\left(\frac{\Delta W}{W_o}\right) \qquad (10)$$

A 12.

Equation (10) indicates that 1% change in total energy at 300°K represents 0.75°C change in temperature. Similarly, a 1% change in emissivity yields the same magnitude of apparent temperature change. This error magnitude changes linearly with temperature and also varies slightly depending upon the system spectral response, but it represents a satisfactory first approximation.

If temperature of the reference surface is non-uniform, the total emitted energy differs from what it would be with a uniform surface. If 10% of the reference surface is 1°C above nominal and 10% is 1°C below nominal, the energy change is only about 10^{-4} watts which represent less than 0.01°C temperature error.

Due to the self calibration feature of the quantitative scanner, changes in optical efficiency or detector sensitivity other than changes in the responsivity appear as a neutral density filter and are compensated for by the initial gain adjustment. Within certain limitations the effects of some types of electronic instability are self calibrated and can be compensated for with elaborate procedures.

2.5. TEMPERATURE INTERPOLATION

With a reference source voltage output at each end of a quantitative scanner temperature range, it is natural to use a linear interpolation to relate other scanner output voltages to other temperatures within this range. For example, if a -2V DC and +2V DC correspond to 0°C and 40°C reference source temperatures, it is tempting to assume 0V DC represents a 20°C apparent temperature. Such an assumption is, of course, in error since the quantitative

A 13

scanner measures energy within a limited spectral region whereas the total emitted energy is proportional to T^4. The magnitude of the error in a linear interpolation depends somewhat upon the temperature of interest, but it depends to a greater degree upon the temperature range of the interpolation and on the spectral region of the measurements.

Figure 2 shows radiated energy vs. temperature for blackbody reference sources in the 3-5 μm and 8-14 μm regions. These curves assume uniform 100% detector response over the particular wavelength region and no response outside the region. Source emissivity is 1.0 and the detector voltage responsivity is assumed to be linear. A linear interpolation between two temperatures is equivalent to drawing a straight line between those two temperatures on figure 2 as shown. The maximum error occurs about midway between the two temperatures and is such that a linear voltage (energy) to temperature interpolation always results in an interpolated temperature lower than the actual temperature which would produce that energy level.

Figure 3 shows the errors for linear interpolation plotted vs. temperature range for the 3-5 μm region as determined graphically from figure 2. Errors for the 8-14 μm range are too small to be determined from figure 2, but they should be around 20-30% of those for 3-5 μm.
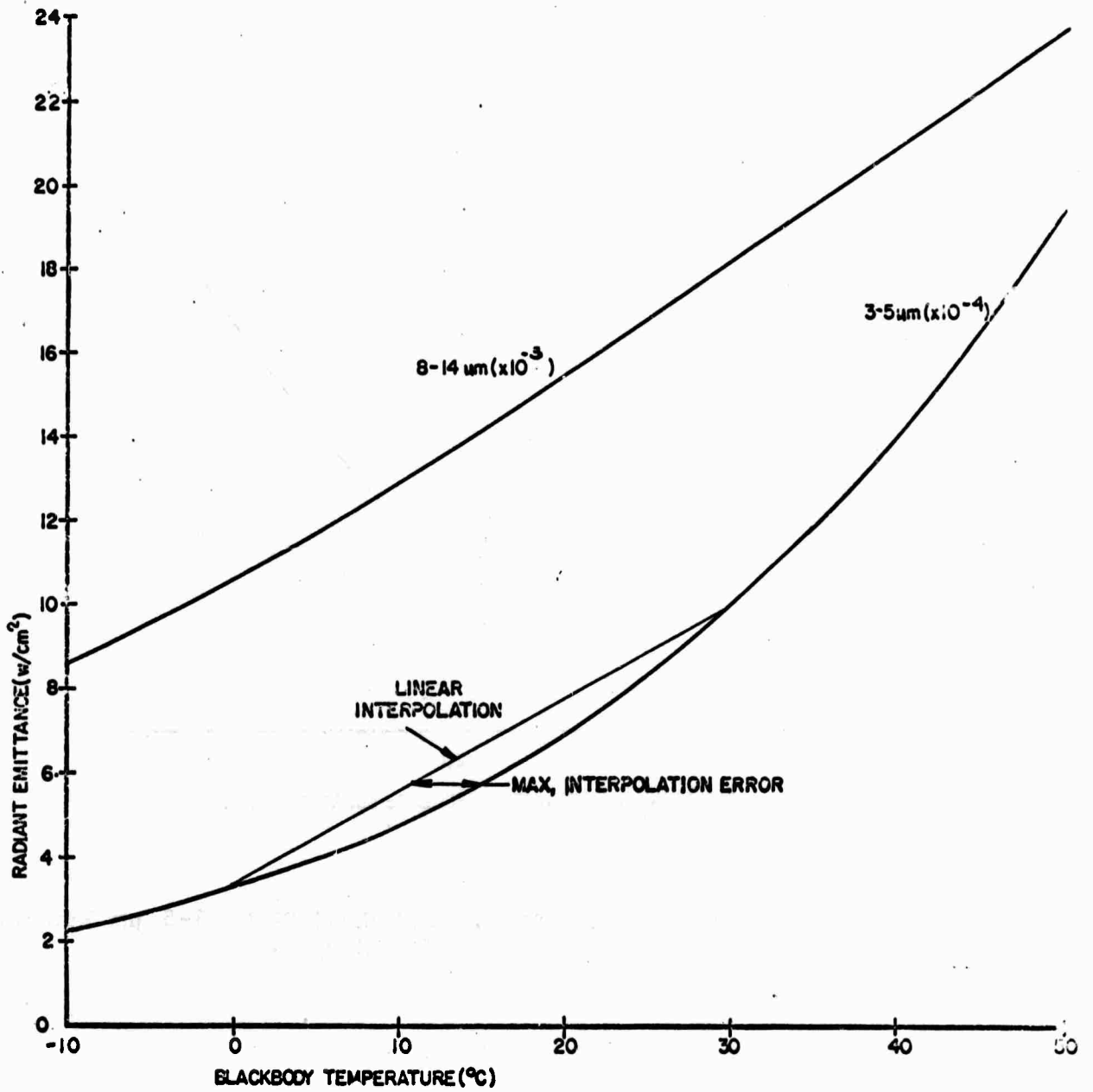
RADIATED ENERGY VS. TEMPERATURE FOR BLACKBODY SOURCES
FIGURE 2
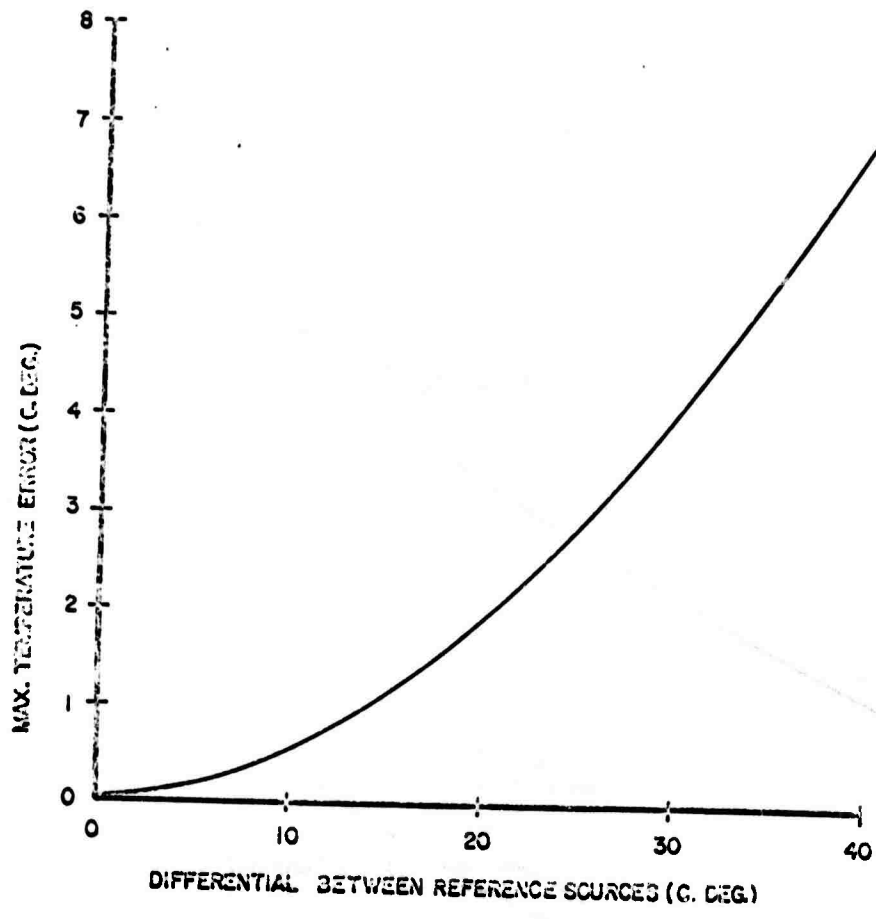
ERRORS OF LINEAR INTERPOLATION IN 3-5 μm REGION
FIGURE 3

A 16

GENERAL DESCRIPTION

The quantitative airborne line scanner is a special purpose instrument designed to both image and measure the thermal radiation from targets of interest. The scanner system consists of the scan head, the control console, the power junction box, and the two-channel temperature controller (see figure 4). Normally, a vertical gyro would be added to the system for aircraft roll compensation, as well as a wideband FM tape recorder for data recording.

The quantitative scanner contains two independent reference-temperature calibration sources physically located within the scanner housing as shown in figure 5. Energy from each of these sources completely fills the scanner aperture for several fields of view of the detector once during each scan line. The reference sources are adjusted, within their range of capability, to correspond to the high and low ends of the temperature range of interest. Sample-hold circuitry automatically maintains a constant system zero level at the average of the two temperature reference signal levels. Since the detector is included in the video system, output shifts due to bias level drift and changing environmental conditions are continuously compensated for.

A functional block diagram of the system is shown in figure 6; an outline drawing with clearance dimensions and mounting points is provided in Appendix II.

Pages 18 and 19 of this excerpt
have been excluded by the authors.

A 17
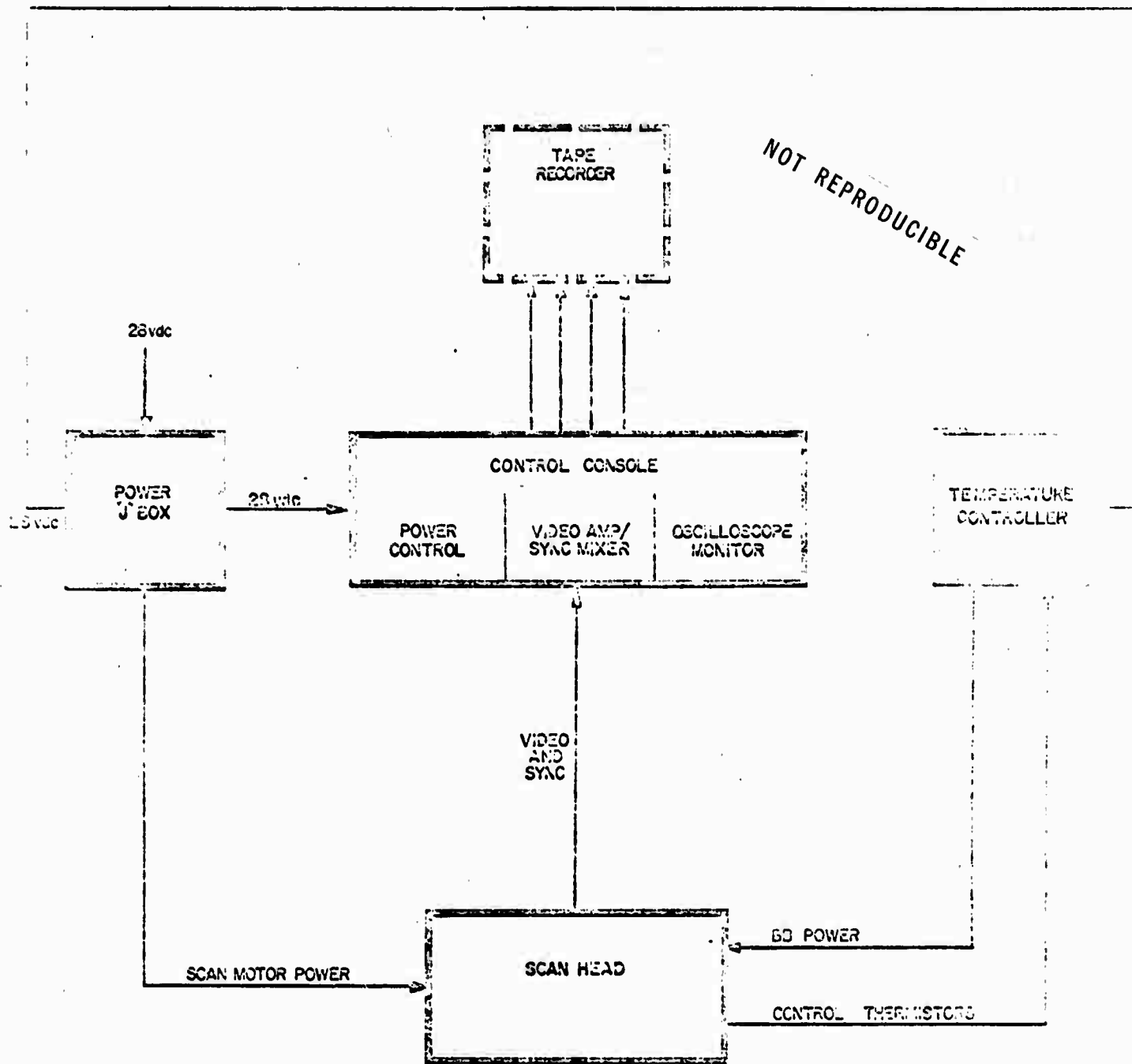
FUNCTIONAL BLOCK DIAGRAM OF THE SCANNING RADIOMETER
FIGURE 6

3.1. SCAN HEAD

The scan head (refer to figure 4) contains the detector mount, the focusing optics, the rotating assembly consisting of the scanning mirror, sync generator slugs and drive motor, and the energy reference sources. These elements are held rigidly in place by a unique frame construction which also provides a mount for the sync generator magnetic pickups. The electronic module which constitutes the detector preamplifier plugs into the top mounting surface. These various scan head subsystems are described in detail in separate sections below.

3.1.1. OPTICAL SYSTEM

The optical system consists of a classic Newtonian telescope whose field of view is traversed by a rotating 45° mirror. The optical system is shown schematically in figure 7 and pictorially in figure 5.

The parabolic primary mirror has a 5-inch diameter clear aperture and a focal length of 6-inches. It has a flat annulus ground on the face normal to the optic axis with the back being ground parallel to this surface. The edge is ground parallel to and concentric with the optic axis. As a result of this finishing, no optical alignment procedure is required other than an initial focus adjustment.

The flat secondary mirror is constructed of pyrex and is shaped to be slightly larger than the conic section it slices from the cone of rays being focused by the parabola. This mirror is permanently cemented to an aluminum block which mounts to the flange face of the scanning mirror shaft.

A 21
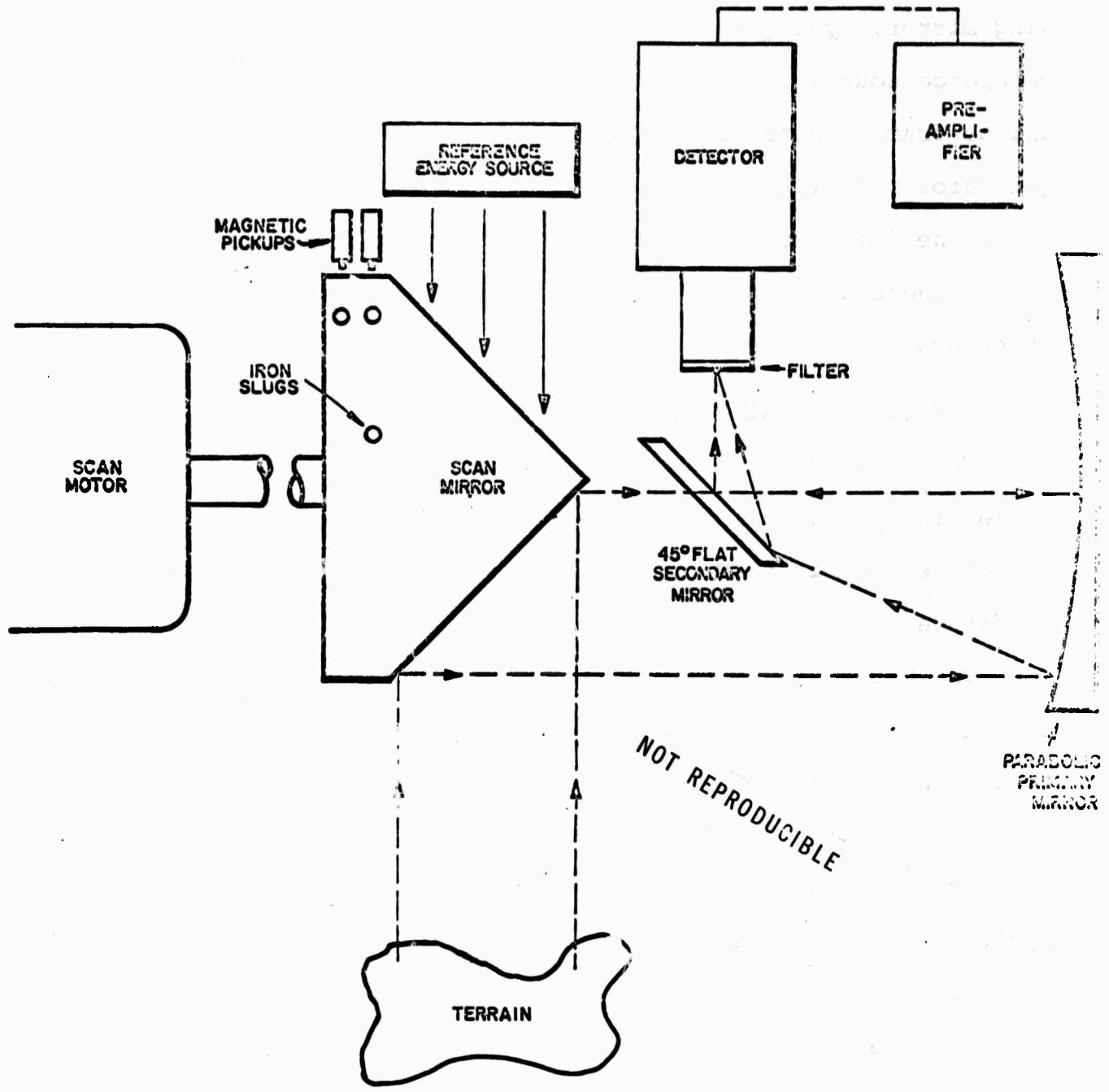
SCANNER OPTICAL RAY DIAGRAM
FIGURE 7

A 22

The scanning mirror is a classic axe blade design; an aluminum cylinder with two 45° inclined faces separated by 180° of rotation. One of these faces has been blackened with a high emissivity coating while the other has been plated with electroless nickel, optically polished and coated with evaporated aluminum to produce a highly reflective surface. The surface is further overcoated with a protective layer of silicon monoxide.

The scanning mirror rotates about its axis on two integral bearings on a fixed shaft. It is driven by a 3600 RPM AC synchronous motor which is powered from a crystal oscillator controlled power supply.

The focal ratio (F) of the scanner optical system is determined by the aperture of the scanning mirror. F is defined by:

$$F = \frac{FL}{D_{eff}}$$

where   FL   = focal length of primary mirror

D_{eff} = the effective diameter of the entrance aperture.

D_{eff} in the quantitative scanner is the equivalent diameter of the area of scanning mirror minus the area of all other obscurations in the optical system. Additional obscurations in this system are limited to the secondary mirror spider shown in figure 8. D_{eff} is given by:

$$D_{eff} = 2\sqrt{\frac{\frac{\pi R^2 - \pi \hbar^2}{2} - A_m}{\pi}}$$

A 23

where   R = radius of scanning mirror = 2.500 in.

$\,\,\,\,\,\,\,\,\,\,\,\,\,$ $\hbar$ = radius of scanning mirror bore = 1.187 in.

$\,\,\,\,\,\,\,\,\,\,\,\,\,$ A_m = area of lower portion of secondary mirror spider.

$$A_m = \frac{\left[R_m^{\,2} - \hbar_m^{\,2} \right] \theta}{2}$$
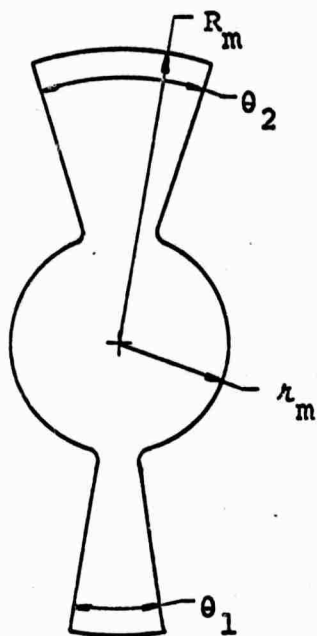
where: R_m = 2.500

$\,\,\,\,\,\,\,\,\,\,\,\,\,\,\,\,\,$ $\hbar_m$ = 1.187

$\,\,\,\,\,\,\,\,\,\,\,\,\,\,\,\,\,$ $\theta_1 = 18° = .1\pi$ radians

$\,\,\,\,\,\,\,\,\,\,\,\,\,\,\,\,\,$ $\theta_2 = 36° \, 40'$

FIGURE 8. SECONDARY MIRROR SPIDER

It will be noted that the radiation collected by the scanning
mirror and subsequently reflected to the parabola, impinges on
different areas of the parabola as the scanning mirror rotates.
This does not create any problem as the high degree of uniformity
of the coatings on the parabola and the flat secondary mirror
obviates the possibility of any significant energy difference at
the detector.

A 24

APPENDIX B

In this Appendix the University of Michigan
Thermal Modeling Program is Described, and
the Modifications Made to Account for Phase
Change are Discussed.

B-0

APPENDIX B

THERMAL MODELING

1.1 Program Description

The thermal model is based on the one-dimensional heat transfer equation

$$\frac{\partial^2 T}{\partial x^2} = \frac{1}{\alpha} \frac{\partial T}{\partial t} \tag{1}$$

where T is the spatially and temporally varying temperature, X is the vertical distance below the surface, t is time, and α is the thermal diffusivity of the medium through which the heat propagates. The thermal diffusivity is related to the thermal conductivity K, heat capacity, C, and the density, ρ of the medium as

$$\alpha = \frac{K}{\rho C}$$

The one-dimensional model is based on the assumption that the most significant heat fluxes are vertical, and that transverse heat flow is negligible. This one-dimensional model adequately describes a geologic section which is uniformly illuminated, has an essentially horizontal surface, and with a horizontal spatial extent significantly greater than the depth of penetration of the annual cycle. In addition, the properties of the media are considered to be homogeneous in its transverse dimension.

Equation (1) may be used to describe the temperature distribution in multi-layered media by considering the media to be composed of stacked, horizontal layers, each of arbitrary thermal properties and arbitrary thicknesses. Each layer is then subjected to two boundary conditions. Across the boundaries between the layers, the temperature profile is required to be continuous. The boundary condition at the bottom of the deepest layer is usually taken to be some temperature realistic for that point. If the point is at a depth below the annual thermal wave penetration, the assignment of a constant temperature is quite appropriate.

While the bottom and intermediate boundary conditions are simple, the upper boundary condition is a statement of the very complicated natural meteorological driving functions which act on the exposed surface. For non-covered surfaces, there are six essential heat-transfer processes which

B-1

must be accounted for:

- conduction
- solar energy absorption
- net thermal radiation
- convection
- rain
- evaporation

An additional transpiration term must be considered for surfaces with vegetation. All of these processes depend on directly measurable meteorological parameters, such as ambient air temperature, horizontal wind velocity, relative humidity, cloud cover, and cloud type, which, in general, are time-dependent. A brief description of each process as treated in the U. of M. program follows:

Conduction. This term accounts for the heat flow between the upper surface and the interior region. It depends on the thermal conductivity of the near-surface material and the temperature gradient in the material evaluated at the surface.

Solar Energy Absorption. This term accounts for the albedo of the surface. It is the sum of the direct and diffuse solar irradiance multiplied by the total solar absorptivity of the surface.

Net Thermal Radiation. The net thermal radiation is specified as the difference between the instantaneous total grey body radiation emitted by the surface and the absorbed energy from a radiating atmosphere. The mean total emittance of the atmosphere is an analytical function of the cloud cover, cloud type, relative humidity, and air temperature. In addition the thermal emissivity of the surface must be known.

Convection. Thermal transfer by the convection process can vary over several orders of magnitude, from a very small value for stable, no-wind conditions to a very large rate for unstable atmospheric conditions and high wind. The convective energy transfer process is described by a semi-empirical, analytical expression involving air temperature, wind speed, and an aerodynamic roughness height for the modeled surface.

Rain. The intensity and temperature of rain falling on the surface may alter the surface temperature by causing the surface temperature to attempt to equilibrate with the rain.

Evaporation. A certain portion of the rainfall (remaining after runoff) is susceptible to evaporation. In computing the rate of heat transfer resulting from evaporation, an analytical formulation was used which accounts for the

effects of wind turbulent mixing and diffusion in the immediate atmosphere. This term depends on the wind speed, the relative humidity and air temperature, and the surface (water) temperature.

In addition to the boundary conditions, the solution of the thermal diffusion equation requires that the spatial-temperature distribution be specified at some time t_o. This temperature distribution is the cumulative result of the effect of the thermal phenomena prevailing prior to t_o. Thus the response of the media to thermal input occurring after t_o will be influenced by the spatial distribution at t_o. However, this influence decreases in time and finally becomes negligible after an interval comparable to the time constant of the system (a year for this particular situation).

The computer program uses as input data the time dependent insolation, horizontal wind speed, ambient air temperature, relative humidity, percent cloud cover and cloud type for many annual cycles. Several of these cycles are used to obtain the initial temperature distribution for the start of the subsequent cycle of interest.

1.2 Thermal Properties

The determination of surface temperature requires the knowledge of the thermal properties of each of the layers of the multi-layered medium. The required thermal properties are thermal conductivity, specific heat and density. These properties vary with temperature, moisture, density and composition. The R & M geologists use the following soil descriptions to describe the cores of their pipeline borings made across the entire State of Alaska:

- organics
- silt
- sand
- clay
- gravel

The thermal properties for these five soil materials were taken from Kersten's study of the thermal properties of Alaskan soils[1]. The particular soils selected for the computer analysis are shown in Table 1. The thermal properties were evaluated at the temperature and moisture content appropriate to the particular case under study.

In addition to the above five soils, essentially pure ice was found in the cores from the Alyeska boreholes. The thermal properties of ice are therefore required.

B-3

TABLE 1 - SOILS FOR THERMAL MODEL

SOIL DESCRIPTION	SOIL NO.	SOIL DESIGNATION
Organics	P4707	Fairbanks Peat
Silt	P4602	Fairbanks Silt Loam
Sand	P4709	Fairbanks Sand
Clay	P4708	Healy Clay
Gravel	P4601	Chena River Gravel

1.3 Atmospheric Data

The computer program required the following atmospheric data, averaged on a monthly basis:

- total solar radiation, langleys/day
- air temperature, $^{\circ}F$
- relative humidity, percent
- wind speed, mph
- sky cover, tenths

In addition, the monthly total precipitation (water equivalent) in inches, is required. The Fairbanks weather data were used for all computer calculations. The monthly average and monthly total values are shown in Tables 2-7.

1.4 Geological Data

The computer analysis required the specification of the various layers comprising the media under study. Since the thermal modeling was to be completed prior to the field program, a variety of multilayered media were selected for study. The particular multilayered samples were selected from the Alyeska boring logs. These logs give the location and subsurface geology of sites along the proposed pipeline route. Seven multilayered samples were selected, five in the area between Fort Yukon and Fairbanks and two near Prudhoe Bay. The requirement for selection was the presence of massive ice at a site, close to which another site or sites showed no significant ice and for which the layers were otherwise similar. It is quite reasonable to assume that the meterological inputs at these close sites were the same. Therefore, comparison of the predicted surface temperatures for these close sites should indicate the presence of the ice beneath the surface of one of the sites. The test cases are described in Table 8.

1.5 Sample Calculation

The annual variation of surface temperature for the test cases, subject to known metereological conditions, was computed using the University of Michigan Thermal Modeling Computer Program[2]. The time interval used for this computation was six days. The U. of M. computer program was not set up to account for the phase change of the water, that is, for the energy requirements associated with the melting and freezing of the interstitial water in the active layer. While the governing equation remains unchanged, a new boundary condition is required at the moving phase change interface. This boundary condition must account for the energy required for or released by the phase change process. Since alteration of the computer program was beyond the scope of this project, approximate techniques were developed to

B-5

TABLE 2

MONTHLY AVERAGE, SOLAR RADIATION*, LANGLEYS/DAY

	1970	1969	1968	1967
JAN	24	14	6	23
FEB	66	75	61	76
MAR	195	223	251	212
APR	354	423	411	382
MAY	521	513	401	527
JUN	490	518	552	627
JUL	465	404	566	465
AUG	321	468	365	322
SEP	199	278	252	204
OCT	86	103	62	95
NOV	32	29	24	26
DEC	6	7	7	4

*Total Solar Radiation (Direct and Indirect) received on a horizontal surface during each month, divided by number of days in that month.

TOTAL ANNUAL SOLAR RADIATION, LANGLEYS

1970	85,752
1969	90,132
1968	91,639
1967	90,821

TABLE 3

FAIRBANKS
MONTHLY AVERAGE AIR TEMPERATURE, °F.

	1971	1970	1969	1968	1967
JAN	-31.7	-16.2	-26.7	-11.0	-15.3
FEB	- 4.6	8.0	-7.3	-5.0	-6.9
MAR	-0.4	20.9	10.1	12.8	9.6
APR	26.7	32.0	36.3	29.2	31.7
MAY	47.3	51.8	49.4	47.6	45.7
JUN		58.0	64.9	59.5	61.6
JUL		62.4	59.4	65.6	59.6
AUG		56.9	49.6	56.5	58.3
SEP		40.6	49.1	42.6	46.6
OCT		16.9	34.0	22.1	24.8
NOV		10.7	1.2	2.3	9.5
DEC		-9.6	4.0	-17.7	-1.6

B-6

TABLE 4

FAIRBANKS
MONTHLY AVERAGE RELATIVE HUMIDITY, PERCENT

	1971	1970	1969	1968	1967
JAN	64.4	57.9	61.4	76.9	59.5
FEB	62.1	57.1	55.6	65.5	52.0
MAR	47.4	50.6	47.9	52.5	64.5
APR	50.1	46.3	40.5	44.5	72.3
MAY	47.4	38.5	44.8	44.6	55.0
JUN		50.9	48.1	61.0	54.1
JUL		61.5	71.3	56.5	70.1
AUG		69.1	64.0	73.1	74.3
SEP		65.5	57.5	65.8	66.9
OCT		73.8	64.5	75.9	75.3
NOV		67.9	67.4	73.0	79.5
DEC		63.4	62.9	63.3	76.3

TABLE 5

FAIRBANKS
MONTHLY AVERAGE WIND SPEED, MPH

	1971	1970	1969	1968	1967
JAN	2.3	4.5	1.1	2.9	1.1
FEB	4.5	6.2	3.4	4.6	2.7
MAR	7.2	7.1	4.5	4.3	4.2
APR	8.3	8.1	6.6	5.9	6.3
MAY	9.1	9.9	9.0	8.9	7.5
JUN		8.8	6.8	7.1	7.3
JUL		7.3	6.8	6.1	6.5
AUG		7.0	8.2	5.7	5.9
SEP		7.6	6.5	6.2	5.9
OCT		5.5	5.3	4.9	5.9
NOV		6.5	4.7	4.5	4.6
DEC		5.3	4.8	3.3	2.8

TABLE 6

FAIRBANKS
MONTHLY AVERAGE SKY COVER, TENTHS

| | 1971 | | 1970 | | 1969 | | 1968 | | 1967 | |
	S to S	M to M*	S to S	M to M*	S to S	M to M*	S to S	M to M*	S to S	M to M*
JAN	6.9	6.7	4.0	4.0	6.6	6.4	7.0	6.5	6.0	5.9
FEB	8.2	8.1	7.9	7.6	6.1	5.5	6.4	6.5	7.9	6.9
MAR	5.4	5.1	7.1	7.1	6.2	6.0	4.8	4.5	6.6	6.2
APR	7.2	7.1	8.0	7.7	6.7	6.5	7.4	7.1	7.9	7.9
MAY	8.2	8.3	7.4	7.2	7.0	6.7	7.0	7.2	7.3	7.2
JUN			8.4	8.4	7.0	7.0	7.7	7.7	6.6	6.8
JUL			8.4	8.4	8.3	8.2	6.1	6.2	8.9	8.8
AUG			8.6	8.7	7.2	7.2	6.2	6.0	7.4	7.5
SEP			8.2	8.0	4.7	4.3	6.4	6.3	7.3	6.6
OCT			7.9	8.4	6.7	6.4	8.3	7.8	7.4	7.0
NOV			7.0	6.7	7.4	7.3	7.0	6.6	7.4	7.3
DEC			7.2	7.3	7.3	6.7	6.4	5.6	8.0	7.8

*S to S = Sunrise to Sunset
*M to M = Midnight to Midnight

TABLE 7

FAIRBANKS
MONTHLY TOTAL PRECIPITATION, WATER EQUIVALENT, INCHES

	1971	1970	1969	1968	1967
JAN	0.33	0.10	0.55	1.19	0.40
FEB	0.63	0.32	0.10	0.15	0.25
MAR	0.20	0.25	0.60	0	1.90
APR	0.11	0.45	0	0.29	0.84
MAY	0.16	0.42	0.95	0.67	0.43
JUN		2.57	0.39	1.52	1.13
JUL		1.81	1.33	0.84	3.34
AUG		1.98	2.04	0.96	6.20
SEP		0.65	0.28	0.15	0.25
OCT		1.84	0.10	0.31	0.32
NOV		3.32	0.54	0.27	0.93
DEC		2.29	0	1.38	1.34

TABLE 8 - TEST CASES

TEST CASE	LAYER	COMPOSITION	THICKNESS
1A	1	Organics	1'
	2	Sand	3'
	3	Ice	6'
1B	1	Organics	1'
	2	Sand	22'
IIA	1	Organics	0.2'
	2	Silt	7.8'
	3	Ice	10'
IIB	1	Organics	1'
	2	Silt	17'
IIC	1	Organics	0.5'
	2	Silt	8.5'
	3	Ice	1'
	4	Silt	8'
IIIA	1	Silt	2.5'
	2	Gravel	20.5'
IIIB	1	Silt	2'
	2	Ice	9'
	3	Silt	5.5'
	4	Gravel	15.5'

accou nt for the phase change.

In the initial modification only the change in the thermal properties of the interstitial water due to freezing and melting was considered. It was assumed that from 1 December to 30 June of each year the interstitial water in the active layer was solid and from 1 July to 30 January of each year the interstitial water in the active layer was liquid*. The active layer was taken to be 1-1/2 feet. The bottom of the lowest layer was at a depth of 23 feet; this depth represents the deepest auger penetration for the test cases. Ground temperature measurements were available from the Fort Yukon test station[3] (Figure 1). At a depth of 22.5 ft., the bottom of the test hole, temperatures of $30^{\circ}F \pm 1^{\circ}F$ were observed. Therefore, the temperature of the bottom of the lowest layer was assumed to be constant at $30^{\circ}F$. The annual variation of surface temperature for the seven test cases was computed.

In the second modification, the first four annual cycles (years 1967-1970) for test cases IA and IB were computed as above. Because of the lengthier computer calculations required, only two test cases were used. Upon computing the temperature distribution at the end of the fourth freeze period (June 30, 1970), the amount of energy required to thaw the known amount of water in each strata within the active layer was calculated and the pre-thaw temperature profile within the active layer was reduced accordingly, subject to the condition of unchanged surface and active layer interface temperatures. The time interval was then changed from 6 days to 10 minutes and the phase-change profile, representing the removal of all of the phase change energy as a step function, was allowed, over a 5-day period, to equilibrate. At the end of the five day equilibration interval the resulting profile was used to represent the July 1 post-thaw profile and the basic program continued. At the end of the thawed season (Nov. 30, 1970) the program was interrupted again to account for freezing of the active layer. The amount of energy removal required to freeze the known amount of water in each strata of the active layer was calculated and the pre-freeze temperature profile within the active layer was increased accordingly, subject to the conditions that the surface temperature and the active layer interface temperatures remain unchanged. The time interval reverted to 10 minutes and the phase change profile (representing the addition of all of the phase change energy as a step function) was allowed, over a five day interval, to equilibrate. At the end of this five day equilibration interval the resulting profile was used to represent the December 1 post-freeze profile and the basic program continued. In such a manner the surface temperature for two of the seven cases was obtained for the period of interest, the thawed interval, July 1 to Nov. 30, 1971.

---

*For ease of computation each month was assumed to have thirty days.
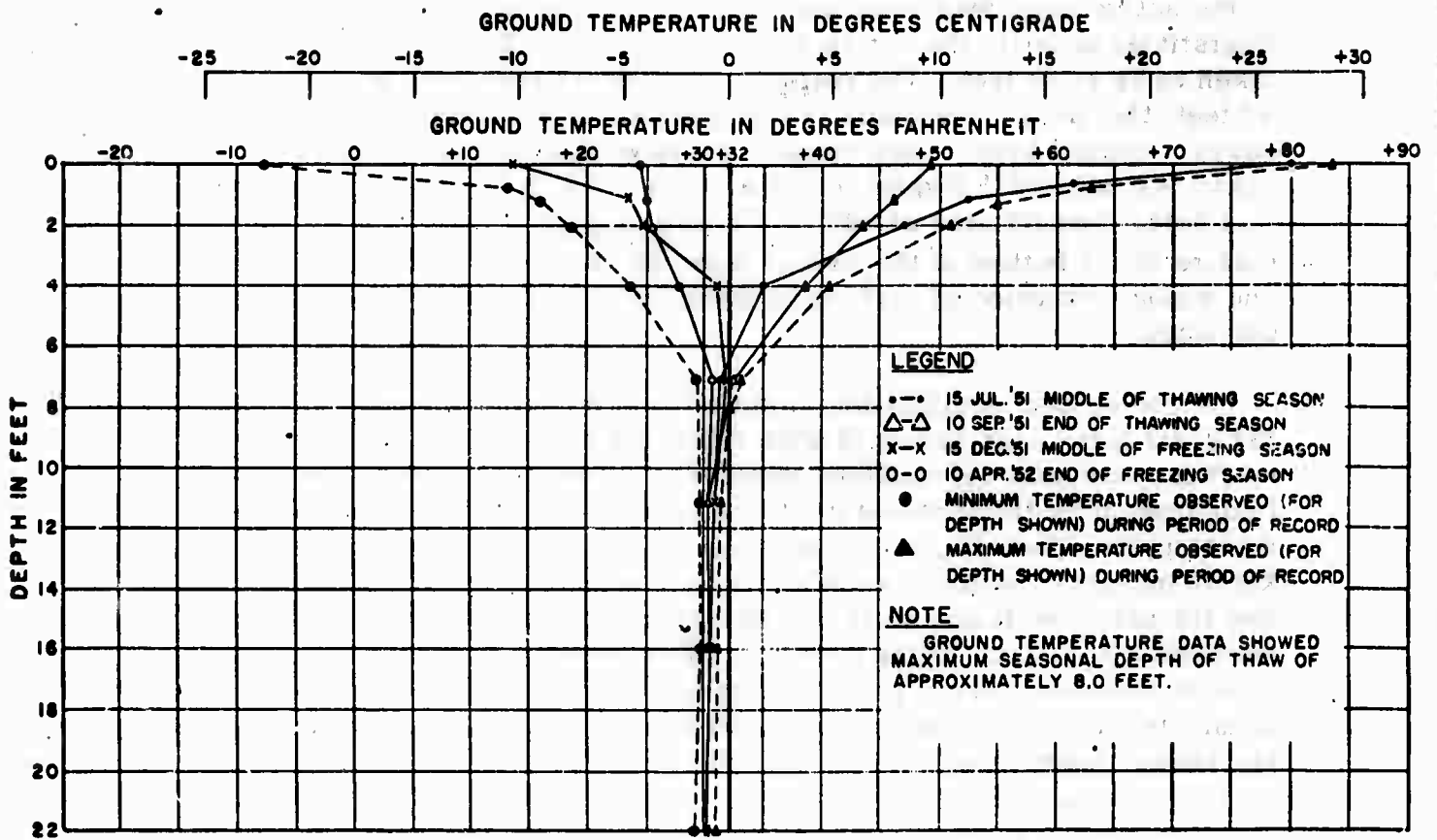
FIGURE 1: Ground Temperature Profiles Measured at the Fort Yukon Test Station, Alaska. (After CRREL Tech. Rpt. 100, Ref 3).

B-11

DEG. C.

-40   -20   0   20   40

0

ORG

ACTIVE LAYER

SAND

DEPTH IN METERS

ICE

FEB 1970

AUG 1971

5

Change of Thermal
Properties

Step Phase Change And
Change of Thermal
Properties
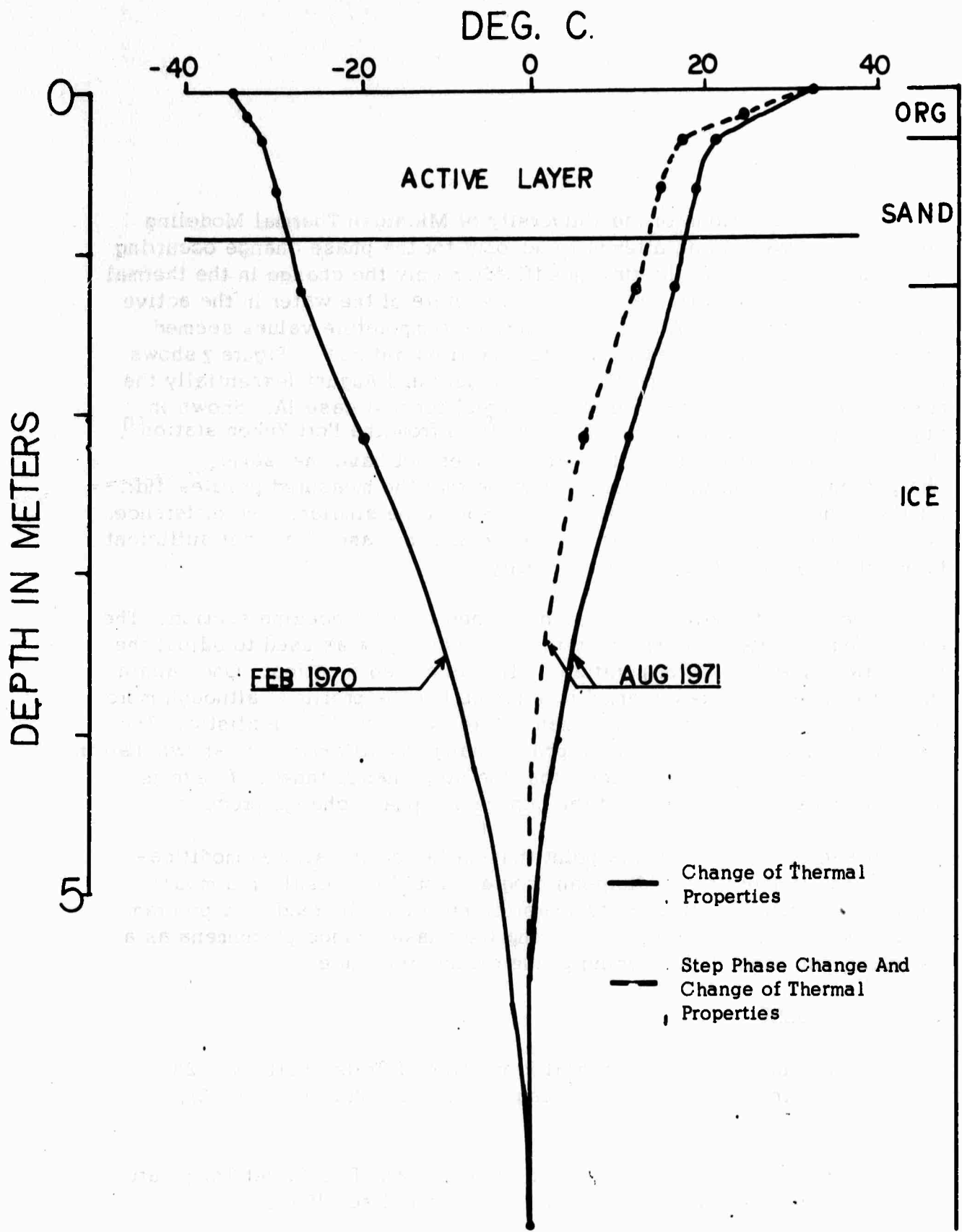
FIGURE 2: The Temperature Profiles for February and August as
Predicted by The U. of M. Model Are Shown. Although The Surface
Temperatures Appear Reasonable, the Profiles at Depth Do Not,
Suggesting The Present Inadequacy of This Model (See Text of
Appendix B).

1.6 Conclusions

Two modifications of the University of Michigan Thermal Modeling Program were made in an attempt to account for the phase change occurring in the active layer. In the first modification only the change in the thermal properties resulting from the change in the state of the water in the active layer was considered. Although the surface temperature values seemed reasonable, the associated temperature profiles did not . Figure 2 shows the predicted temperature profiles for February and August (essentially the minimum and maximum surface temperatures) for test case 1A. Shown in Figure 1 are the measured temperature profiles from the Fort Yukon station[3]. It can be seen that the predicted profile does not have the same sharp decay towards the undisturbed value that the measured profiles did; for the model to be realistic, the profile should be similar. The differences however, between the media at Fort Yukon and for case IA are not sufficient to account for this observed dissimilarity.

The second modification was described in the preceding section. The energy required for or released by the phase change was used to adjust the pre-thaw or pre-freeze temperature profile as a step function. Once again the surface temperatures seemed reasonable but the profiles, although more similar to the measured profiles than before, were still not realistic. The August profile, based on the step phase change modification, is shown also in Figure 2. It is likely, therefore, that the step change thaw or freeze is an inadequate representation of the continuous phase change process.

It seems apparent at this point that further computational modifications of the University of Michigan program would not result in a model capable of producing realistic temperature profiles. Instead, the program itself should be modified by introducing the phase change phenomena as a boundary condition at the moving phase change interface.

1.7 References

1. Kersten, Miles S., Thermal Properties of Soils, Bull. No. 28, U. of Minn., Inst. of Technology, Eng. Exp. Sta., Vol. Lll, No. 21, June 1, 1949.

2. Bornemeier, D., Bennet, R., and Norman, R., Target Temperature Modeling, Rept. No. 1588-5-F, RADC TR 69-404, Dec. 1969.

3. Ground Temperature Observations, Fort Yukon, Alaska, U. S. Army C.R.R.E.L., Technical Rept. #100, July 1962.

APPENDIX C

Flight Logs.

DATE 8/19/71 TAKE OFF 09:45
FLIGHT NO. 1 LANDING 11:20 (1:35)
OPERATING BASE ANCHORAGE
PROJECT D.&R.T.
TAPE RECORDER

RUN	TIME ON OFF	TARGET	SPEED	ALTITUDE	READING	CELL-FILTER	DIR REC	TAPED	CELL-FILTER	DIR REC	TAPED	TAPE NUMBER	REMARKS
		FERRY: ANCHORAGE TO GULKANA											

DATE 8/19/71 TAKE OFF 16:10
FLIGHT NO. 2 LANDING 17:50 (1:40) Solid Overcast / Light Rain
OPERATING BASE GULK
PROJECT D.&R.T.
TAPE RECORDER

RUN	TIME ON OFF	TARGET	SPEED	ALTITUDE	HEADING	CELL-FILTER	DIR REC	TAPED	CELL-FILTER	DIR REC	TAPED	TAPE NUMBER	REMARKS
1		Enroute Site										1	
2	16:27	GULK #1	100	1300	305							2A1	Pan Photo #1, 8 frames
3	16:31	#5			290							2A2	7 frames
4	16:36	#6			250							2A3	8 frame
5	16:38	#2			310							2A4	9 frame
6	16:52	#3			160							2A5	13 frames
7	16:56	#3			355							2A6	17 frame
8	16:59	#4			165							2A7	13 frame
9	17:11	#7			360							2A8	14 frame
10	17:18	#8			025							2A9	Pan Film Out, 6 frames
11	17:21	#9			300							2A10	Pan Cassette #2, 6 fram
12	17:24	#9		750	300							2A11	No Photo
13	17:29	#7		750	180							2A12	No Photo

C-1

DATE __8/20/71__ TAKE OFF __15:30__
FLIGHT NO. __3__ LANDING __17:35__ (2:05) Overcast
OPERATING BASE __GULK__ Sprinkling
PROJECT __D.&R.T.__
TAPE RECORDER __

CHANNEL
1 ____ 2 ____
3 ____ 4 ____
5 ____ 6 ____
7 ____

RUN	TIME ON OFF	TARGET	SPEED	ALTITUDE	HEADING	CELL-FILTER	DIR REC	TAPED	CELL-FILTER	DIR REC	TAPED	TAPE NUMBER	REMARKS
1	15:48	GULK #7	100	2000	360							3A1	Pan Photo #2, 7 frames
2	15:51	#8			210							3A2	17 frames
3	15:56	#9			120							3A3	5 frames
4	16:03	#34			170							3A4	13 frame
5	16:09	#34			350							3A5	9 frame
6	16:13	#14			120							3A6	11 frame
7	16:19	#7	90	750	355							3A7	No Photo
8	16:25	#8			205							3A8	
9	16:30	#9			120							3B1	
10	16:39	#1			290							3B2	
11	16:43	#2			110							3B3	
12	16:50	#3			355							3B4	
13	16:57	#4			350							3B5	

DATE __8/20/71__ TAKE OFF __22:25__
FLIGHT NO. __4__ LANDING __24:05__ (1:40) Overcast
OPERATING BASE __GULK__
PROJECT __D.&R.T.__
TAPE RECORDER __

CHANNEL
1 ____ 2 ____
3 ____ 4 ____
5 ____ 6 ____
7 ____

RUN	TIME ON OFF	TARGET	SPEED	ALTITUDE	HEADING	CELL-FILTER	DIR REC	TAPED	CELL-FILTER	DIR REC	TAPED	TAPE NUMBER	REMARKS
1	22:52	GULK #7	90	750	360							4A1	
2	22:00	#9			205							4A2	
3	23:09	#8			200							4A3	
4	23:13	#8			205							4A4	
5	23:19	#1			300							4A5	
6	23:23	#2			120							4A6	
7	23:28	#4			160							4A7	
8	23:36	#3			160							4A8	
9	23:42	#1			330							4A9	
10	23:48	#1			300							4B1	

C-2

DATE __8/21/71__ TAKE OFF __04:00__
FLIGHT NO. __5__ LANDING __05:15__ (1:15) Overcast
OPERATING BASE __GULK__
PROJECT __D.&R. T.__
TAPE RECORDER _____

RUN	TIME ON/OFF	TARGET	SPEED	ALTITUDE	HEADING	CELL-FILTER	TIR REC	TAPED	CELL-FILTER	DIR REC	TAPED	TAPE NUMBER	REMARKS
1	04:15	GULK #7	90	750	360							5A1	
2	04:19	#8			205							5A2	
3	04:25	#9			120							5A3	
4	04:29	#9			120							5A4	
5	04:37	#1			300							5A5	
6	04:40	#2			120							5A6	
7	04:46	#3			160							5A7	
8	04:52	#4			160							5A8	
9	04:56	#4½			160							5B1	

CHANNEL
1 _____ 2 _____
3 _____ 4 _____
5 _____ 6 _____
7 _____

DATE __8/21/71__ TAKE OFF __10:12__
FLIGHT NO. __6__ LANDING __11:27__ (1:15) Broken/Scattered
OPERATING BASE __GULK__
PROJECT __D.&R.T.__
TAPE RECORDER _____

RUN	TIME ON/OFF	TARGET	SPEED	ALTITUDE	HEADING	CELL-FILTER	DIR REC	TAPED	CELL-FILTER	DIR REC	TAPED	TAPE NUMBER	REMARKS
1	10:27	GULK #7	90	750	360							6A1	
2	10:32	#8			205							6A2	
3	10:38	#9			120							6A3	
4	10:43	#4			160							6A4	
5	10:48	#2			120							6A5	
6	10:53	#1			300							6A6	
7	10:59	#3			160							6A7	

CHANNEL
1 _____ 2 _____
3 _____ 4 _____
5 _____ 6 _____
7 _____

C-3

DATE 8/22/71 **TAKE OFF** 04:05
FLIGHT NO. 7 **LANDING** 05:40 (1:35)
OPERATING BASE GULK
PROJECT D.&R.T.
TAPE RECORDER

CHANNEL
1 _____ 2 _____
3 _____ 4 _____
5 _____ 6 _____
7 _____

RUN	TIME ON	OFF	TARGET	SPEED	ALTITUDE	HEADING	CELL-FILTER	DIR REC	TAPED	CELL-FILTER	DIR REC	TAPED	TAPE NUMBER	REMARKS
1	04:16		Gulk #7	100	4K	360							7A1	
2	04:22		#8			205							7A2	
3	04:30		#9			120							7A3	
4	04:36		#34			170							7A4	
5	04:42		#14			300							7A5	
6	04:50		#7	90	750	360							7A6	
7	04:56		#8			205							7B1	
8	05:00		#9			120							7B2	
9	05:03		#3			170							7B3	
10	05:08		#2			120							7B4	
11	05:12		#1			300							7B5	
12	05:17		#4			170							7B6	

DATE 8/22/71 **TAKE OFF** 11:25
FLIGHT NO. 8 **LANDING** 12:30 (1:05)
OPERATING BASE GULK
PROJECT D.&R.T.
TAPE RECORDER

Weather: Broken

CHANNEL
1 _____ 2 _____
3 _____ 4 _____
5 _____ 6 _____
7 _____

RUN	TIME ON	OFF	TARGET	SPEED	ALTITUDE	HEADING	CELL-FILTER	DIR REC	TAPED	CELL-FILTER Frame No.	DIR REC	TAPED	TAPE NUMBER	REMARKS
1			Abort	120	3K					#1 { 7				Photo EKTA(IR) ROLL #1 1/250 @ f/5.6
2	11:38		#7			360				15				Mag Malfunction 1/250 @ f/4.0
3	11:52		#8			205				{ 14				Roll #2
4	11:57		#7			360	PHOTO ONLY			20				
5	12:02		#9							30				
6	12:06		#34			170				#2 40				
7	12:12		#14			120				52				

DATE __8/22/71__ TAKE OFF __12:55__
FLIGHT NO. __9__ LANDING __14:05__   (1:10)
OPERATING BASE __BULK__
PROJECT __D.&R.T.__
TAPE RECORDER _____

CHANNEL
1 _____   2 _____
3 _____   4 _____
5 _____   6 _____
7 _____

RUN	TIME ON	OFF	TARGET	SPEED	ALTITUDE	READING	CELL-FILTER	PER REC	TAPED	CELL-FILTER	DIR REC	TAPED	TAPE NUMBER	REMARKS
			FERRY GULKANA TO ANCHORAGE											

DATE __8/23/71__ TAKE OFF _____
FLIGHT NO. __10 & 11__ LANDING _____
OPERATING BASE _____
PROJECT __D.&R.T.__
TAPE RECORDER _____

CHANNEL
1 _____   2 _____
3 _____   4 _____
5 _____   6 _____
7 _____

RUN	TIME ON	OFF	TARGET	SPEED	ALTITUDE	READING	CELL-FILTER	DIR REC	TAPED	CELL-FILTER	DIR REC	TAPED	TAPE NUMBER	REMARKS
			FLT. #10 FERRY ANCHORAGE TO BETTLES											
			Off: 12:00											
			Down: 15:15											
			3:15											
			●											
			FLT. #11 FERRY BETTLES TO BARROW											
			Off: 16:03											
			Down: 18:43 2:30											

C-5

DATE 8/24/71   TAKE OFF 01:45
FLIGHT NO. 12   LANDING 03:30   (1:45)
OPERATING BASE Barrow
PROJECT D.&R.T.
TAPE RECORDER

CHANNEL
1 —— 2 ——
3 —— 4 ——
5 —— 6 ——
7 ——

RUN	TIME ON OFF	TARGET	SPEED	ALTITUDE	HEADING	CELL-FILTER	DIR REC	TAPED	CELL-FILTER	DIR REC	TAPED	TAPE NUMBER	REMARKS
1	02:05	---	90	1000								8A1	Radar Spikes
2	02:11	BAR #3			15-125							8A2	Tape Batt. Off
3	02:15	#4			130							8A3	Ripple fm. Batt Charger
4	02:28	#6			340							8A4	
5	02:31	#8			120							8A5	
6	02:47	#5			320							8A6	
7	02:51	#5½			130							8B7	
8	02:57	#5½			130							8B1	
9	03:02	#7			340							8B2	
10	03:06	#1			200-220							8B3	
11	03:09	#2			020-040							8B4	

DATE 8/24/71   TAKE OFF 17:15
FLIGHT NO. 13   LANDING 18:45   (1:30)   Overcast @ 800 ft.
OPERATING BASE Barrow
PROJECT D.&R.T.
TAPE RECORDER

CHANNEL
1 —— 2 ——
3 —— 4 ——
5 —— 6 ——
7 ——

RUN	TIME ON OFF	TARGET	SPEED	ALTITUDE	HEADING	CELL-FILTER	DIR REC	TAPED	CELL-FILTER	DIR REC	TAPED	TAPE NUMBER	REMARKS
1	17:24	BAR #8	80	500	115							9A1	Pan Photo #3, 24 frame
2	17:28	#8 Repeat			115							9A2	No Camera
3	17:35	#6			320							9A3	13 frames
4	17:40	#7			150							9A4	15 frames
5	17:44	#5½			320							9A5	21 frames
6	17:49											9A6	5 frames
7	17:54	#5			130							9A7	Pan Photo #4, 8 frame
8	18:00	#5			130							9B1	10 frame
9	18:03	#4			320							9B2	9 frame
10	18:09											9B3	18 frame
11	18:18											9B4	4 frames in middle
12	18:27											9B5	4 frames in middle
13		TEST								•		10A1	
14	18:37	BAR #1										10A2	7 frames & 5 frames
15	18:43	SEV										10A3	

C-6

DATE __8/25/71__ TAKE OFF __12:43__
FLIGHT NO. __14__ LANDING __16:25__   (3:42)
OPERATING BASE __Barrow__
PROJECT __D.&R.T.__
TAPE RECORDER _____

CHANNEL
1 _____ 2 _____
3 _____ 4 _____
5 _____ 6 _____
7 _____

RUN	TIME ON	OFF	TARGET	SPEED	ALTITUDE	HEADING	CELL-FILTER	DIR REC	TAPED	CELL-FILTER	DIR REC	TAPED	TAPE NUMBER	REMARKS
		FERRY BARROW TO FAIRBANKS											

DATE __8/26/71__ TAKE OFF __14:20__
FLIGHT NO. __15__ LANDING __15:31__   (1:11)
OPERATING BASE __Fairbanks__
PROJECT __D.&R.T.__
TAPE RECORDER _____

CHANNEL
1 _____ 2 _____
3 _____ 4 _____
5 _____ 6 _____
7 _____

RUN	TIME ON	OFF	TARGET	SPEED	ALTITUDE	HEADING	CELL-FILTER	DIR REC	TAPED	CELL-FILTER	DIR REC	TAPED	TAPE NUMBER	REMARKS
		FERRY FAIRBANKS TO BIG DELTA											
		14	16:25											

DATE 8/26/71 TAKE OFF 21:35
FLIGHT NO. 16 LANDING 23:05   Weather: Clear
OPERATING BASE Big Delta
PROJECT D.&R.T.
TAPE RECORDER

RUN	TIME ON OFF	TARGET	SPEED	ALTITUDE	HEADING	CELL-FILTER	DIR REC	TAPED	CELL-FILTER	DIR REC	TAPED	TAPE NUMBER	REMARKS
1	21:48	Abort	90	750								11A1	
2	21:54	BD #1			280							11A2	
3	22:02	Repeat #1			100							11A3	
4	22:12	#2			010							11A4	
5	22:15	#3			240							11A5	
6	22:27	#1	90	3K	100							11B1	Break in Tape Run
7	22:42	#2			010							11B2	
8	22:46	#3			240							11B3	
9	22:50	River										11B4	

DATE 8/27/71 TAKE OFF 04:18
FLIGHT NO. 17 LANDING 05:20   (1:02)
OPERATING BASE Big Delta
PROJECT D.&R.T.
TAPE RECORDER

RUN	TIME ON OFF	TARGET	SPEED	ALTITUDE	HEADING	CELL-FILTER	DIR REC	TAPED	CELL-FILTER	DIR REC	TAPED	TAPE NUMBER	REMARKS
1	04:32	BD #1	120	4K	105							12A1	
2	04:40	#2			005							12A2	
3	04:43	#3			245							12A3	
4	04:50	#1	90	750	105-85							12A4	
5	05:02	#2			010							12B1	
6	05:05	#3			245							12B2	

DATE __8/27/71__ TAKE OFF __10:45__
FLIGHT NO. __18__ LANDING __12:50__ (2:05) Weather: Clear
OPERATING BASE __Big Delta__
PROJECT __D.&R.T.__
TAPE RECORDER _____

CHANNEL
1 _____ 2 _____
3 _____ 4 _____
5 _____ 6 _____
7 _____

RUN	TIME ON OFF	TARGET	SPEED	ALTITUDE	READING	CELL-FILTER	DIR REC	TAPED	CELL-FILTER Frame No.	DIR REC	TAPED	TAPE NUMBER	REMARKS
1	10:54	BD #1	120	4K	260-280				19			13A1	EK(IR) #1 1/250 @ f/4.0
2	11:00	#1 Repeat			105-90	'			41			13A2	
3	11:09	#2			010				46			13A3	
4	11:13	#3			245				53			13A4	
1A		Camera Run Out over TAPS Line							~70				
5	11:25	#2	110	2K	010				9			13A5	EK(IR) #3
6	11:29	#3			245				15			13A6	
7	11:33	#1 False Start			105-90	'			20			13A7	
8	11:40	BD #1	110	2K	105-90	.			46			13B1	
9	11:49	#2	90	750	010				54			13B2	Camera Malfunction
0	11:58	#2			010				9				EK(IR) #4 No Scanner
1	12:01	#3			245				24			13B3	
2	12:04	#1	90	750	260				39			13B4	Camera on twice 1/250 @ f/5.6 No Scanner
3	12:14	#2		2K	010	No Scanner Photo Only			45				
4	12:19	#3			245	" " " "			55				
5	12:21	#1				" " " "			60				
6	12:24	#1 cont.				" " " "			73				

DATE __8/27/71__ TAKE OFF __21:25__
FLIGHT NO. __#19__ LANDING __22:25__ (1:00)
OPERATING BASE __Big Delta__
PROJECT __D.&R.T.__
TAPE RECORDER _____

CHANNEL
1 _____ 2 _____
3 _____ 4 _____
5 _____ 6 _____
7 _____

RUN	TIME ON OFF	TARGET	SPEED	ALTITUDE	READING	CELL-FILTER	DIR REC	TAPED	CELL-FILTER	DIR REC	TAPED	TAPE NUMBER	REMARKS
1	21:31	BD #2 (abort)	90	750	020							14A1	
2	21:34	BD #2			020							14A2	
3	21:37	BD #3			245							14A3	
4	21:40	BD #1			105-95							14A4	
5	21:49	BD #2	110	2K	020							14A5	
6	21:56	BD #1	120	4K	105-115							14A6	
7	22:06	BD #2			025							14B1	
8	22:09	BD #3			245							14B2	

DATE 8/28/71 TAKE OFF 04:03
FLIGHT NO. #20 LANDING 05:13 (1:10) Light Ground Fog
OPERATING BASE Big Delta
PROJECT D.&R.T.
TAPE RECORDER

CHANNEL
1		2	
3		4	
5		6	
7			

RUN	TIME ON	OFF	TARGET	SPEED	ALTITUDE	HEADING	CELL-FILTER	DIR REC	TAPED	CELL-FILTER	DIR REC	TAPED	TAPE NUMBER	REMARKS
1	04:15		BD #1	120	4K	107-97							15A1	
2	04:24		BD #2			025							15A2	
3	04:27		BD #3			245							15A3	
4	04:34		BD #2	110	2K	025							15A4	
5	04:40		BD #1	90	750	110							15A5	Tape Drop Outs
6	04:50		BD #2			025							15B1	
7	04:54		BD #3			245							15B2	
8	04:56		BD #1			110							15B3	Repeat Run #5

DATE 7/28/71 TAKE OFF 12:30
FLIGHT NO. #21 LANDING 14:05 (1:35)
OPERATING BASE Big Delta
PROJECT D.&R.T.
TAPE RECORDER

CHANNEL
1		2	
3		4	
5		6	
7			

RUN	TIME ON	OFF	TARGET	SPEED	ALTITUDE	HEADING	CELL-FILTER	TAR REC	TAPED	CELL-FILTER	DIR REC	TAPED	TAPE NUMBER	REMARKS
		FERRY - BIG DELTA TO ANCHORAGE												

APPENDIX D

Vegetation at Shaw Creek Flats

VEGETATION; D&RTCo. TEST SITE, SHAW CREEK FLATS, ALASKA.

TREES
Betula papyrifera   Marsh
Larix laricina   (Du Roi) K. Koch
Picea glauca   (Moench) Voss
P. mariana   (Mill.) B.S.P.
Populus balsamnifera   L.

SHRUBS
Arctostáphylus rubra   (Rehd.&Wilson) Fern
Betula glandulosa   Michx.
Ledum palustre groenlandicum   (Oeder) Hult.
Portentilla fruticosa   L.
Salix spp.
Vaccinium uliginosum alpinum   (Bigel.) Hult.
V. vitis-idaes   L.

HERBS
Calamagrostis canadensis   (Michx.) Beauv.

MOSSES
Homalothecium hitens   (Hedw.) H. Robins
Hylocomium splendens   (Hedw.) B.S.G.
Tolytrichum juniperinum   (Hedw.)

LICHENS
Alectoria sp.
Cetraria sp.
Cladonia spp.
Hypogymnia sp.
Parmeleus sp.
Peltegeria sp.
Usnea sp.

identified by
Barbara Murray
Herbarium
University of Alaska

FIGURE 1: (Following Page) Ground Conditions at the Shaw Creek
Flats Site in the Immediate Area of Boreholes TH8-2, 8-3, 8-4, 8-5,
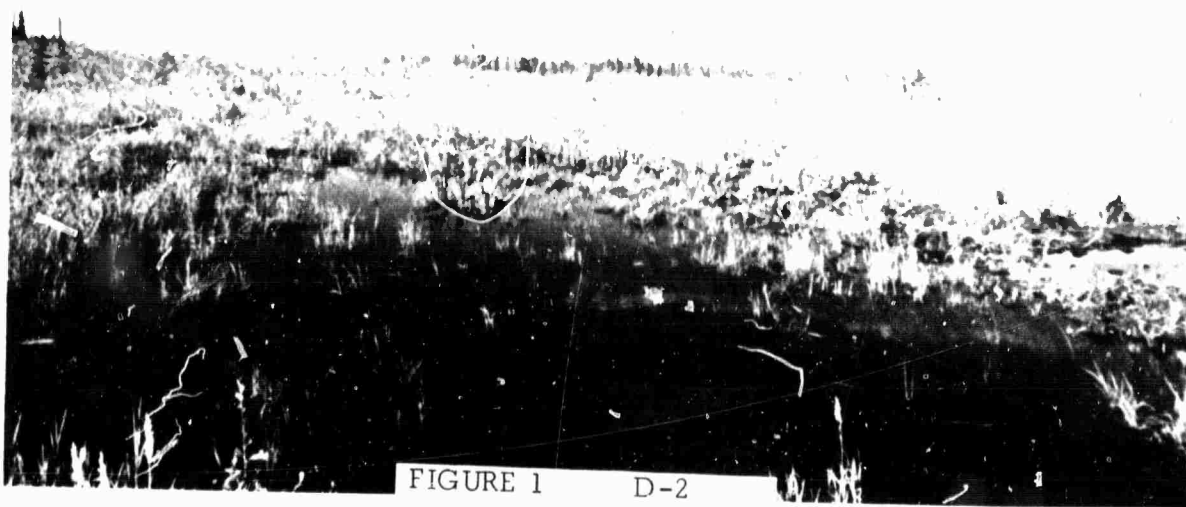and 8-45 A&B.   Photos Top to Bottom are Facing E.S,W. August 1971

D-1

FIGURE 1   D-2